https://www.mdc-berlin.de/de/veroeffentlichungstypen/clinical-journal-club

Als gemeinsame Einrichtung von MDC und Charité fördert das Experimental and Clinical Research Center die Zusammenarbeit zwischen Grundlagenwissenschaftlern und klinischen Forschern. Hier werden neue Ansätze für Diagnose, Prävention und Therapie von Herz-Kreislauf- und Stoffwechselerkrankungen, Krebs sowie neurologischen Erkrankungen entwickelt und zeitnah am Patienten eingesetzt. Sie sind eingeladen, uns beizutreten. Bewerben Sie sich!

Prurigo pigmentosa — also known as keto rash — is an inflammatory dermatosis that manifests as pruritic, erythematous papules on the chest, back, or neck that may progress to a reticular pattern over time. It has been associated with ketosis in the context of ketogenic diets (as in this patient), diabetes mellitus, and fasting. Treatment involves tetracycline therapy and resolution of ketosis.

A previously healthy 20-year-old man presented to the dermatology clinic with a 4-week history of an itchy rash on his upper chest and shoulders. Two months before presentation, he had started a carbohydrate-restricted ketogenic diet for weight loss. Physical examination is shown. Which of the following is the most likely diagnosis?

Confluent and reticulated papillomatosis

Contact dermatitis

Erythema dyschromicum perstans

Prurigo pigmentosa

Tinea corporis

Prurigo pigmentosa (PP) ist eine seltene, chronisch-entzündliche Hauterkrankung, die stark juckende, rötliche Knötchen (Papeln) verursacht, welche typischerweise am Oberkörper (Brust, Rücken, Nacken) auftreten und beim Abheilen netzartige (retikuläre) dunkle Flecken (Hyperpigmentierungen) hinterlassen; sie ist auch als "Keto-Rash" bekannt und wird oft mit ketogenen Diäten, Diabetes oder Fettreduktion in Verbindung gebracht, wobei orale Antibiotika wie Doxycyclin oder Minocyclin oft gut wirken, aber die Pigmentflecken bestehen bleiben können.

Carotid artery stenosis is the narrowing of the carotid arteries in the neck, typically from plaque buildup (atherosclerosis), restricting blood flow to the brain and increasing stroke risk. It often has no symptoms but can cause sudden weakness, vision loss, or speech issues, requiring diagnosis via ultrasound or CT/MRI scans, with treatments ranging from lifestyle changes and medication to angioplasty/stenting or surgery.

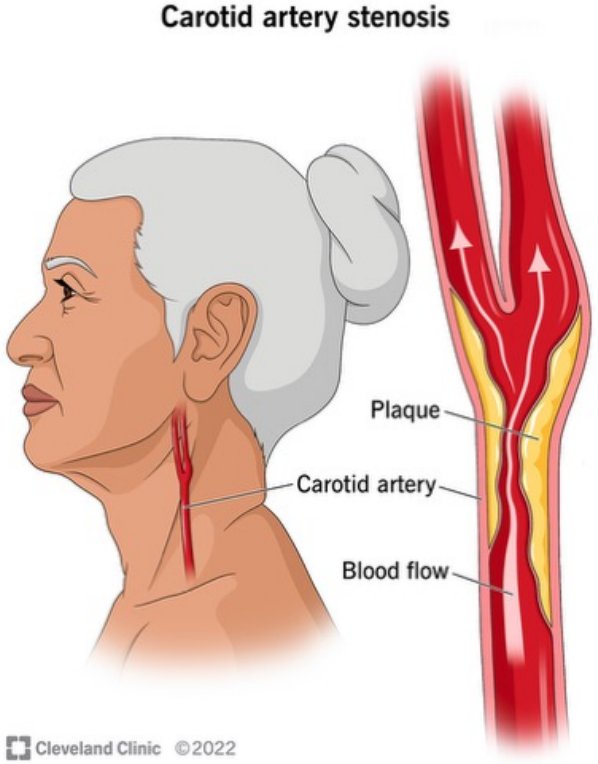

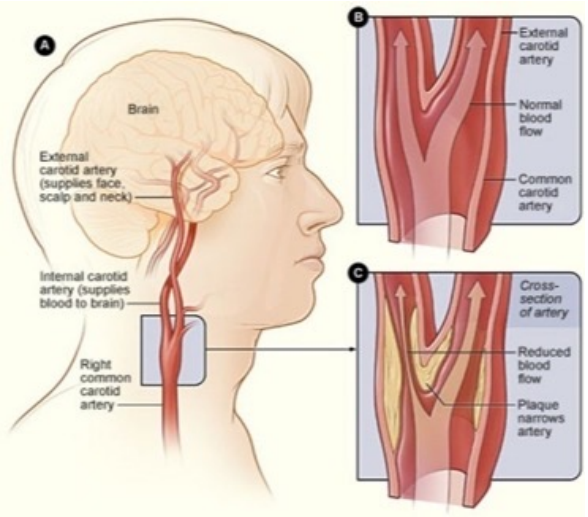

How about LDL <70 mm Hg and Blood Pressure down to normal (to 120/80 mm Hg)?

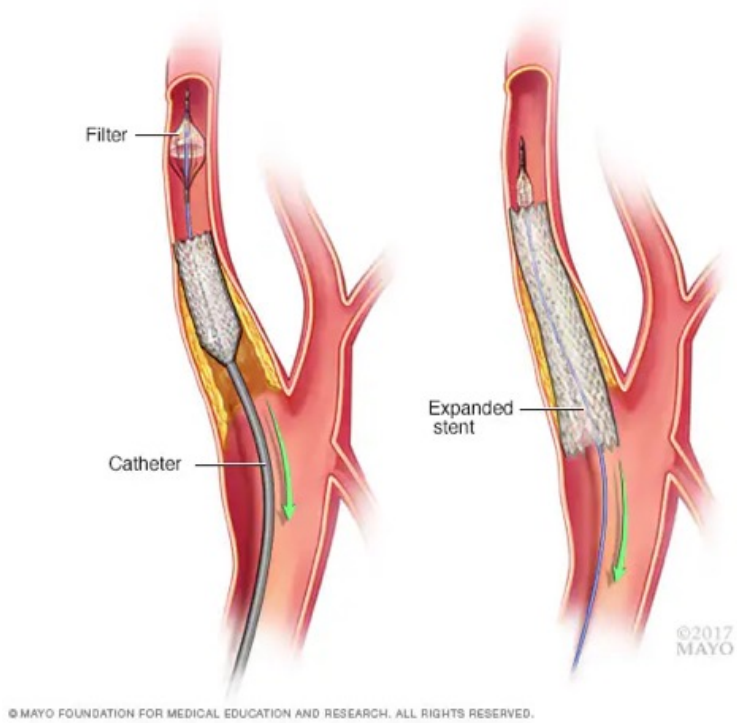

Stenting

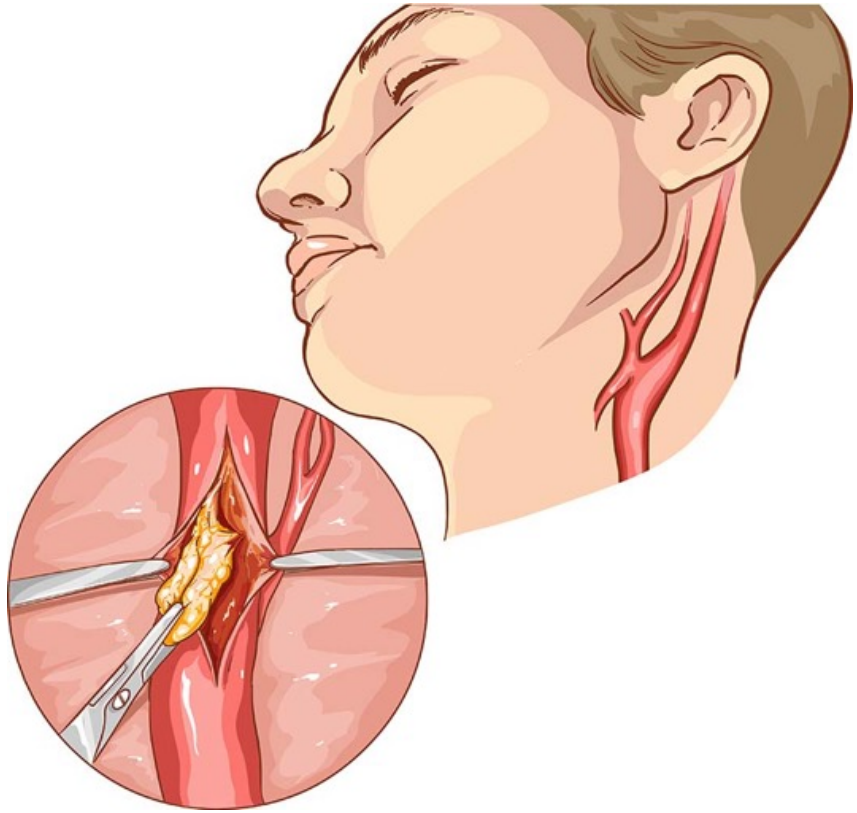

Endarterectomy

Medical Management and Revascularization for Asymptomatic Carotid Stenosis

Improvements in medical therapy, carotid-artery stenting, and carotid endarterectomy call into question the preferred management of asymptomatic carotid stenosis. Whether adding revascularization to intensive medical management would provide greater benefit than intensive medical management alone is unclear.

We conducted two parallel, observer-blinded clinical trials that enrolled patients with high-grade (≥70%) asymptomatic carotid stenosis across 155 centers in five countries. The stenting trial compared intensive medical management alone (medical-therapy group) with carotid-artery stenting plus intensive medical management (stenting group); the endarterectomy trial compared intensive medical management alone (medical-therapy group) with carotid endarterectomy plus intensive medical management (endarterectomy group). The primary outcome was a composite of any stroke or death, assessed from randomization to 44 days, or ipsilateral ischemic stroke, assessed during the remaining follow-up period up to 4 years.

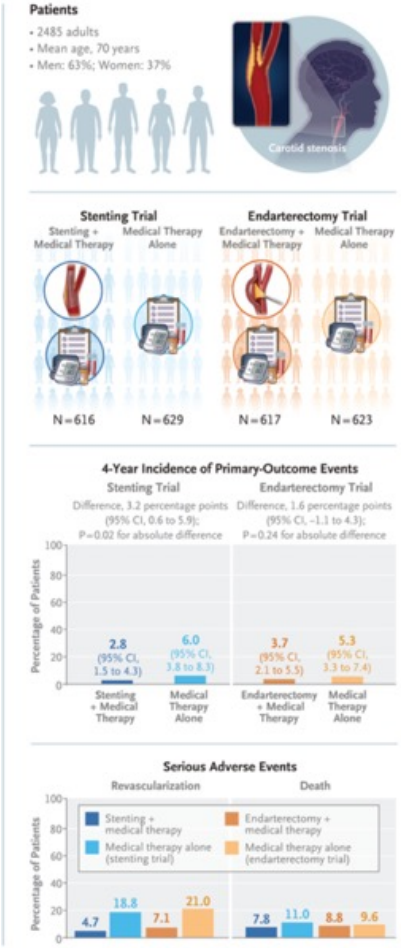

The treatment of high-grade carotid-artery stenosis varies considerably internationally. Some countries limit revascularization primarily to patients with symptoms, whereas others more commonly recommend that asymptomatic patients undergo revascularization. In the United States, 75 to 80% of patients who undergo carotid-artery stenting or endarterectomy are asymptomatic. Randomized trials from the 1990s and early 2000s showed that carotid endarterectomy led to a lower risk of stroke among asymptomatic patients with high-grade stenosis than medical therapy. Improvements in carotid endarterectomy, carotid-artery stenting, and medical therapy and the results of two recent small trials have challenged our understanding of appropriate treatments. Here, we present results from the Carotid Revascularization and Medical Management for Asymptomatic Carotid Stenosis Trials (CREST-2), which tested whether carotid-artery stenting or carotid endarterectomy plus intensive medical management would be superior to intensive medical management alone for preventing stroke in patients with high-grade carotid stenosis without recent stroke symptoms.

Patient Selection and Randomization

Patients 35 years of age or older were eligible if they had no history of stroke, transient ischemic attack (TIA), or amaurosis fugax in the carotid-artery territory within 180 days before randomization. Also required were stenosis of at least 70% as assessed by Doppler ultrasonography showing a peak systolic velocity of at least 230 cm per second and any of the following findings: an end diastolic velocity of at least 100 cm per second, a peak systolic velocity ratio of the internal to common carotid artery of at least 4.0, or at least 70% stenosis on computed tomographic angiography (CTA) or magnetic resonance angiography (MRA); or at least 70% stenosis on catheter angiography alone. Patients were excluded if they had a previous disabling stroke, unstable angina, or atrial fibrillation prompting anticoagulation. Patient eligibility and trial assignment were established by the trial site, guided by differences in eligibility criteria specific to carotid-artery stenting or carotid endarterectomy. Patients underwent randomization by means of a Web-based system, with stratification according to trial and center.

Intensive Medical Management

The intensive medical management protocol was the same for all the patients, except for the period of antiplatelet use before and after carotid-artery stenting and carotid endarterectomy. Site investigators managed cardiovascular risk factors with protocol-driven central oversight. Primary targets were a systolic blood pressure of less than 130 mm Hg (the initial target of <140 mm Hg was reduced in 2018 after guideline changes) and a low-density lipoprotein (LDL) cholesterol level of less than 70 mg per deciliter (1.80 mmol per liter). Elevated levels of glucose and glycated hemoglobin and lifestyle factors (cigarette smoking, excess body weight, and physical inactivity) were also monitored and managed. Health coaching was provided by telephone. If requested by the patient, medications to address risk factors were provided at no cost, including alirocumab.

Stenting and Endarterectomy

Revascularization procedures were performed in accordance with guidelines and operators' standard procedures. Carotid-artery stenting was performed with local anesthesia for femoral access, with or without conscious sedation. Embolic protection was required. Starting 48 hours before the procedure, patients who underwent carotid-artery stenting received aspirin at a dose of 325 mg daily and clopidogrel at a dose of 75 mg twice daily. After the stenting procedure, patients received clopidogrel at a dose of 75 mg daily and aspirin at a dose of 75 to 325 mg daily for 30 days, followed by a dose of 70 to 325 mg daily thereafter. Alternative antiplatelet regimens were used when clopidogrel or aspirin could not be used. Patients who underwent carotid endarterectomy received aspirin at a dose of 325 mg daily for at least 48 hours before the procedure and 70 to 325 mg daily thereafter.

Follow-up Assessments

In-person follow-up occurred at 12 to 36 hours after the revascularization procedure; at 44 days; at 4, 8, and 12 months; and every 6 months thereafter to 48 months. This follow-up included a medical history, the Questionnaire Verifying Stroke Free Status, the modified Rankin scale score (range, 0 [no symptoms] to 6 [death]), the National Institutes of Health Stroke Scale (NIHSS) score (range, 0 to 42, with higher scores indicating greater neurologic deficit), vital signs, and laboratory studies. Magnetic resonance imaging (MRI) or computed tomography (CT) of the head was recommended in patients who had an increase in the NIHSS score of at least 2 points from baseline. If stroke or TIA was suspected during follow-up, an additional visit was scheduled, which included CT (or CTA) or MRI (or MRA) and other testing as indicated. For patients unable to return to the clinic and during the coronavirus disease 2019 pandemic, telephone and virtual visits were conducted. The last patient who was randomly assigned to each treatment group was followed for 1 year. All the adverse events were reported by the sites to the independent medical monitor, with serious unexpected events reported within 24 hours. Results of Doppler ultrasonography were obtained annually, overseen by the imaging core.

Primary and Secondary Outcomes

The primary outcome was a 4-year composite of any stroke (ischemic or hemorrhagic) or death, assessed from randomization to 44 days (periprocedural period), or ipsilateral ischemic stroke, assessed during the remaining follow-up period up to 4 years (postprocedural period). The primary outcome was analyzed according to the intention-to-treat principle (i.e., in all the patients who had undergone randomization).

Characteristic	Stenting Trial (N = 1245)		Endarterectomy Trial (N = 1240)	
	Medical Therapy Alone (N = 629)	Stenting (N = 616)	Medical Therapy Alone (N = 623)	Endarterectomy (N = 617)
Age — yr	69.7±7.7	69.3±8.1	70.4±7.6	70.7±7.8
Female sex — %	38.2	36.9	39.0	35.3
Race — %†				
White	90.1	92.9	88.3	90.0
Black	6.2	5.7	6.9	6.0
Other, not reported, or missing data	3.7	1.5	4.8	4.1
Hispanic ethnic group — %†	4.7	4.8	3.9	4.4
Previous stroke or TIA on target lesion >180 days before randomization — %	4.9	8.0	8.4	8.9
Risk factors — %				
Hypertension	87.4	88.0	84.9	85.1
Diabetes	37.8	40.7	38.0	34.4
Dyslipidemia	93.3	92.0	90.0	91.5
Current smoking	21.0	18.8	21.2	21.1
Previous cardiovascular disease or CABG	54.5	53.7	43.3	44.3
Blood pressure — mm Hg				
Systolic	138.8±20.2	138.2±20.2	137.9±19.8	139.3±20.2
Diastolic	73.2±10.8	73.1±11.2	72.6±10.2	73.1±10.7
LDL cholesterol — mg/dl‡	76.7±34.6	77.1±36.5	81.3±33.9	80.3±33.6
Body-mass index§	28.7±5.6	29.3±5.5	28.5±5.4	28.7±5.3
Stenosis at randomization — %				
Index artery				
≥70% stenosis	97.6	97.7	97.1	97.4
Peak systolic velocity ≥389 cm/sec¶	33.5	31.1	32.9	37.2
Nonindex artery: ≥50% stenosis	34.4	37.0	37.2	35.7
Modified Rankin scale score of 0 — %‖	87.8	88.8	87.9	87.0
CHA_2DS_2-VASc score of ≥4 — %**	56.9	60.1	53.8	55.9
Current treatment with any antiplatelet agent before procedure — %	—	100	—	99.2
Carotid-artery stenting procedure				
Median target-lesion length (IQR) — mm	—	18 (12–20)	—	—
Embolic protection placed — %	—	99.6	—	—
Carotid endarterectomy procedure: general anesthesia — %	—	—	—	89.0

Analysis of Primary Outcome and Components.

3% difference

2% difference

Variable	Stenting Trial		Endarterectomy Trial	
	Medical Therapy Alone	Stenting	Medical Therapy Alone	Endarterectomy
Primary 4-yr composite outcome*				
Event rate (95% CI) — %	6.0 (3.8 to 8.3)	2.8 (1.5 to 4.3)	5.3 (3.3 to 7.4)	3.7 (2.1 to 5.5)
Absolute difference (95% CI) — percentage points†	3.2 (0.6 to 5.9)		1.6 (−1.1 to 4.3)	
P value for difference	0.02		0.24	
Relative risk (95% CI)†	2.13 (1.15 to 4.39)		1.43 (0.78 to 2.72)	
Components of primary outcome				
Periprocedural period: stroke or death				
No. of events/no. of patients	0/629	8/616	3/623	9/617
Percent of patients with event (95% CI)	0.0 (0.0 to 0.6)	1.3 (0.6 to 2.5)	0.5 (0.1 to 1.4)	1.5 (0.7 to 2.8)
Difference (95% CI) — percentage points	−1.3 (−2.2 to 0.4)		−1.0 (−2.1 to 0.1)	
Postprocedural period: ipsilateral ischemic stroke				
No. of person-yr	1686	1714	1761	1823
No. of events/no. of patients	28/600	7/582	23/600	10/596
Annual event rate per person-yr (95% CI) — %	1.7 (1.1 to 2.4)	0.4 (0.2 to 0.9)	1.3 (0.9 to 2.0)	0.5 (0.3 to 1.0)
Relative risk (95% CI)	4.07 (1.78 to 9.31)		2.38 (1.13 to 5.00)	

Good control of risk factors

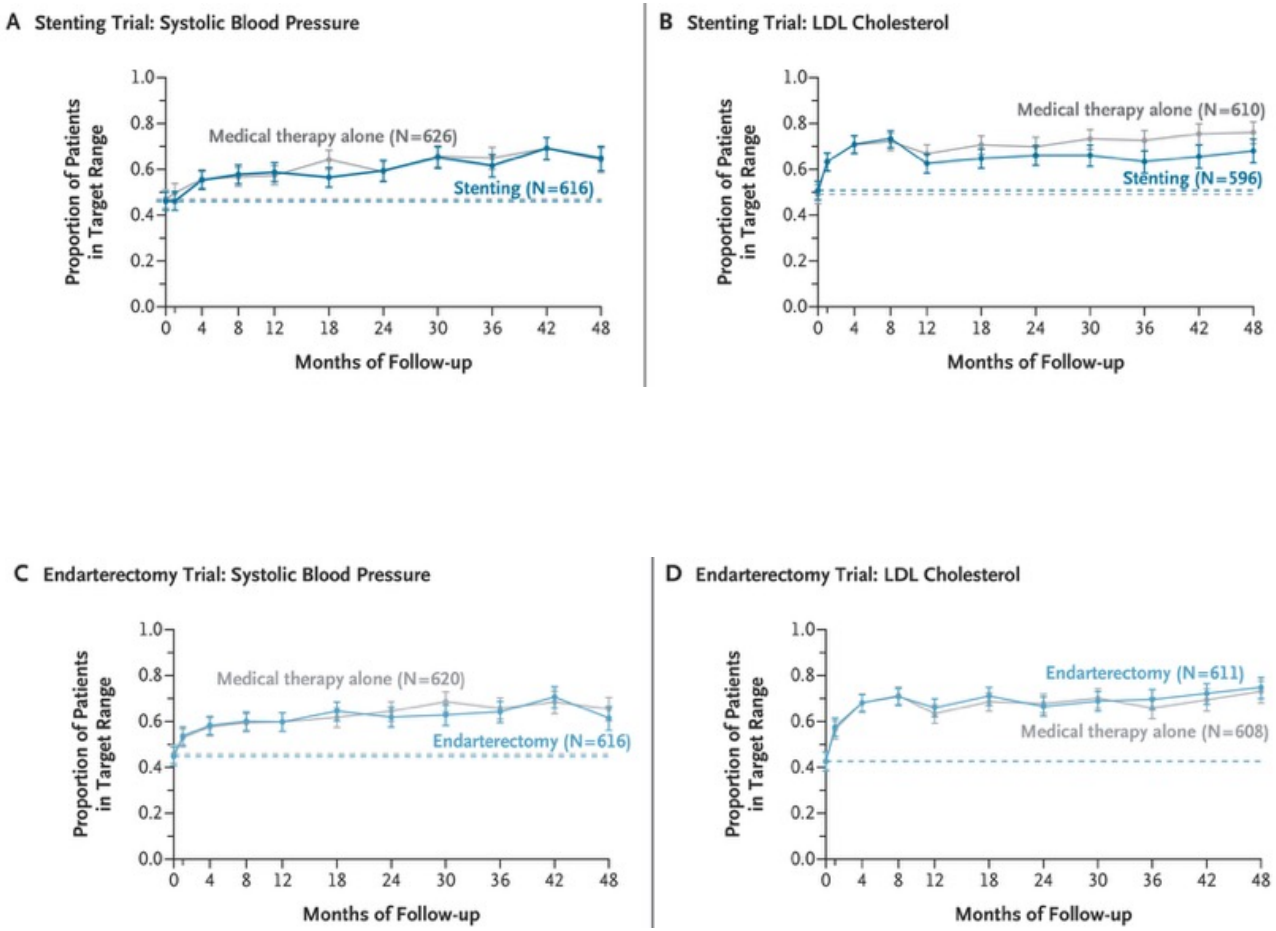

Proportion of Patients with Risk-Factor Values in Target Range over Time.

The stenting trial compared intensive medical management (medical therapy alone) with carotid-artery stenting plus intensive medical management (stenting), and the endarterectomy trial compared intensive medical management (medical therapy alone) with carotid endarterectomy plus intensive medical management (endarterectomy). Shown are changes in risk-factor values (systolic blood pressure and low-density lipoprotein [LDL] cholesterol) from baseline to 48 months for the stenting trial (Panels A and B) and the endarterectomy trial (Panels C and D). The target systolic blood pressure was less than 130 mm Hg (changed from <140 mm Hg in 2018). The target LDL cholesterol level was less than 70 mg per deciliter (1.80 mmol per liter). Dashed lines represent the proportion of patients meeting the treatment threshold goals in each group at baseline; these values overlap in Panel D. The first postbaseline assessment was conducted at 44 days after randomization. Patients were followed beyond the occurrence of a primary-outcome event for risk-factor control. In all panels, I bars indicate 95% confidence intervals.

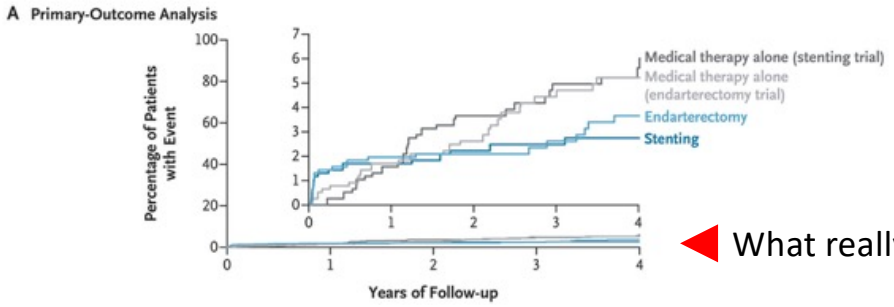

What really happened

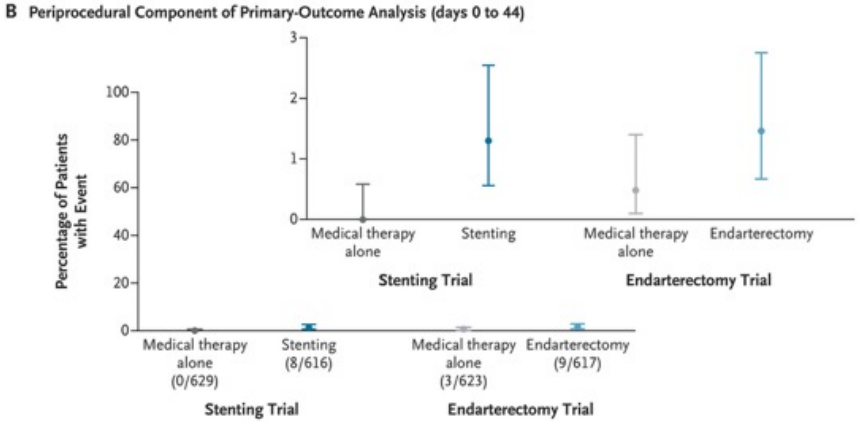

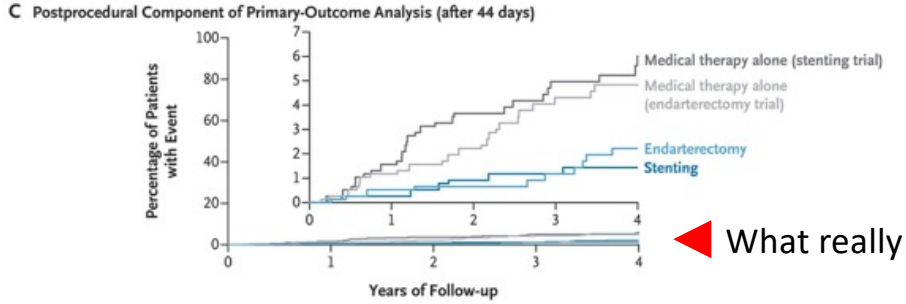

What really happened

Four-Year Event Rates for the Primary Outcome and Individual Components of the Primary Outcome.

Panel A shows Kaplan–Meier estimates of the 4-year incidence of primary-outcome events in the stenting and endarterectomy trials, according to trial group. The primary outcome was a composite of any stroke or death, assessed from randomization to 44 days, or ipsilateral ischemic stroke, assessed during the remaining follow-up period up to 4 years. Panel B shows the periprocedural component of the primary outcome (i.e., stroke or death from randomization [day 0] to 44 days). Numbers in parentheses below the labels on the horizontal axis are the numbers of events and of patients in trial group. I bars indicate 95% confidence intervals. Panel C shows the postprocedural component of the primary outcome (i.e., ipsilateral ischemic stroke during the remaining portion of the 4-year follow-up). In all panels, the inset shows the same data on an expanded y axis.

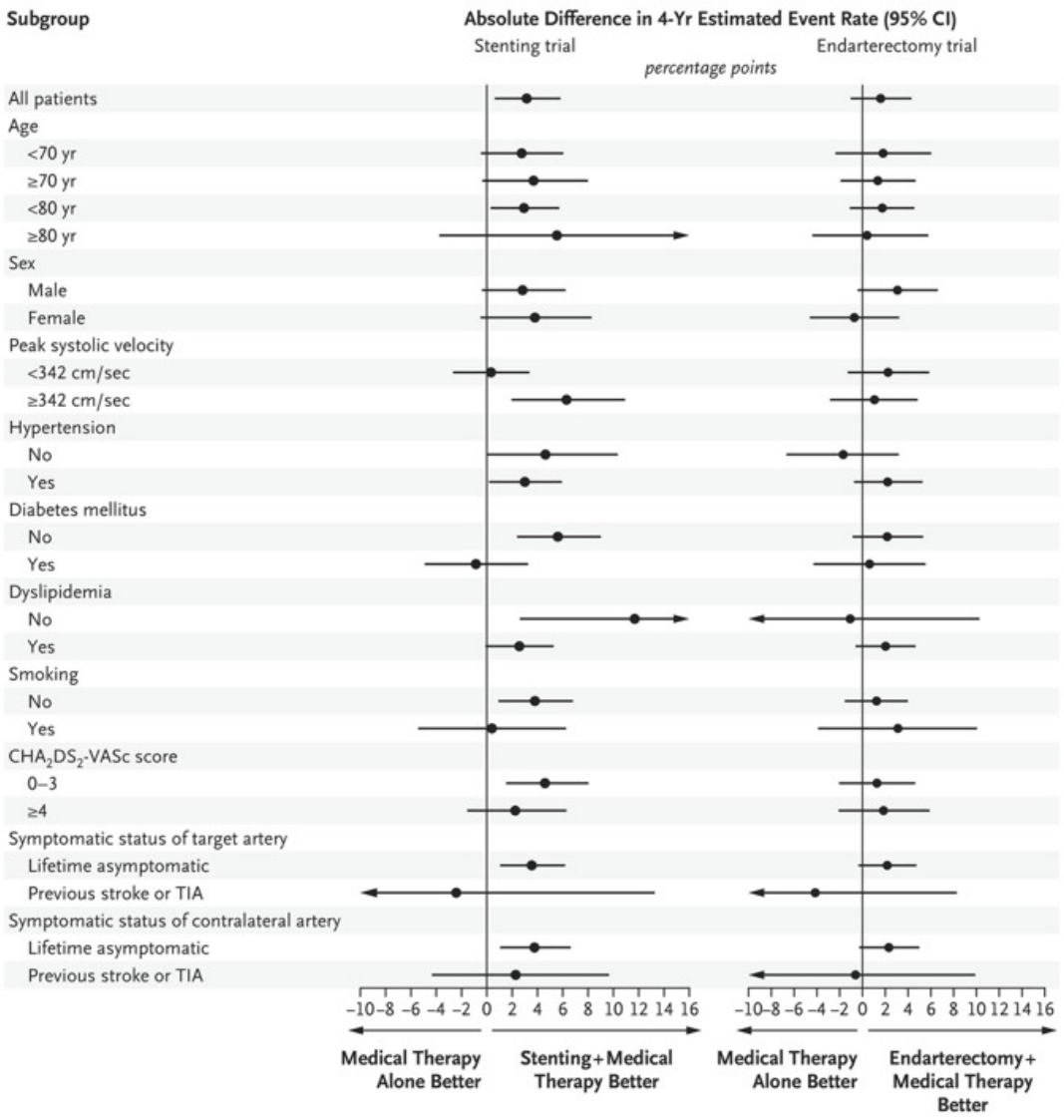

Absolute Between-Group Differences in the 4-Year Estimated Event Rate in the Stenting and Endarterectomy Trials, According to Risk-Factor Subgroups.

Shown are absolute between-group differences in the 4-year incidence of primary-outcome events in the stenting and endarterectomy trials. The CHA_2DS_2-VASc scale is used to assess the risk of stroke among patients with atrial fibrillation; scores range from 0 to 9, with higher scores indicating a greater risk of stroke. Confidence intervals are not adjusted for multiplicity and should not be used to infer treatment effects. Arrows indicate that the 95% confidence interval extends outside the graphed area. Full data regarding the subgroup analyses are provided in Figure S8A through S8K. TIA denotes transient ischemic attack.

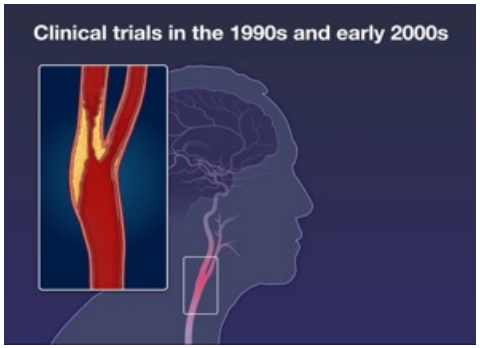
Clinical trials in the 1990s and early 2000s

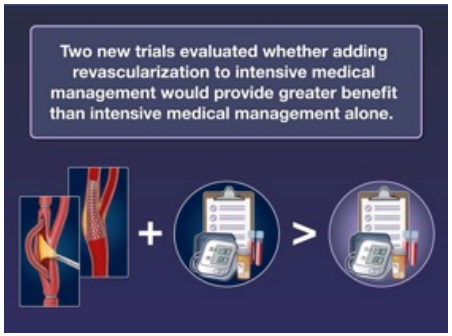
Two new trials evaluated whether adding revascularization to intensive medical management would provide greater benefit than intensive medical management alone.

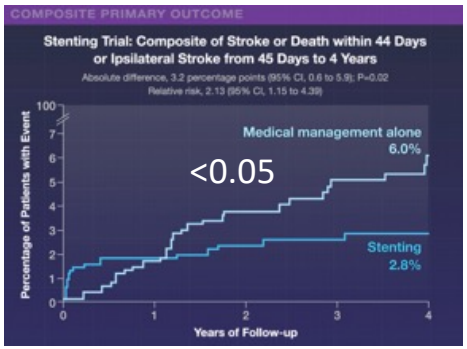
COMPOSITE PRIMARY OUTCOME
Stenting Trial: Composite of Stroke or Death within 44 Days or Ipsilateral Stroke from 45 Days to 4 Years
Absolute difference, 3.2 percentage points (95% CI, 0.6 to 5.9); P=0.02
Relative risk, 2.13 (95% CI, 1.15 to 4.39)
Medical management alone
6.0%
<0.05
Stenting
2.8%
Percentage of Patients with Event
Years of Follow-up

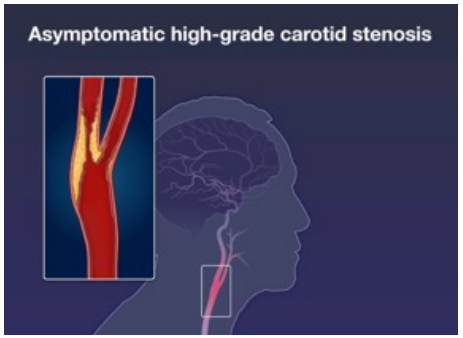
Asymptomatic high-grade carotid stenosis

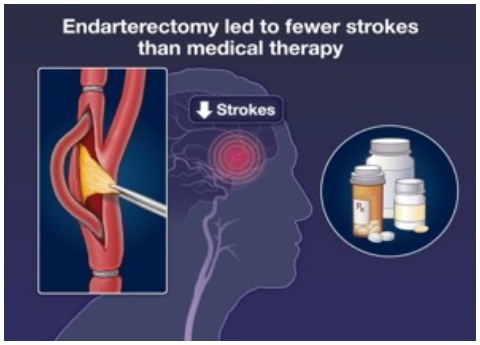
Endarterectomy led to fewer strokes than medical therapy
Strokes

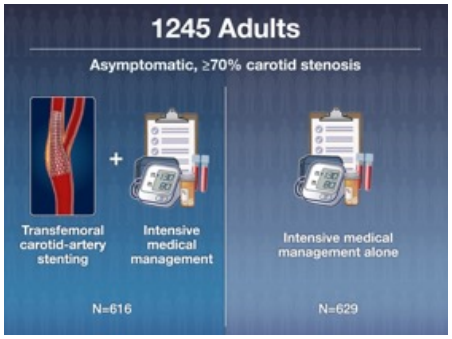
1245 Adults
Asymptomatic, ≥70% carotid stenosis
Transfemoral carotid-artery stenting
Intensive medical management
Intensive medical management alone
N=616
N=629

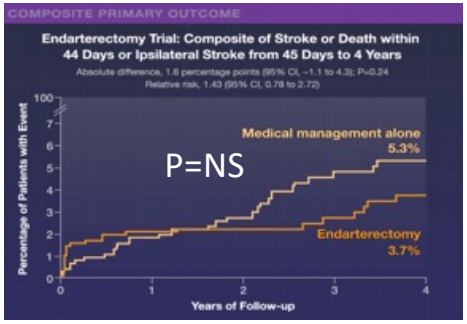
COMPOSITE PRIMARY OUTCOME
Endarterectomy Trial: Composite of Stroke or Death within 44 Days or Ipsilateral Stroke from 45 Days to 4 Years
Absolute difference, 1.6 percentage points (95% CI, −1.1 to 4.3); P=0.24
Relative risk, 1.43 (95% CI, 0.78 to 2.72)
Medical management alone
5.3%
P=NS
Endarterectomy
3.7%
Percentage of Patients with Event
Years of Follow-up

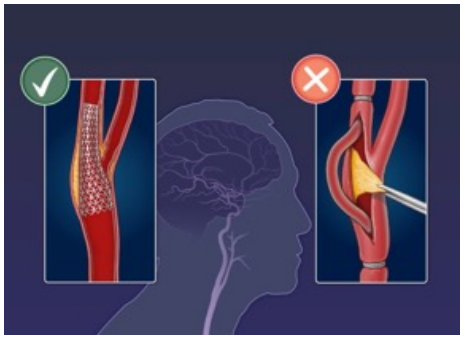

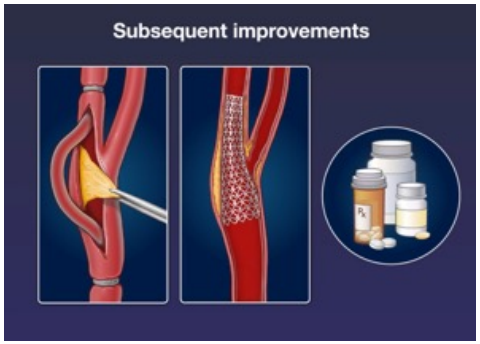
Subsequent improvements

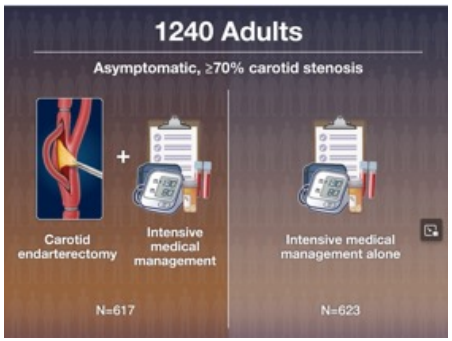
1240 Adults
Asymptomatic, ≥70% carotid stenosis
Carotid endarterectomy
Intensive medical management
Intensive medical management alone
N=617
N=623

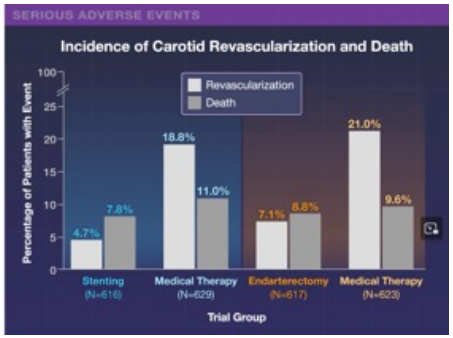
SERIOUS ADVERSE EVENTS
Incidence of Carotid Revascularization and Death
Revascularization
Death
Percentage of Patients with Event
4.7%
7.8%
18.8%
11.0%
7.1%
8.8%
21.0%
9.6%
Stenting (N=616)
Medical Therapy (N=629)
Endarterectomy (N=617)
Medical Therapy (N=623)
Trial Group

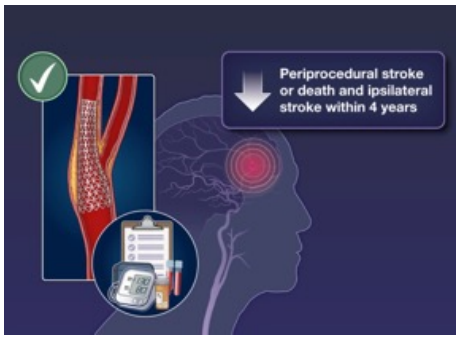
Periprocedural stroke or death and ipsilateral stroke within 4 years

Managing Asymptomatic Carotid Stenosis

The management of carotid-artery stenosis that has not caused recent symptoms — asymptomatic carotid stenosis — has been controversial. Clinical trials that began more than 30 years ago showed a small benefit of carotid endarterectomy as compared with medical treatment, but improvements in medical prevention of stroke call into question whether endarterectomy is still beneficial. Carotid-artery stenting has emerged as a less invasive but unproven alternative to endarterectomy for the treatment of asymptomatic carotid stenosis.

The CREST-2 investigators are to be congratulated for conducting a large-scale trial investigating the management of asymptomatic carotid stenosis on the background of intensive medical therapy. What we need now are trials focusing on identification of the small proportion of patients with carotid stenosis in whom symptoms develop despite the use of medical therapy. The most promising approach uses magnetic resonance imaging of carotid-artery plaque to identify intraplaque hemorrhage, a strong risk factor for stroke.

Die trockene altersbedingte Makuladegeneration (AMD) ist die häufigere Form dieser Augenerkrankung, bei der es durch Stoffwechselablagerungen (Drusen) zu einem langsamen Absterben von Sehzellen im Bereich des schärfsten Sehens kommt.

- **Nahrungsergänzungsmittel (AREDS2):** Die Einnahme spezieller Kombinationen aus Lutein, Zeaxanthin, Vitamin C, E, Zink und Kupfer wird bei intermediären Stadien empfohlen, um das Risiko eines Übergangs in das Spätstadium zu senken.
- **Neue Medikamente (Komplement-Inhibitoren):** In den USA sind Wirkstoffe wie Syfovre oder Izervay bereits zugelassen, die das Fortschreiten der geografischen Atrophie (Spätstadium) verlangsamen können. In der EU hatte die EMA die Zulassung für diese Substanzen Anfang 2025 zunächst kritisch gesehen; Patienten sollten ihren Augenarzt nach dem aktuellen Verfügbarkeitsstatus in Deutschland für 2026 fragen.
- **Lasertherapie & Photobiomodulation:** Neuere, nicht-invasive Verfahren wie die Photobiomodulation (Lichttherapie) oder spezielle Laserbehandlungen werden eingesetzt, um die Netzhautregeneration zu stimulieren und Drusen zu reduzieren.

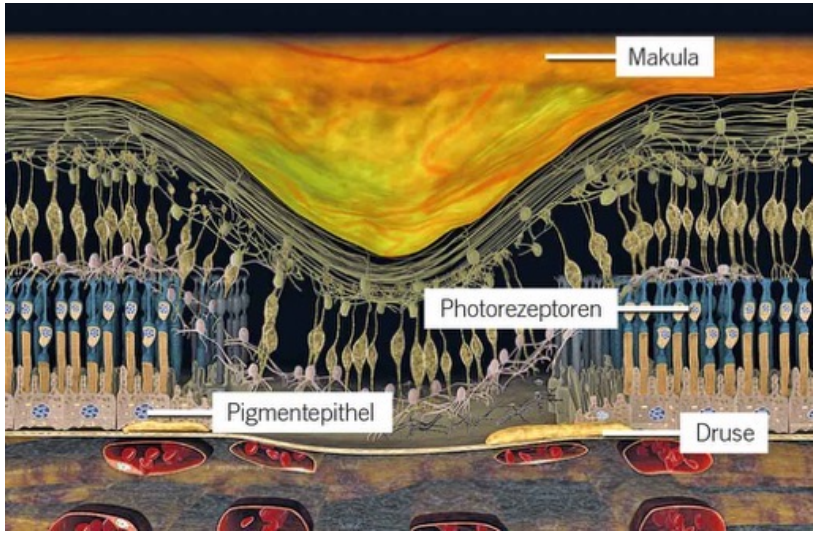

Das PRIMA-Implantat ist ein bahnbrechendes Netzhaut-Prothesensystem für Patienten mit trockener altersbedingter Makuladegeneration (AMD), das einen winzigen, drahtlosen photovoltaischen Chip unter die Netzhaut implantiert, der mit einer speziellen Brille zusammenarbeitet, um Lichtmuster zu erfassen und in elektrische Signale umzuwandeln, wodurch ein Teil des zentralen Sehvermögens wiederhergestellt wird, was das Lesen und das Erkennen von Gesichtern ermöglicht. Es ist eine weniger invasive Alternative zu Gehirnimplantaten und hat in klinischen Studien gezeigt, dass es die visuelle Acuity verbessert, indem es die Funktion der zerstörten Photorezeptoren ersetzt.

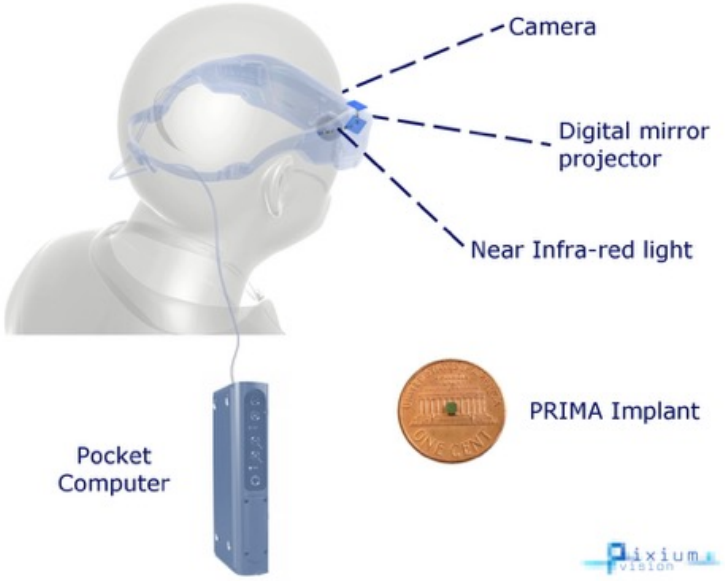

*These images are for illustrative purpose and not fully representative of the actual device used in the clinical study

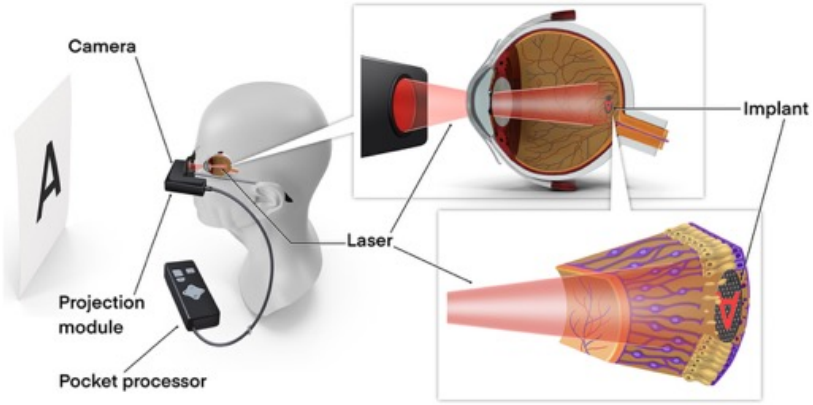

Subretinal Photovoltaic Implant to Restore Vision in Geographic Atrophy Due to AMD

Geographic atrophy due to age-related macular degeneration (AMD) is the leading cause of irreversible blindness and affects more than 5 million persons worldwide. No therapies to restore vision in such persons currently exist. The photovoltaic retina implant microarray (PRIMA) system combines a subretinal photovoltaic implant and glasses that project near-infrared light to the implant in order to restore sight to areas of central retinal atrophy.

We conducted an open-label, multicenter, prospective, single-group, baseline-controlled clinical study in which the vision of participants with geographic atrophy and a visual acuity of at least 1.2 logMAR (logarithm of the minimum angle of resolution) was assessed with PRIMA glasses and without PRIMA glasses at 6 and 12 months. The primary end points were a clinically meaningful improvement in visual acuity (defined as ≥0.2 logMAR) from baseline to month 12 after implantation and the number and severity of serious adverse events related to the procedure or device through month 12.

Conclusions

In this study involving 38 participants with geographic atrophy due to AMD, the PRIMA system restored central vision and led to a significant improvement in visual acuity from baseline to month 12.

The PRIMA implant, which has an area of 2 mm by 2 mm and a thickness of 30 µm, is a thin crystalline silicon array comprising 378 photovoltaic pixels that are each 100-µm wide. The array is implanted subretinally within the atrophic lesion. A frame-mounted camera on the PRIMA glasses captures images and projects them, after processing, onto the implant with the use of near-infrared light (wavelength, 880 nm) (Figure 1). The pixels in the implant convert near-infrared light into electrical pulses to stimulate retinal bipolar cells, which restores the flow of visual information. Unlike a wired prosthesis, the photovoltaic nature of the implant enables wireless operation combined with a straightforward implantation technique. The lenses in the PRIMA glasses are transparent, so participants have natural vision and prosthetic central vision simultaneously.

After extensive preclinical testing, a first-in-human clinical trial evaluated the feasibility of the PRIMA system in five participants with geographic atrophy due to AMD. Although the primary end point of the feasibility trial was light perception with the implant, after optimization and training, three participants reliably recognized sequences of letters and had acuity closely matching the maximum resolution of 20/420 allowed by the pixel width (100 µm). At 4 years, these three participants could read small fonts, with a mean Snellen visual acuity of 20/135.

We conducted the PRIMAvera study to assess the efficacy and safety of the PRIMA system in patients with geographic atrophy due to AMD.

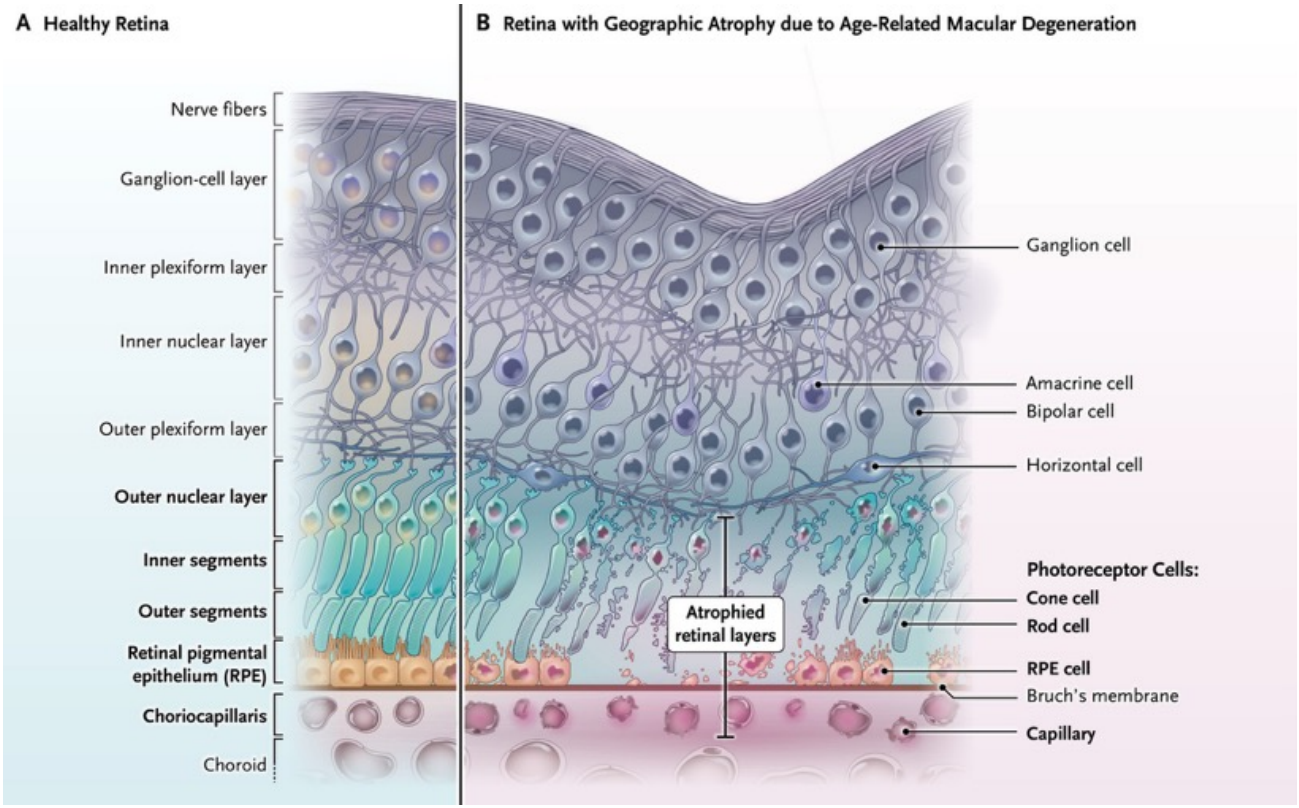

The Photovoltaic Retina Implant Microarray (PRIMA) System.
Shown is the anatomy of a healthy retina (Panel A) and a retina with geographic atrophy due to age-related macular degeneration (Panel B).

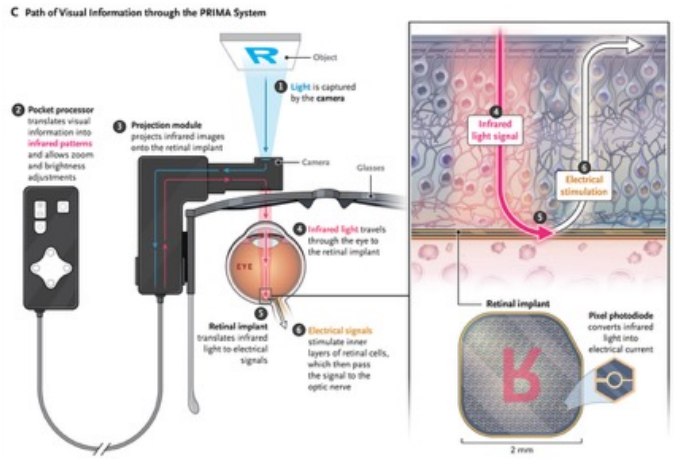

The PRIMA system (Panel C) combines a subretinal photovoltaic implant, a pocket processor, and glasses that project near-infrared light to the implant to restore sight to areas of central retinal atrophy. The camera captures light reflecting from an image (e.g., a letter R) and sends the visual information to the pocket processor. Processed information is then sent to the glasses and projected onto the implant by means of near-infrared light (wavelength 880 nm); the letter R on the implant is shown in red to indicate that the wavelength of the projected image differs from that of the light reflected by the original letter R. To achieve continuous, uninterrupted central visual perception, the projector operates at a frame rate of 30 Hz, and the processor adjusts perceptual brightness by controlling the pulse duration from 0.7 to 9.8 ms at a peak irradiance of 3.5 mW per square millimeter. The implant has an area of 2 mm by 2 mm and is composed of pixels with a width of 100 µm. Each pixel includes an active electrode in the center, a hexagonal return electrode mesh, and two photodiodes filling the space between the active and the return electrode. The photodiodes convert the near-infrared light into electrical current in order to stimulate the nearby inner retinal neurons, which process the electrical information in the retina. This information is then transferred via the optic nerve to the brain, where it is interpreted as a visual image.

Methods

Study Design and Oversight

PRIMAvera was an open-label, prospective, single-group, baseline-controlled, confirmatory clinical efficacy and safety study of the PRIMA system. The study was conducted at 17 clinical sites across five European countries.

Participants

Recruitment activities included chart review, referral by health care providers, and community outreach. Participants were eligible for inclusion if they were 60 years of age or older, had a diagnosis of geographic atrophy due to AMD in both eyes as confirmed on fundus autofluorescence imaging and optical coherence tomography (OCT), had a visual acuity of at least 1.2 logMAR (logarithm of the minimum angle of resolution [smaller values indicate better visual acuity]; Snellen equivalent, 20/320) in the study eye, and had atrophy involving the fovea of the study eye that was larger than the implant (i.e., >2.4 mm in diameter). All the participants provided written informed consent.

End Points

The primary efficacy end point was a clinically meaningful improvement in visual acuity from baseline to month 12 after implantation. Clinically meaningful improvement was defined as an improvement (i.e., decrease) of at least 0.2 logMAR (corresponding to an increase of ≥10 letters) on a standard Early Treatment Diabetic Retinopathy Study chart.

Figures

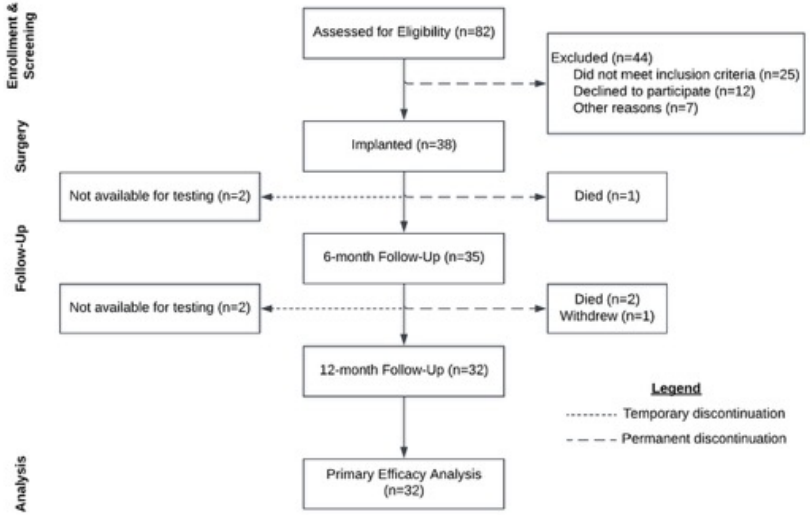

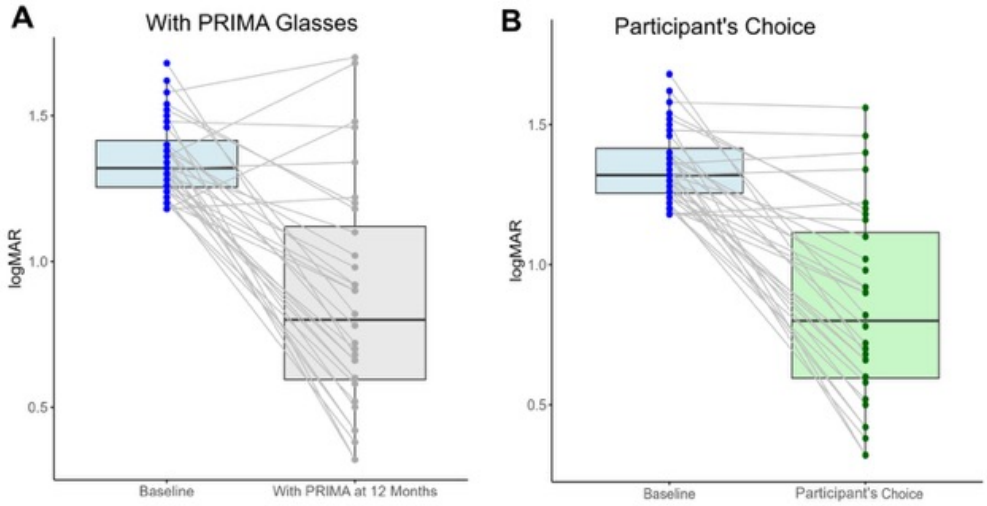

Single participant visual acuity (in logMAR) values at baseline and 12 months, comparison between with PRIMA Glasses and Participant's Choice. Boxplots of visual acuity data distribution showing single participant's values for baseline, in blue, with PRIMA glasses at 12 months, in gray, and for Participant's Choice at 12 months, in green.

Efficacy Analyses.

Variable	Primary Analyses: ≥0.2 logMAR Improvement		Post Hoc Analyses: ≥0.3 logMAR Improvement	
	no. with event/ total no.	*% with event (95% CI)*	*no. with event/ total no.*	*% with event (95% CI)*
Analysis of observed data†	26/32	81 (64–93)‡	25/32	78 (60–91)
Multiple imputation§	NA	80 (66–94)‡	NA	77 (62–92)

* A binomial test was used to assess the percentage of participants with a clinically meaningful improvement in visual acuity from baseline to month 12 (primary efficacy end point) as compared with the null hypothesis that a primary efficacy end-point event would occur in 50% or fewer participants. Clinically meaningful improvement was defined as an improvement (i.e., decrease) of at least 0.2 logMAR (logarithm of the minimum angle of resolution; corresponding to an increase of ≥10 letters) on a standard Early Treatment Diabetic Retinopathy Study chart. Multiple imputation was used in the analysis of the primary efficacy end point in order to account for missing data at month 12; data from the analysis of observed data are also reported. A post hoc analysis with methods similar to those used in the primary efficacy end-point analysis was conducted to assess the percentage of participants with an improvement in visual acuity of at least 0.3 logMAR from baseline to month 12. NA denotes not applicable.

† The analyses included 32 participants with nonmissing data at 12 months. Exact 95% confidence intervals were computed in the primary and post hoc analyses.

‡ P<0.001 for comparison with the null hypothesis.

§ The analyses included 38 participants, of whom 6 had missing data at month 12. The missing data were estimated with a multiple-imputation approach, which does not provide the exact percentage of participants with an end-point event but rather an estimated percentage computed over 100 imputed datasets. Logit 95% confidence intervals were computed in the primary and post hoc analyses.

Serious Adverse Events.

Event	Participants (N=38)	Serious Adverse Events
	no. (%)	*no.*
Ocular hypertension	6 (16)	6
Peripheral retinal break	5 (13)	5
Full-thickness macular hole	3 (8)	3
Subretinal hemorrhage	3 (8)	4
Choroidal neovascularization	2 (5)	2
Choroidal hemorrhage	1 (3)	1
Choroidal fold	1 (3)	1
Proliferative vitreoretinopathy	1 (3)	1
Retinal detachment	1 (3)	1
Retinal hemorrhage	1 (3)	1
Thrombophlebitis	1 (3)	1

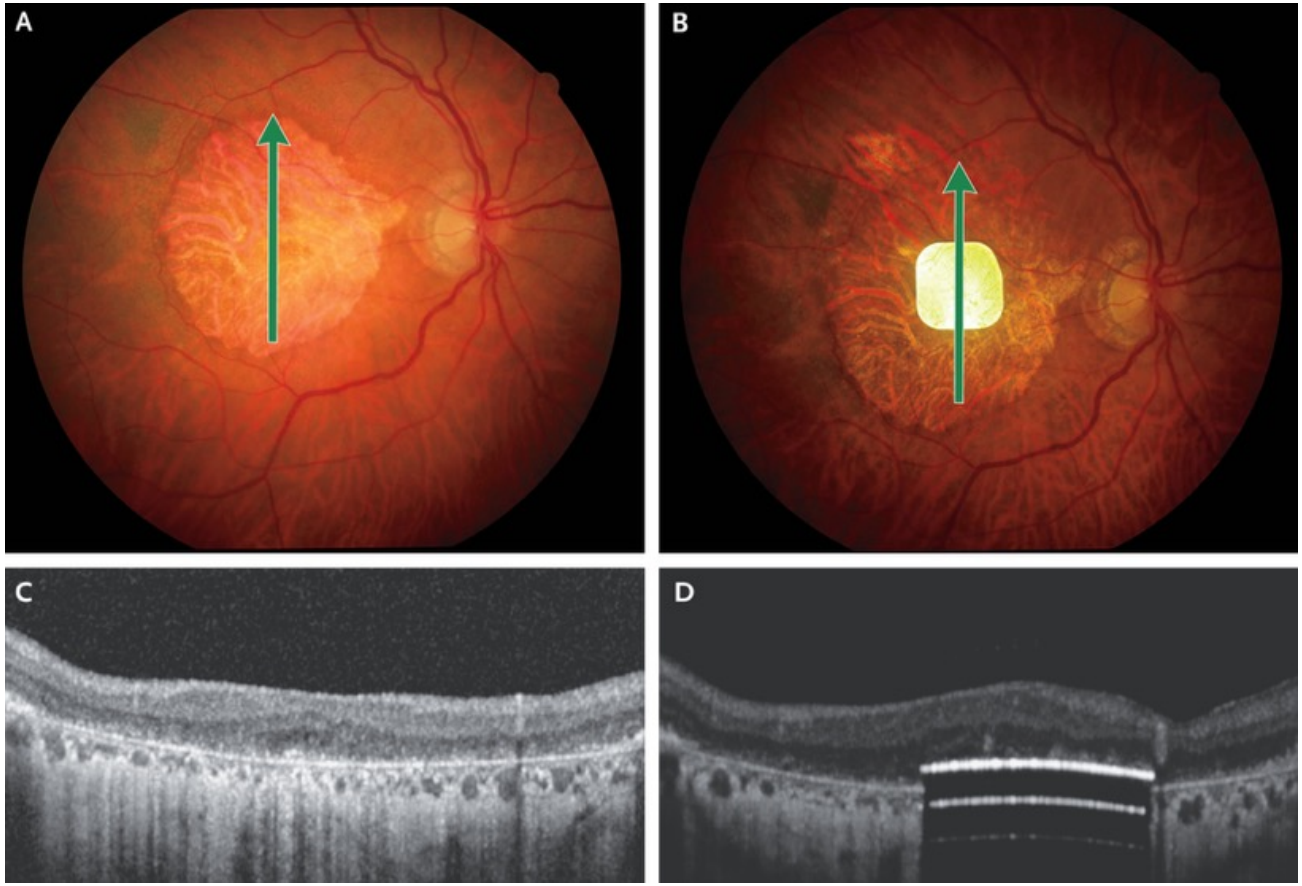

Retinal Imaging before and after Implantation.

Shown are images before and after implantation of the PRIMA photovoltaic array in a study participant's eye. The size of retinal atrophy was 21.49 mm^2 at baseline, and the array was implanted 5 years after the diagnosis of acute macular degeneration. Images obtained with color fundus photography show geographic atrophy before implantation (Panel A) and the subretinal implant 12 months after surgery (Panel B). Arrows indicate the direction of optical coherence tomographic scanning. Also shown are optical coherence tomographic images of the degenerated retina before implantation (Panel C) and the implant under the degenerated retina in proximity to the inner nuclear layer at month 12 (Panel D). The implant is not transparent and therefore creates a shadow, which covers the underlying choroid. The multiple lines below the implant surface are artifacts due to multiple reflections within the implant.

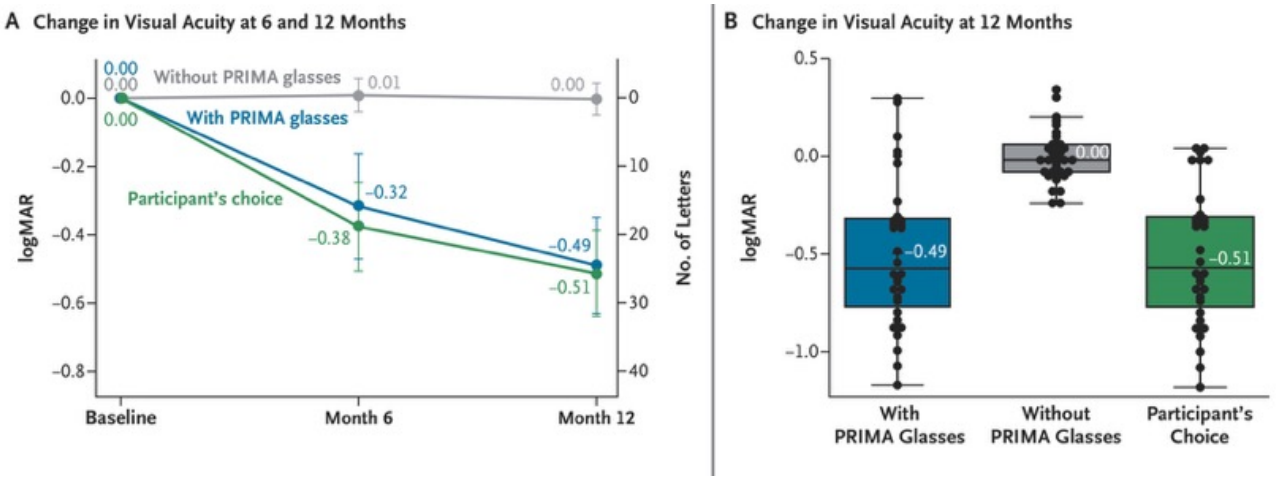

Change from Baseline in Visual Acuity.

The best-corrected visual acuity without PRIMA glasses and with PRIMA glasses was assessed at months 6 and 12 after implantation of the PRIMA photovoltaic array. The mean change from baseline to months 6 and 12 was analyzed according to three conditions: with PRIMA glasses (blue line), without PRIMA glasses (gray line), and participant's choice (the better visual acuity between the assessment without glasses and the assessment with glasses; green line) (Panel A). Mean changes are expressed as logMAR (logarithm of the minimum angle of resolution) values (y axis on left) and number of letters (y axis on right) on a standard Early Treatment Diabetic Retinopathy Study chart. Negative logMAR values indicate improvements from baseline, and the I bars indicate exact 95% confidence intervals. The confidence intervals were not adjusted for multiplicity and should not be used in place of hypothesis testing or to infer definitive treatment effects. Also shown (Panel B) are the changes from baseline to month 12 in visual acuity with PRIMA glasses (blue), without PRIMA glasses (gray), and with participant's choice (green) overall and in individual participants. Negative logMAR values indicate improvements from baseline. In the box-and-whisker plots, the white numbers indicate the mean, the center lines the median, the top and bottom of the boxes the interquartile range, the I bars 1.5 times the interquartile range, and the black dots values for individual participants.

Discussion

In the current study, the PRIMA system resulted in meaningful improvement in vision in a representative sample of participants with profound vision loss due to AMD-induced geographic atrophy with foveal involvement. Visual acuity improved from baseline to month 12 after implantation by at least 0.2 logMAR (≥10 letters) in 81% of the participants and by at least 0.3 logMAR (≥15 letters) in 78% with the PRIMA system. The mean improvement from baseline at 12 months was 0.51 logMAR (25.5 letters), and the maximum improvement was 1.18 logMAR (59 letters). Moreover, 84% of the participants reported using the device at home for reading letters, numbers, or words. With the use of digital enhancements offered by the PRIMA glasses, such as the zoom function, these participants were able to read fonts smaller (Snellen equivalent, up to 20/42) than the theoretical resolution achievable with the 100-µm pixels (Snellen equivalent, approximately 20/400).

The data at 12 months in this clinical study showed that the PRIMA subretinal implant restored meaningful central vision in persons with geographic atrophy due to AMD, thus enabling the performance of visual tasks such as reading and writing. Although no retinal implants have been explanted in humans, the wireless design allows for replacement with higher resolution next-generation implants or implantation of multiple arrays in a tiled pattern at the atrophic area with minimal incision.

Migräne bei Kindern äußert sich oft mit beidseitigen Kopfschmerzen, Übelkeit, Erbrechen, Blässe, Licht-/Lärmempfindlichkeit und Abgeschlagenheit, kann aber auch nur als Bauchschmerzen auftreten ("Bauchmigräne"), besonders bei jüngeren Kindern. Häufig schlafen betroffene Kinder während einer Attacke ein und wachen beschwerdefrei auf, Attacken sind kürzer als bei Erwachsenen (oft 1-2 Std.). Stress, Schlafmangel, Flüssigkeitsmangel und bestimmte Auslöser (wie enge Kleidung) spielen eine große Rolle, Behandlung umfasst Ruhe, Dunkelheit, evtl. Medikamente (Ibuprofen) und nicht-medikamentöse Maßnahmen wie Stressreduktion.

Symptome

- **Kopfschmerz:** Oft beidseitig, Stirn, dumpf bis pochend.
- **Begleitsymptome:** Übelkeit, Erbrechen, Bauchschmerzen (können auch allein auftreten).
- **Vegetativ:** Blässe, kalte Hände/Füße, Müdigkeit, Appetitlosigkeit, vermehrter Harndrang.
- **Sensorisch:** Überempfindlichkeit gegen Licht, Lärm, Gerüche.
- **Besonderheiten:** Abwesenheit, Schlaf als Heilmittel, manchmal Schwindel oder "Alice-im-Wunderland-Syndrom" (Verzerrung von Größe/Form) bei Aura.

„Alice im Wunderland“ (Originaltitel: *Alice's Adventures in Wonderland*) ist ein weltberühmter Kinderbuchklassiker des britischen Autors **Lewis Carroll** aus dem Jahr 1865.

Das **Calcitonin Gene-Related Peptide (CGRP)** ist ein körpereigenes Neuropeptid, das im zentralen und peripheren Nervensystem vorkommt. Es spielt eine Schlüsselrolle in der Entstehung von **Migräne** und anderen Kopfschmerzerkrankungen.
Hier sind die wichtigsten Fakten auf Deutsch:

- **Funktion:** CGRP ist einer der stärksten bekannten gefäßerweiternden Stoffe im Körper. Es ist an der Schmerzweiterleitung und an neurogenen Entzündungsprozessen beteiligt.
- **Rolle bei Migräne:** Während einer Migräneattacke steigt der CGRP-Spiegel im Blut deutlich an. Das Peptid erweitert die Blutgefäße der Hirnhaut und sensibilisiert die Schmerznerven (Trigeminusnerv).

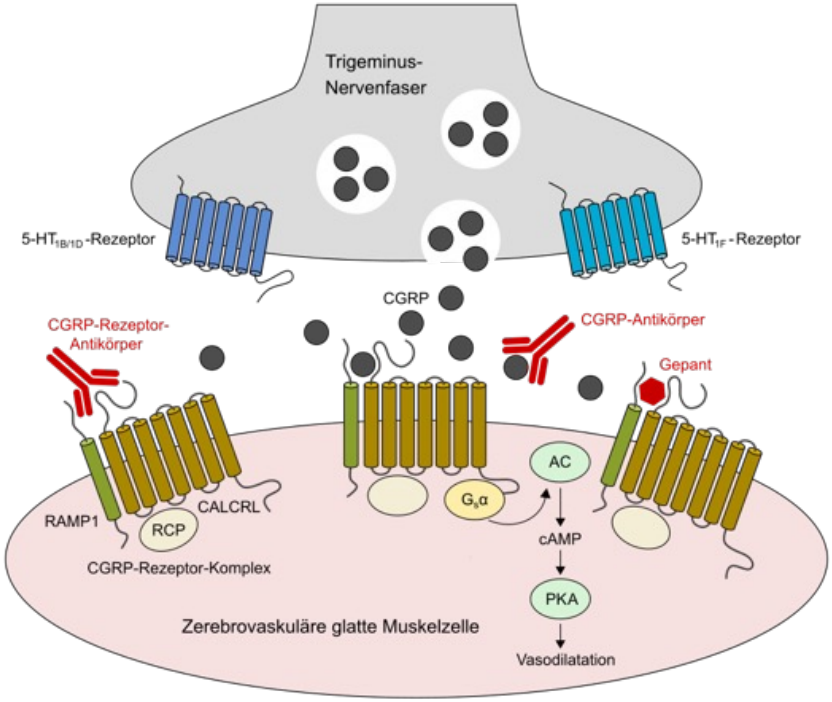

Fremanezumab in Children and Adolescents with Episodic Migraine

Fremanezumab, a humanized monoclonal antibody that selectively targets calcitonin gene–related peptide, is approved for the prevention of migraine in adults. Evidence from randomized, controlled trials in children and adolescents is needed.

We randomly assigned participants 6 to 17 years of age with a diagnosis of episodic migraine (defined as migraine for ≥6 months and a history of ≤14 headache days per month) to receive monthly subcutaneous injections of fremanezumab (120 mg for participants with a body weight of <45 kg and 225 mg for those with a body weight of ≥45 kg) or matched placebo for 3 months. Participants were allowed to use migraine-specific medications to treat acute headaches. The primary end point was the change from baseline in the average number of migraine days per month. Key secondary end points included the change in the number of days per month with headache of at least moderate severity and a reduction of 50% or more in the number of migraine days per month.

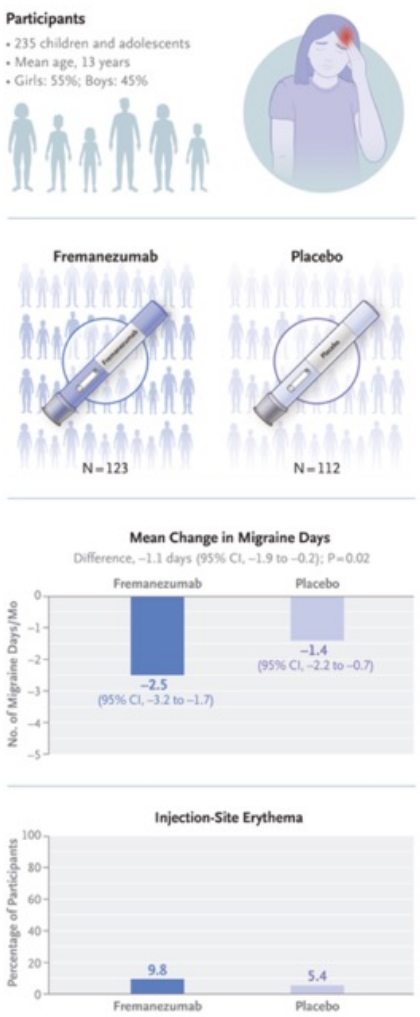

Migraine is a common neurologic disorder in childhood and adolescence, with an estimated overall prevalence of 11%. Children and adolescents with migraine, as well as their families, face a substantial burden due to their attacks, including lost schooling and workdays, poor educational performance, and missed social activities. Although lifestyle modifications and treatment of acute attacks represent the mainstay of migraine management in children and adolescents, current options for preventive treatment have limited efficacy.

Fremanezumab, a humanized monoclonal antibody that selectively targets calcitonin gene–related peptide (CGRP), is approved in adults for the preventive treatment of episodic and chronic migraine in several countries, including the United States, and across Europe, Asia, and South America. Fremanezumab has been shown to significantly reduce headache frequency, use of acute headache medication, and headache-related disability in adults with episodic and chronic migraine.

The potential of monoclonal antibodies that target the CGRP pathway in children and adolescents has been observed in retrospective cohort studies, and although they are recommended by the American Headache Society in certain cases, there is a need for evidence from prospective, randomized, controlled trials in this population. As such, we conducted a phase 3, multicenter, randomized, placebo-controlled trial with a 3-month double-blind period to evaluate the efficacy and safety of fremanezumab in children and adolescents with episodic migraine. The results of the trial have led to Food and Drug Administration approval of the drug for the prevention of episodic migraine in children and adolescents.

Trial Participants

This trial was conducted at 89 sites, 74 of which enrolled at least one participant, in nine countries from August 20, 2020, to March 13, 2024. The trial included participants 6 to 17 years of age with a diagnosis of episodic migraine (defined as migraine for ≥6 months and a history of ≤14 headache days per month), with or without aura (consistent with the International Classification of Headache Disorders, 3rd edition). Participants had to have at least 4 headache days per month in each of the 3 months before screening. Up to 30% of participants using a stable dose of no more than two concomitant migraine-preventive medications for at least 2 months before screening could be included.

Trial Design

This multicenter, parallel-group, randomized, placebo-controlled trial consisted of a 28-day baseline period and a 3-month double-blind period. During the baseline period, participants were required to maintain a headache diary with data entry on at least 21 days and were permitted to use acute migraine medication, except for those containing opioids or barbiturates, and migraine-preventive medications that had been taken at a stable dose for at least 2 months before screening.

Primary and Key Secondary End Points

The primary end point was the least-squares mean change from baseline in the average number of migraine days per month during the 3-month double-blind period. A migraine day was defined as a calendar day (00:00 to 23:59) in which the participant reported any of the following three events: at least 2 consecutive hours of headache that was accompanied by at least two migraine symptoms.

Characteristic	Fremanezumab (N=123)	Placebo (N=112)
Age		
Mean — yr	13.3±2.7	13.4±3.0
Distribution — no. (%)		
6–11 yr	32 (26)	32 (29)
12–17 yr	91 (74)	80 (71)
Female sex — no. (%)	66 (54)	64 (57)
Race — no. (%)†		
White	96 (78)	84 (75)
Nonwhite	9 (7)	7 (6)
Unknown or not reported‡	18 (15)	21 (19)
Weight		
Mean — kg	52.6±15.5	52.1±15.8
Distribution — no. (%)		
<45 kg	36 (29)	33 (29)
≥45 kg	87 (71)	79 (71)
Body-mass index§	20.50±3.98	20.57±3.88
Time since initial migraine diagnosis — yr	4.4±3.0	4.4±3.1
Migraine with aura — no. (%)	41 (33)	30 (27)
Migraine days per month	7.8±3.1	7.5±2.8
Days per month with headache of at least moderate severity	8.2±3.1	7.9±2.8
Days per month in which acute headache medication was used	5.8±3.6	5.6±3.4
PedMIDAS total score¶	44.4±26.5	46.5±43.6
Child-reported PedsQL total score‖	72.0±13.1	72.7±13.7

Primary and Ranked Secondary End Points.

End Point	Fremanezumab (N=123)	Placebo (N=111)	Difference	P Value
Primary end point				
LS mean change from baseline in average number of migraine days per month during the 3-month double-blind period (95% CI)	−2.5 (−3.2 to −1.7)	−1.4 (−2.2 to −0.7)	−1.1 (−1.9 to −0.2)	0.02
Secondary end points				
LS mean change from baseline in average number of days per month with headache of at least moderate severity during the 3-month double-blind period (95% CI)	−2.6 (−3.4 to −1.8)	−1.5 (−2.3 to −0.7)	−1.1 (−2.1 to −0.2)	0.02
Reduction of ≥50% in number of migraine days per month during the 3-month double-blind period — % of participants	47.2	27.0	20.1	0.002
LS mean change from baseline in average number of days per month in which acute headache medication was used during the 3-month double-blind period (95% CI)	−2.1 (−2.6 to −1.5)	−1.0 (−1.6 to −0.4)	−1.1 (−1.8 to −0.4)	0.002
LS mean change from baseline in PedMIDAS total score at month 3 (95% CI)	−21.6 (−28.1 to −15.1)	−15.3 (−22.0 to −8.7)	−6.3 (−13.7 to 1.2)	0.10†
LS mean change from baseline in PedsQL total score at month 3 (95% CI)	5.7 (3.1 to 8.3)	6.2 (3.5 to 8.9)	−0.5 (−3.5 to 2.5)	

Adverse Events According to Trial Group.

Event	Fremanezumab, 120 mg (N=36)	Fremanezumab, 225 mg (N=87)	All Fremanezumab (N=123)	Placebo (N=112)
	number of participants (percent)			
Any adverse event	20 (56)	48 (55)	68 (55)	55 (49)
Adverse event related to fremanezumab or placebo†	6 (17)	17 (20)	23 (19)	21 (19)
Severe adverse event	2 (6)	2 (2)	4 (3)	4 (4)
Serious adverse event	1 (3)	1 (1)	2 (2)	3 (3)
Blood and lymphatic system disorders	0	0	0	1 (<1)
Immune thrombocytopenia	0	0	0	1 (<1)
Infections and infestations	0	1 (1)	1 (<1)	0
Hepatitis infectious mononucleosis	0	1 (1)	1 (<1)	0
Nervous system disorders	1 (3)	0	1 (<1)	2 (2)
Migraine	1 (3)	0	1 (<1)	1 (<1)
Hemiparesis	0	0	0	1 (<1)
Adverse event leading to discontinuation of participation in the trial‡	1 (3)	0	1 (<1)	0
Adverse event leading to death	0	0	0	0
Adverse events occurring in ≥5% of participants in any group				
General disorders and administration-site conditions	5 (14)	21 (24)	26 (21)	21 (19)
Injection-site erythema	1 (3)	11 (13)	12 (10)	6 (5)
Injection-site pain	0	6 (7)	6 (5)	6 (5)
Injection-site swelling	1 (3)	5 (6)	6 (5)	1 (<1)
Pyrexia	0	4 (5)	4 (3)	1 (<1)
Vaccination-site pain§	2 (6)	0	2 (2)	1 (<1)
Infections and infestations	9 (25)	24 (28)	33 (27)	31 (28)
Nasopharyngitis	3 (8)	8 (9)	11 (9)	8 (7)
Covid-19	2 (6)	5 (6)	7 (6)	6 (5)
Upper respiratory tract infection	2 (6)	4 (5)	6 (5)	5 (4)
Gastroenteritis	0	4 (5)	4 (3)	1 (<1)
Nervous system disorders	3 (8)	6 (7)	9 (7)	6 (5)
Dizziness	0	5 (6)	5 (4)	0
Headache	2 (6)	0	2 (2)	2 (2)

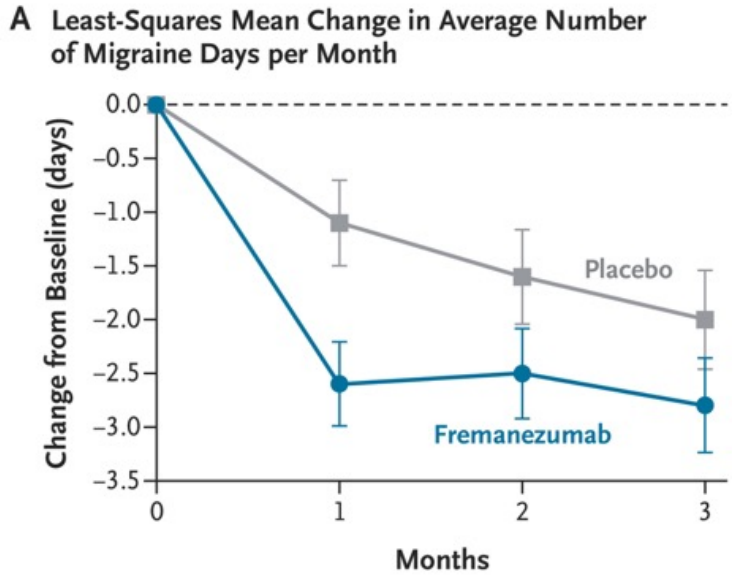

Change in Migraine Days per Month and Reduction of 50% or More in Migraine Days per Month.

Least-squares means (±SE) are shown from a mixed-effects model for repeated measures.

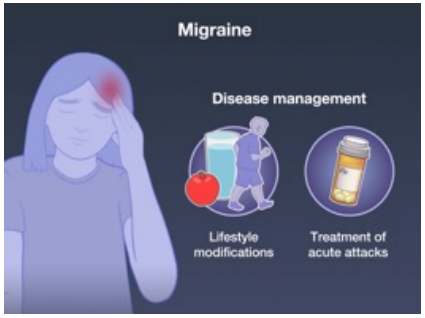
Migraine
Disease management
Lifestyle modifications
Treatment of acute attacks

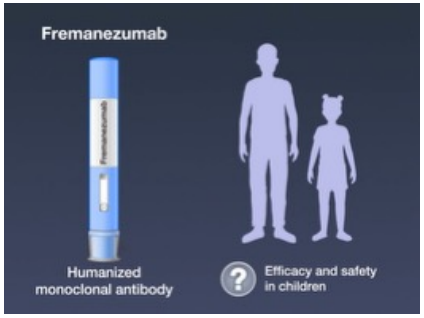
Fremanezumab
Humanized monoclonal antibody
Efficacy and safety in children

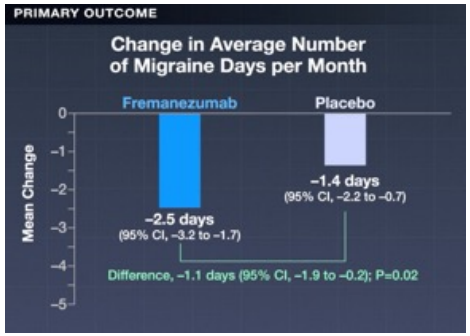
PRIMARY OUTCOME
Change in Average Number of Migraine Days per Month
Fremanezumab
Placebo
Mean Change
0
−1
−2
−3
−4
−5
−2.5 days
(95% CI, −3.2 to −1.7)
−1.4 days
(95% CI, −2.2 to −0.7)
Difference, −1.1 days (95% CI, −1.9 to −0.2); P=0.02

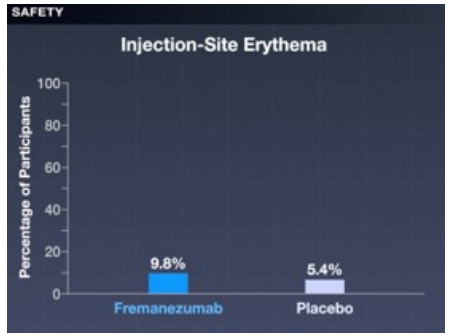
SAFETY
Injection-Site Erythema
Percentage of Participants
100
80
60
40
20
0
9.8%
5.4%
Fremanezumab
Placebo


Migraine
Current preventive treatments have limited efficacy


Trial
• 235 Children and adolescents
• 6 to 17 years of age
• Diagnosis of migraine
• With or without aura
• 4 to 14 headache days in each of the previous 3 months

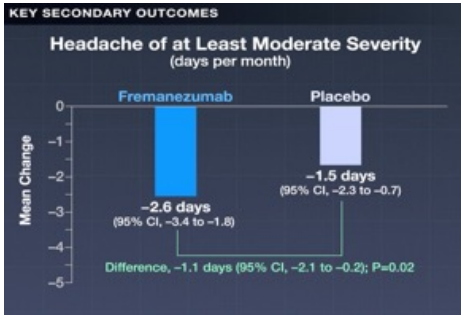
KEY SECONDARY OUTCOMES
Headache of at Least Moderate Severity
(days per month)
Fremanezumab
Placebo
Mean Change
0
−1
−2
−3
−4
−5
−2.6 days
(95% CI, −3.4 to −1.8)
−1.5 days
(95% CI, −2.3 to −0.7)
Difference, −1.1 days (95% CI, −2.1 to −0.2); P=0.02

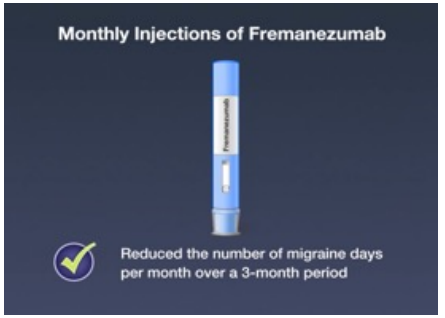
Monthly Injections of Fremanezumab
Reduced the number of migraine days per month over a 3-month period

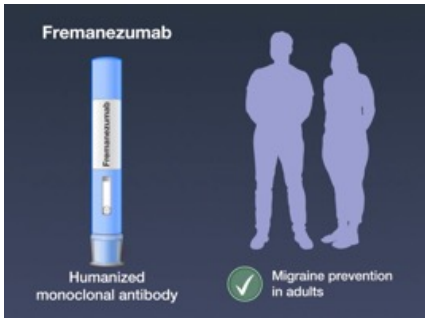
Fremanezumab
Humanized monoclonal antibody
Migraine prevention in adults

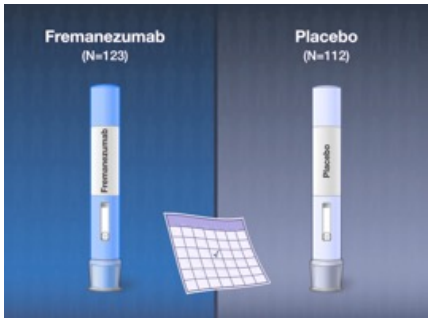
Fremanezumab
(N=123)
Placebo
(N=112)

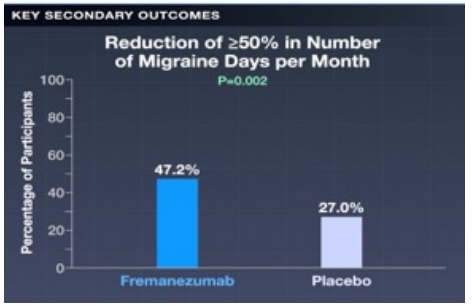
KEY SECONDARY OUTCOMES
Reduction of ≥50% in Number of Migraine Days per Month
P=0.002
Percentage of Participants
100
80
60
40
20
0
47.2%
27.0%
Fremanezumab
Placebo

Autoimmune Hemolytic Anemia (AIHA) is a rare blood disorder where the immune system mistakenly creates antibodies that attack and destroy the body's own red blood cells (RBCs), drastically shortening their lifespan and causing anemia, leading to fatigue, shortness of breath, pale skin, rapid heart rate, jaundice, and dark urine. AIHA can be primary (idiopathic) or secondary to other conditions like autoimmune diseases (lupus) or cancers (lymphoma, leukemia), with common types including warm AIHA and cold agglutinin disease, managed with corticosteroids, immunosuppressants, or other therapies.

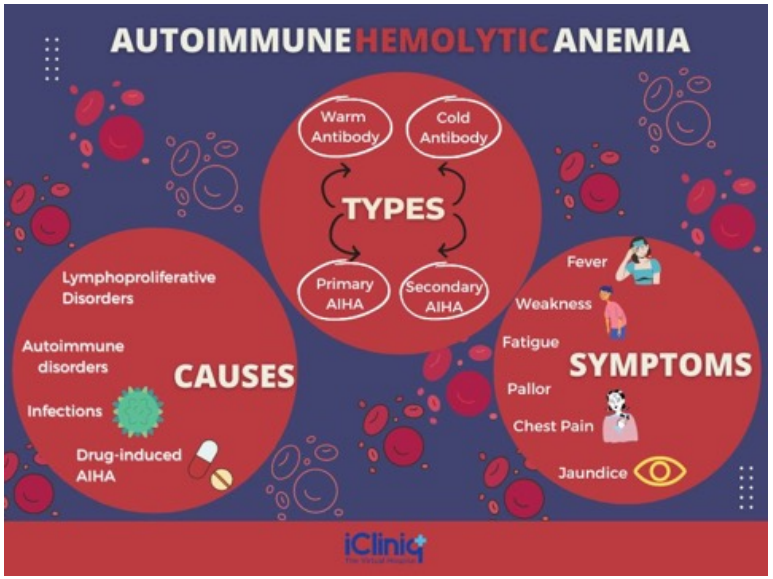

Symptoms

- **Fatigue & Weakness:** Due to lack of oxygen-carrying red blood cells.
- **Pale or Jaundiced Skin:** Yellowish tint from red blood cell breakdown.
- **Shortness of Breath & Rapid Heart Rate:** The body tries to compensate for low RBCs.
- **Fever & Chills**.
- **Dark Urine & Enlarged Spleen**.
- **Cold Sensitivity:** Especially in cold agglutinin disease, causing painful bluish fingers/toes.

Causes & Triggers

- **Autoimmune Diseases:** Lupus, rheumatoid arthritis, Hashimoto's thyroiditis.
- **Cancers:** Chronic lymphocytic leukemia (CLL), lymphoma.
- **Infections:** Epstein-Barr virus (EBV).
- **Medications:** Certain antibiotics, NSAIDs.
- **Primary/Idiopathic:** No underlying cause identified.

CD19 CAR T-cells are a type of immunotherapy where a patient's T-cells are genetically engineered to recognize and attack cancer cells (or autoreactive B-cells) that express the CD19 protein, leading to remarkable success in treating B-cell leukemias, lymphomas, and even some autoimmune diseases, by eliminating these malignant or problematic B-cells and inducing long-lasting remissions. This powerful therapy works by giving T-cells a synthetic receptor (CAR) that links antibody-like binding to the CD19 antigen with T-cell activation signals, clearing the target cells and sometimes causing side effects like cytokine release syndrome (CRS) and neurological issues.

Autogenic CAR T cells

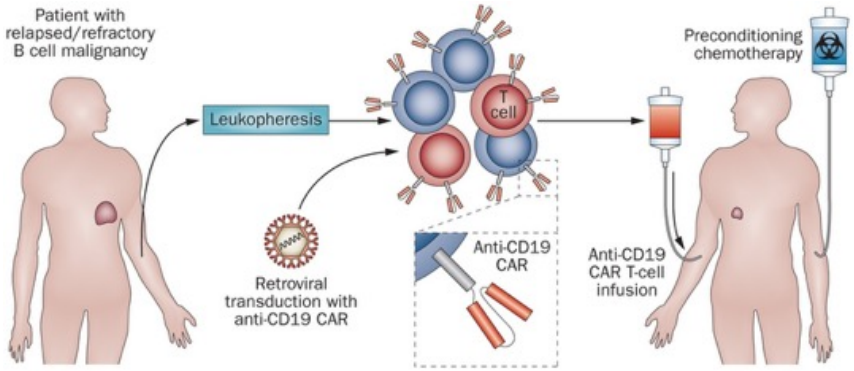

Antibody-producing cells

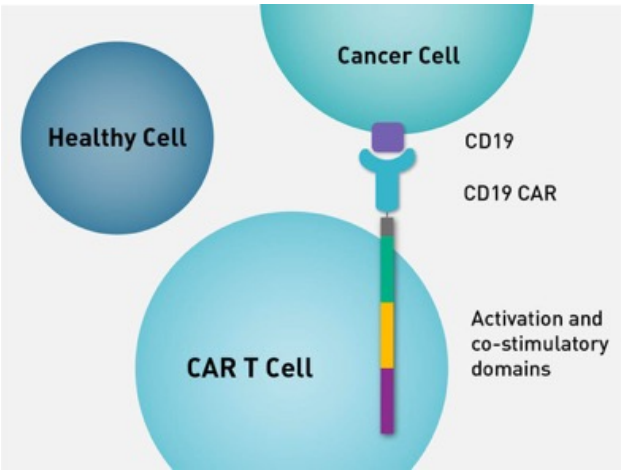

How it Works

1.T-Cell Collection: A patient's T-cells are drawn from their blood.
2.Genetic Engineering: These T-cells are modified in a lab to express Chimeric Antigen Receptors (CARs) that target CD19.
3.Expansion: The modified CAR T-cells are grown in large numbers.
4.Infusion: The engineered CAR T-cells are infused back into the patient.
5.Targeting: The CAR T-cells find and kill any B-cells (including cancer cells) expressing CD19.

CD19 CAR T-Cell Therapy for Autoimmune Hemolytic Anemia

Background

In patients with autoimmune hemolytic anemia (AIHA), the risk of relapse is high owing to persistent autoreactive B-cell activity. Multirefractory AIHA is a more advanced stage of disease that is defined by a lack of response to at least three lines of therapy. CD19-directed chimeric antigen receptor (CAR) T-cell therapy results in profound B-cell depletion and may be a useful approach to achieving drug-free remission in multirefractory AIHA.

Methods

We enrolled patients from a compassionate-use program and those from a phase 1 study who had primary multirefractory AIHA. Each patient received a single infusion of autologous CD19 CAR T cells. The primary objective was to assess the safety profile — the incidence, characteristics, and severity of adverse events, including cytokine-release syndrome and immune effector cell–associated neurotoxicity syndrome. Secondary objectives included efficacy and pharmacokinetic features. A complete response was defined by resolution of symptoms, an increased hemoglobin level, and normalization of hemolysis markers. B-cell reconstitution and the origin of relapse were analyzed with flow cytometry, single-cell RNA sequencing, and paired B-cell receptor sequencing.

Conclusions

CD19 CAR T-cell therapy had expected toxic effects and resulted in sustained remission in patients with multirefractory AIHA.

Autoimmune hemolytic anemia (AIHA), a complex disorder mediated by autoantibodies against red cells, leads to the accelerated destruction of red cells and severe anemia. The annual incidence of AIHA is 18 to 24 cases per million persons worldwide. AIHA is classified as warm, cold (including cold agglutinin disease), or mixed on the basis of isotype and the temperature at which the autoantibodies are most reactive. AIHA in patients with immune thrombocytopenia or autoimmune neutropenia is referred to as Evans's syndrome. Despite the distinct clinical subtypes, all forms of AIHA involve autoantibodies mediated by autoreactive B cells or plasma cells. Although AIHA is considered to be benign, all-cause mortality among patients with the condition is 5 to 9 times that in the general population, depending on the AIHA subtype and geographic region.

Earlier studies of AIHA included patients with refractory AIHA, which usually involves only one or two treatment failures. In this study, we assessed the safety and efficacy of CD19 CAR T-cell therapy in patients with multirefractory AIHA, a more advanced stage of disease that is defined by a lack of response to at least three lines of therapy. We also investigated the underlying mechanisms of multirefractory AIHA relapse after CAR T-cell therapy.

Patients and Study Design

From September 2023 through October 2024, patients with multirefractory AIHA who were participating in a compassionate-use program or a phase 1 study were screened and enrolled. Eligibility criteria were a diagnosis of primary AIHA, including warm, cold, or mixed AIHA or Evans's syndrome; receipt of at least three previous lines of therapy that had failed to result in long-term control; a hemoglobin level of less than 10 g per deciliter at screening; a score of 2 or less on the Eastern Cooperative Oncology Group performance-status scale (range, 0 to 5, with higher scores reflecting greater disability); and adequate organ function, including liver and pulmonary function. Among the exclusion criteria were a diagnosis of a lymphoproliferative disorder, secondary AIHA caused by medication or infection, an inadequate washout period for previous medications, previous organ transplantation or hematopoietic stem-cell transplantation, and the presence of hereditary hemolytic anemia or other acquired hemolytic disorders.

Objectives

The primary objective was to assess the safety profile — the incidence, characteristics, and severity of adverse events, including cytokine-release syndrome and immune effector cell–associated neurotoxicity syndrome (ICANS). Secondary objectives included preliminary efficacy and pharmacokinetic features. Efficacy was independently assessed by senior specialists at the hospital. Response categories included complete response, hematologic complete response with compensated hemolysis, partial response, overall response, and no response.

Variable	Compassionate-Use Program					Phase 1 Clinical Study						Overall
						Dose Level 1			Dose Level 2			Median (IQR)
	Patient 1	*Patient 2*	*Patient 3*	*Patient 4*	*Patient 5*	*Patient 6*	*Patient 7*	*Patient 8*	*Patient 9*	*Patient 10*	*Patient 11*	
Demographic characteristics												
Age — yr	57	9	48	10	22	46	53	50	35	47	64	47 (22–53)
Sex	M	F	F	F	F	F	M	F	F	F	F	—
Primary AIHA subtype†	Cold	Evans's syndrome	Warm	Warm	Mixed	Warm	Warm	Warm	Evans's syndrome	Warm	Warm	—
Disease duration — mo	81	98	76	25	157	7	7	59	224	15	71	71 (15–98)
Follow-up duration — mo	21.9	7.3	19.5	18.1	8.5	15.0	13.5	12.2	10.7	9.8	8.7	12.2 (8.7–18.1)
Laboratory testing												
Hemoglobin level — g/dl	5.6	6.4	7.3	6.1	6.0	6.1	8.6	7.4	5.7	9.3	8.1	6.4 (6.0–8.1)
Reticulocyte count — no./μl	1328×10^2	6287×10^2	5525×10^2	7816×10^2	1698×10^2	7810×10^2	4592×10^2	4888×10^2	8785×10^2	976×10^2	3772×10^2	4888×10^2 (1698×10^2–7810×10^2)
Platelet count — no./liter	197.5×10^9	266×10^9	225×10^9	142×10^9	835.5×10^9	125.5×10^9	144.5×10^9	348.5×10^9	134×10^9	135×10^9	258×10^9	197.5×10^9 (135×10^9–266×10^9)
Neutrophil count — no./μl	2830	7980	4470	3450	2170	6260	5380	4200	4950	340	4530	4470 (2830–5380)
B-cell count — no./μl	51	612	20	157	73	33	0	330	0	0	27	33 (0–157)
LDH level — U/liter	316.8	639.4	661.7	458.1	254.6	826.9	336.3	330.3	771.9	205.3	406.9	406.9 (316.8–661.7)
Unconjugated bilirubin level — μmol/liter	78.3	127.5	50.2	142.4	67.1	122.0	54.4	42.3	76.1	15.2	51.8	67.1 (50.2–122.0)
Plasma-free hemoglobin level — mg/liter	398.4	297.7	357.2	369.5	42.5	146.3	240.3	246	508.8	76.3	69.2	246 (76.3–369.5)
Haptoglobin level — g/liter	<0.07	<0.07	<0.07	<0.08	<0.08	<0.06	<0.06	<0.06	<0.06	0.49	<0.07	—
Positive direct antiglobulin test	Yes	Yes	Yes	Yes	Yes	Yes	Yes	Yes	Yes	Yes	Yes	—
Cold agglutinin titer‡	1:1024	1:32	1:4	1:4	1:1024	1:4	1:16	1:4	1:8	1:16	1:8	1:8 (1:4–1:32)
Positive monoclonal protein test§	Yes	No	No	No	No	No	No	No	No	No	No	—
Other positive tests¶	Yes	No	No	No	No	No	No	No	No	No	No	—
Positive monospecific direct antiglobulin test‖	Yes	Yes	Yes	Yes	Yes	Yes	Yes	Yes	Yes	Yes	Yes	—
Organ involvement												
Splenomegaly**	Yes (stage III)	Yes (stage II)	Yes (stage I)	Yes (stage III)	NE	Yes (stage II)	Yes (stage II)	No	Yes (stage II)	Yes (stage II)	No	—
Hepatomegaly	Yes	No	No	No	No	No	No	No	No	No	Yes	—
Thromboembolic event	Yes	No	No	No	No	No	Yes	No	No	Yes	No	—

Summary of Adverse Events.

Adverse Event	Total (N=11)
Overall — no. of events	67
Grade ≥1 adverse events — no. of patients (%)	11 (100)
Event of special interest	
Overall — no. of events	37
Grade ≥3 adverse events — no. of patients (%)	
Infection	2 (18)
CRS*	0
ICANS*	0
Low IgG level†	1 (9)
Early ICAHT‡	0
Late ICAHT‡	1 (9)
Treatment discontinuation because of adverse event — no. of patients (%)	0

Adverse Events According to Patient.

Adverse Event	Compassionate-Use Program					Phase 1 Study					
						Dose Level 1			Dose Level 2		
	Patient 1	*Patient 2*	*Patient 3*	*Patient 4*	*Patient 5*	*Patient 6*	*Patient 7*	*Patient 8*	*Patient 9*	*Patient 10*	*Patient 11*
CRS	Yes (grade 1)	Yes (grade 2)	No	Yes (grade 1)	Yes (grade 1)	No	Yes (grade 1)	Yes (grade 1)	Yes (grade 1)	Yes (grade 1)	Yes (grade 1)
ICANS	Yes (grade 1)	No	No	No	No	No	No	No	No	No	No
Event resulting in tocilizumab use	No	No	No	No	No	No	No	No	No	No	No
Event resulting in glucocorticoid use	Yes	No	No	No	No	No	No	No	No	No	Yes
Early ICAHT	No	Yes (grade 2)	No	Yes (grade 1)	No	Yes (grade 1)	No	No	Yes (grade 1)	Yes (grade 1)	Yes (grade 1)
Late ICAHT	Yes (grade 1)	No	No	No	No	No	No	No	No	Yes (grade 3)	No
Early low IgG level*	No	Yes (grade 2)	No	Yes (grade 2)	No	No	No	No	No	No	No
Late low IgG level*	Yes (grade 1)	Yes (grade 3)	No	Yes (grade 2)	No	No	No	No	Yes (grade 1)	No	No
Thromboembolism†	Yes (grade 2)	No	No	No	No	No	No	No	No	No	No
Infection‡											
At <3 mo	Yes	No	Yes	No	No	No	Yes	No	No	No	No
At 3 to <6 mo	No	Yes	Yes	Yes	No	No	No	Yes	No	No	No
At 6 to <12 mo	No	Yes	Yes	No	—	No	No	Yes	Yes	—	—
At ≥12 mo	Yes	—	No	No	—	No	No	No	—	—	—

Cytpkine release syndrome (CRS)

Immune effector cell–associated neurotoxicity syndrome (ICANS).

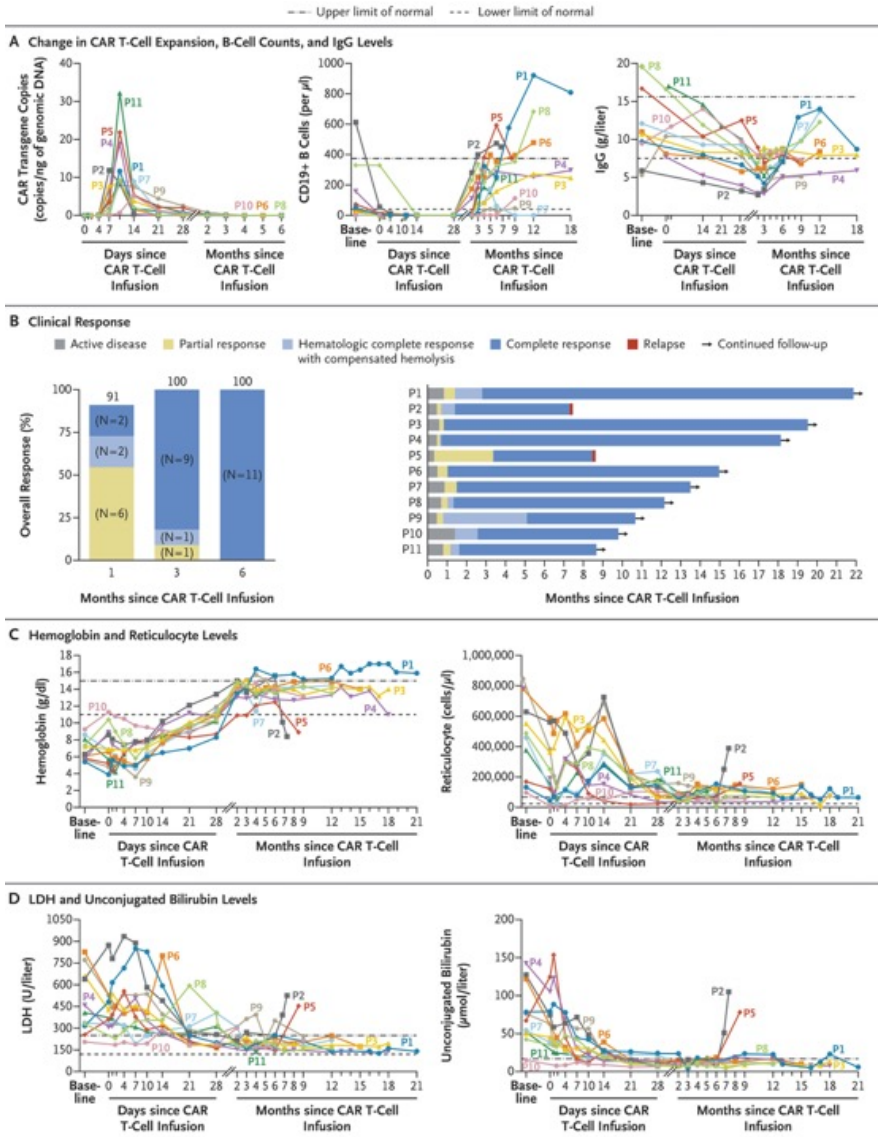

Clinical Efficacy.

Chimeric antigen receptor (CAR) T-cell expansion, B-cell counts, and IgG levels at baseline and after CD19 CAR T-cell infusion in 11 patients (P1 through P11) with multirefractory autoimmune hemolytic anemia (AIHA) are shown in Panel A. The overall response at 1, 3, and 6 months after infusion (left) and a swimmer plot showing the clinical response and follow-up duration for each patient (right) are shown in Panel B. A complete response was defined by the resolution of symptoms, a hemoglobin level of at least 110 g per liter in female patients or at least 120 g per liter in male patients, and normalization of hemolysis markers, including bilirubin and lactate dehydrogenase (LDH) levels; the absence of clonal B cells and IgM was also needed in patients with cold AIHA. A hematologic complete response with compensated hemolysis was defined by the same hemoglobin thresholds as those in the definition of complete response, with partial but not full normalization of hemolysis markers. A partial response was defined by a hemoglobin level of at least 100 g per liter or a level that had increased by at least 20 g per liter from baseline, plus a transfusion-free period of at least 7 days. Patients 2 and 5 had relapse at 7.3 and 8.5 months, respectively. Relapse was defined by the recurrence of hemolysis, as characterized by worsening symptomatic anemia (a hemoglobin level of <100 g per liter or a level that had decreased by at least 20 g per liter), plus the need for additional drug therapy, red-cell transfusion, or both, after a response. Also shown are hemoglobin and reticulocyte levels (Panel C) and LDH and unconjugated bilirubin levels (Panel D) at baseline and after the receipt of CD19 CAR T-cell therapy. Patients 1 through 5 were in a compassionate-use program and received CAR T cells at a single dose of 1.0×10^6 per kilogram of body weight. Patients 6 through 11 were in a phase 1 study and received CAR T cells at a single dose of 0.5×10^6 (Patients 6, 7, and 8) or 1.0×10^6 (Patients 9, 10, and 11) per kilogram.

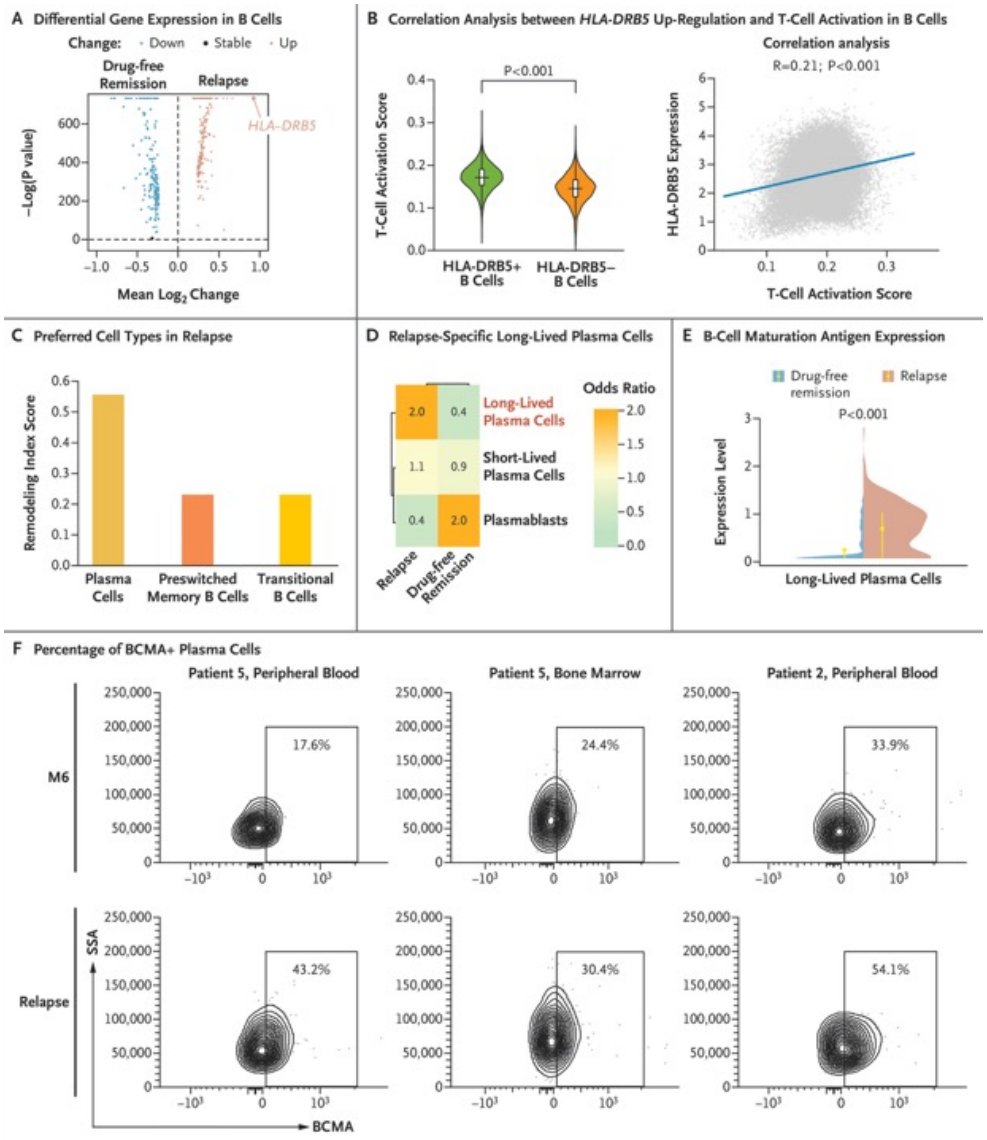

Cellular and Molecular Mechanisms of Relapse.

A volcano plot of differential gene expression between patients with drug-free remission and those with relapse after the receipt of CAR T-cell therapy is shown in Panel A. The change indicates the ratio of gene expression in patients with drug-free remission to gene expression in patients with relapse. *HLA-DRB5* is a major histocompatibility complex class II gene. A violin plot of the T-cell activation score among HLA-DRB5+ B cells and HLA-DRB5− B cells (left) and correlation analysis of HLA-DRB5 expression and T-cell activation scores among B cells (right) are shown in Panel B. The green and orange regions indicate the distribution density, the horizontal lines the mean, the top and bottom of the boxes the interquartile range, and the top and bottom of the vertical lines the maximum and minimum, respectively. T-cell activation was assessed with the Seurat module function, which is used to calculate T-cell activation scores on the basis of a prespecified group of T-cell–activation genes; higher scores indicate higher aggregate expression of genes associated with T-cell activation. The significance of the correlation was assessed with the Pearson correlation test. In Panel C, the B-cell subpopulations with the top three remodeling index scores are indicated. The remodeling index quantifies compositional changes in the B-cell population, with higher scores indicating greater remodeling during relapse. Also shown is a heatmap of the odds ratio of plasma-cell subsets (in Panel D) and a violin plot of the expression level of B-cell maturation antigen (BCMA) in long-lived plasma cells (in Panel E) for patients with relapse and those with drug-free remission. The blue and pink shaded regions indicate the distribution density. The significance of the between-group difference in expression levels was assessed with the Wilcoxon rank-sum test. Changes in total BCMA+ plasma cell (BCMA+CD38+CD138+) subsets in peripheral blood and bone marrow are shown in Panel F for the two patients with relapse after CD19 CAR T-cell therapy. SSA denotes side scatter.

Discussion

In this study, clinical evaluation of CD19-targeted CAR T-cell therapy in patients with multirefractory AIHA showed no unexpected safety signals and rapid remission, including prolonged remission in many of the patients. All 11 patients had a complete response, discontinued immunosuppressive therapy, and had apparent improvements in quality of life. Multirefractory AIHA is typically associated with life-threatening anemia, thromboembolic complications, and markedly reduced quality of life. The median baseline score on the FACIT-Fatigue scale was 34.0 in the current study, which is similar to scores in patients with advanced cancer. CAR T-cell therapy appeared to alleviate these symptoms and improve quality of life, with mild cytokine-release syndrome in 9 patients, ICANS of grade 1 in 1 patient, and no persistent hematologic toxic effects. A total of 15 infections were recorded, 80% of which were grade 1 or 2 in severity, with no infections of grade 4 resulting in hospitalization.

Our results highlight CD19-targeted CAR T-cell therapy as a promising strategy for inducing rapid remission in patients with multirefractory AIHA. Although these early findings are encouraging, additional clinical trials are necessary to confirm these findings and refine treatment strategies.

Sudden Cardiac Arrest in Athletes

Summary

The incidence of sudden cardiac arrest in athletes varies according to age, race and ethnic group, sex, sport, and social determinants of health. The common causes of sudden cardiac arrest include cardiomyopathies, electrical disorders, coronary-artery anomalies, and other cardiac structural abnormalities. There has not been an increase in the incidence of sudden cardiac arrest in athletes during the time frame of the coronavirus disease 2019 (Covid-19) pandemic. Primary prevention is based on cardiovascular screening before participation, and secondary prevention on implementation of emergency action plans. Diagnostic evaluation of athletes who survive sudden cardiac arrest should mirror that of age-matched nonathletes, with additional sport-specific considerations, and should be performed by medical professionals with expertise in the interpretation of test results in the context of athletic adaptation. An increasing body of evidence indicates that many athletes can return to play after disease-specific treatment, without an increase in risk, and professional societies now consider return to participation in sports to be reasonable or appropriate through shared decision making for numerous cardiac conditions.

Incidence of cardiac arrest with/without death

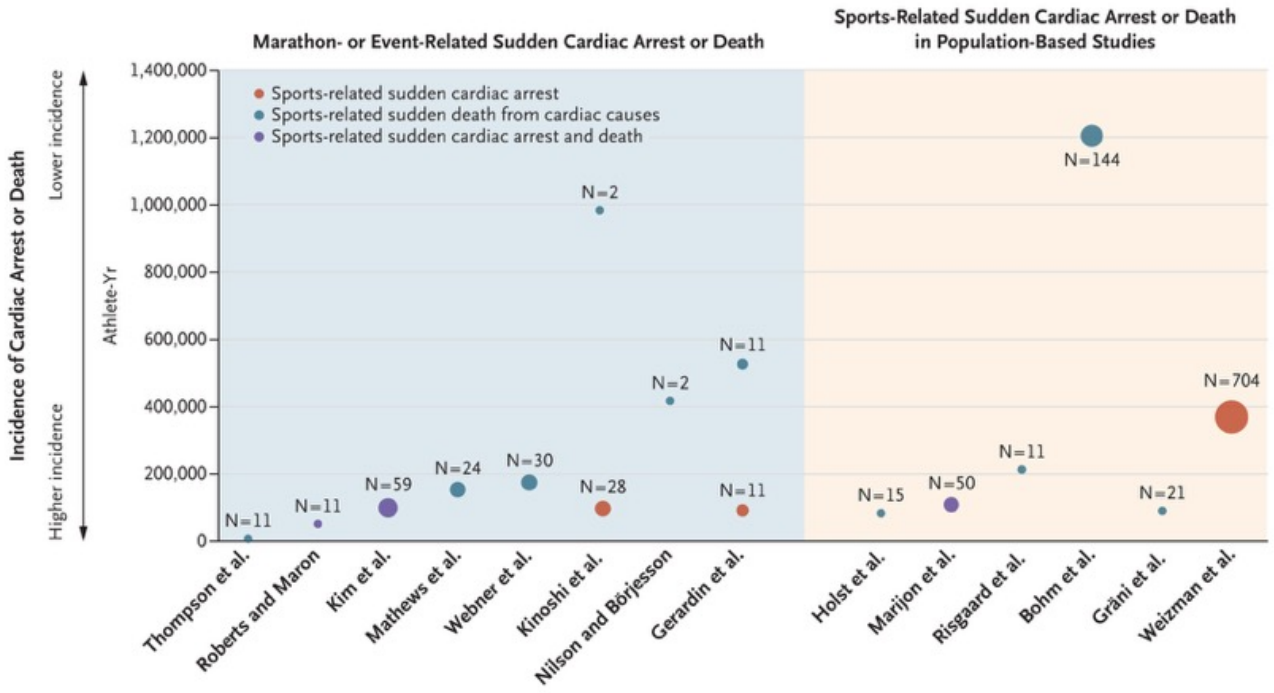

Incidence of Sports-Related Sudden Cardiac Arrest or Death.

The y axis shows the incidence of sudden cardiac arrest or sudden death from cardiac causes as 1 case in 200,000 to 1,400,000 athlete-years, with the highest incidence shown at the bottom of the axis. Numbers of cases reported in studies by Bohm et al.,[2] Gerardin et al.,[3] Gräni et al.,[4] Holst et al.,[5] Kim et al.,[6] Kinoshi et al.,[7] Marijon et al.,[8] Mathews et al.,[9] Nilson and Börjesson,[10] Risgaard et al.,[11] Roberts and Maron,[12] Thompson et al.,[13] Webner et al.,[14] and Weizman et al.[15] are shown, with larger circles indicating higher numbers of cases. The incidence from the study by Weizman et al. (largest circle) includes data from men only.

KEY POINTS

Sudden Cardiac Arrest in Athletes

- The incidence of sudden cardiac arrest in athletes varies according to age, race and ethnic group, sex, social determinants, and sport.
- Causes of sudden cardiac arrest include cardiomyopathies, electrical disease, coronary-artery anomalies, and other structural abnormalities. The incidence of sudden cardiac arrest in college athletes has not increased during the time frame of the coronavirus disease 2019 (Covid-19) pandemic.
- Prevention strategies include both screening for cardiovascular disease before participation in the sport and emergency action planning.
- Diagnostic evaluation of athletes who survive sudden cardiac arrest should follow that for nonathletes in the same age group, but with attention to sport-specific causes, and should be performed by medical professionals with expertise in the interpretation of test results in the context of athletic adaptation.
- Accumulating data indicate that many athletes who survive sudden cardiac arrest can return to sports without excess risk after undergoing appropriate disease-specific treatment. For many — although not all — cardiac diseases, professional societies now view a return to play after sudden cardiac arrest as reasonable or something that may be considered, through shared decision making, with emergency action plans and follow-up in place.
- As some athletes who survive sudden cardiac arrest are returning to play, decisions about management of cardiac conditions should take sports participation into account.

Study	Country	Type of Cardiac Arrest or Death	Population	Age Range yr	No. of Cases	HCM %	Idiopathic LVH, Fibrosis, or Cardiomyopathy NOS %	Coronary-Artery Anomalies %	Arrhythmogenic Cardiomyopathy %	DCM %	AN-SUD %	CAD %	Myocarditis-Related %	Aortic Dissection %	Commotio Cordis %	Other %
Corrado et al.	Italy	SDC	Competitive athletes	12–35	46	2	0	13	26	2	2	22	11	2		20
Harmon et al.	U.S.	SDC	High-school athletes	14–18	50	14	26	8	2	0	18	6	14	0	0	12
Thiene et al.	Italy	SDC	Athletes	<40	75	5	0	16	27	0	11	23	4	0	0	15
Egger et al.	Many	SCA/D	Recreational, competitive, and elite soccer players	≤35	104	11	9	13	4	1		14	13	0	7	36
Peterson et al.	U.S.	SCA/D	Athletes	11–29	209	21	13	12	6	3	19	2	4	3	0	16
Finocchiaro et al.	U.K.	SDC	Athletes	18–35	128	3	12	9	8	3	52	1	0	0	5	7
Bohm et al.	Germany, France	EA-SCA/D	Recreational and competitive athletes	18–35	25	8	4	0	0	4	24	20	16	0	0	24
Petek et al.	U.S.	SDC	Competitive athletes	18–26	118	13	17	8	5	2	19	6	7	4	2	17
Total					**755**	**12**	**11**	**10**	**8**	**2**	**20**	**8**	**6**	**1**	**2**	**20**

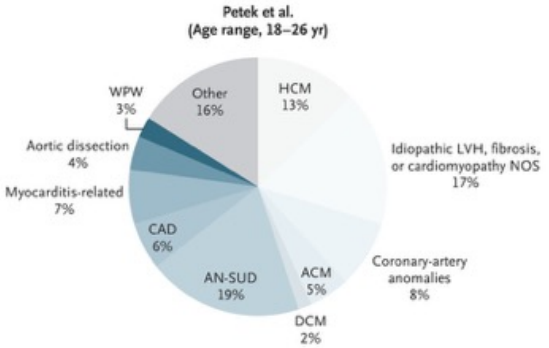

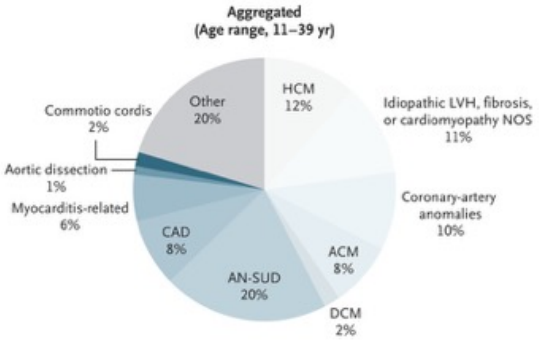

Cardiac Causes of Sudden Death in Athletes.

Only data from studies that included autopsy-negative, sudden, unexplained death (AN-SUD) among possible causes are shown. Data are from Bohm et al.,[36] Corrado et al.,[28] Egger et al.,[37] Finocchiaro et al.,[33] Harmon et al.,[22] Petek et al.,[27] Peterson et al.,[24] and Thiene et al.[38] ACM denotes arrhythmogenic cardiomyopathy, CAD coronary artery disease, DCM dilated cardiomyopathy, EA-SCA/D exercise-associated sudden cardiac arrest or death, HCM hypertrophic cardiomyopathy, LVH left ventricular hypertrophy, NOS not otherwise specified, SCA/D sudden cardiac arrest or death, SDC sudden death from cardiac causes, and WPW the Wolff–Parkinson–White syndrome.

While a normal 12-lead ECG is an excellent indicator of immediate cardiac health, it does not completely rule out the risk of sudden cardiac arrest (SCA). Clinical data indicates that a normal ECG has a very high **negative predictive value (99.4%)** over a 10-year period, meaning the likelihood of an event remains very low for those with normal results.

ECG costs next to nothing and picks up alot

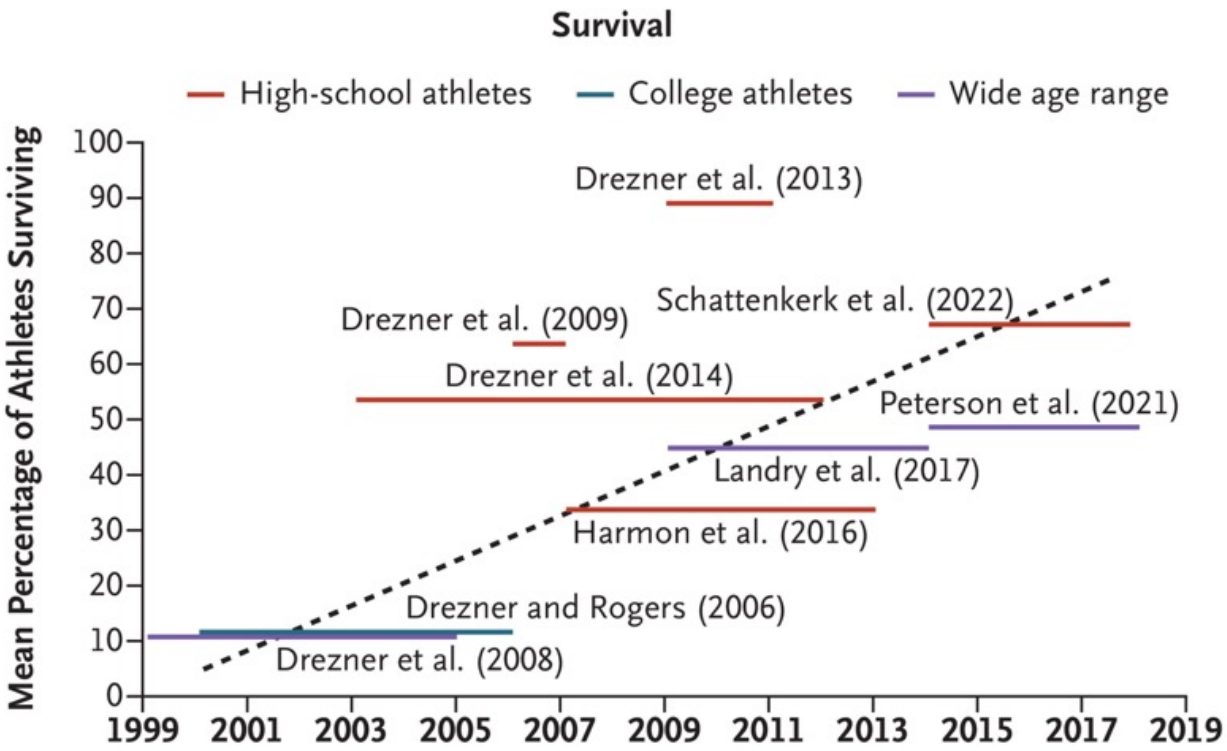

Survival after Sudden Cardiac Arrest in Young, Competitive Athletes in North America.

The horizontal lines represent the time frame of the studies. Data are from Drezner and Rogers,[50] Drezner et al.,[21,51–53] Harmon et al.,[22] Landry et al.,[54] Peterson et al.,[24] and Schattenkerk et al.[31] The dashed line provides a visual representation of the trajectory.

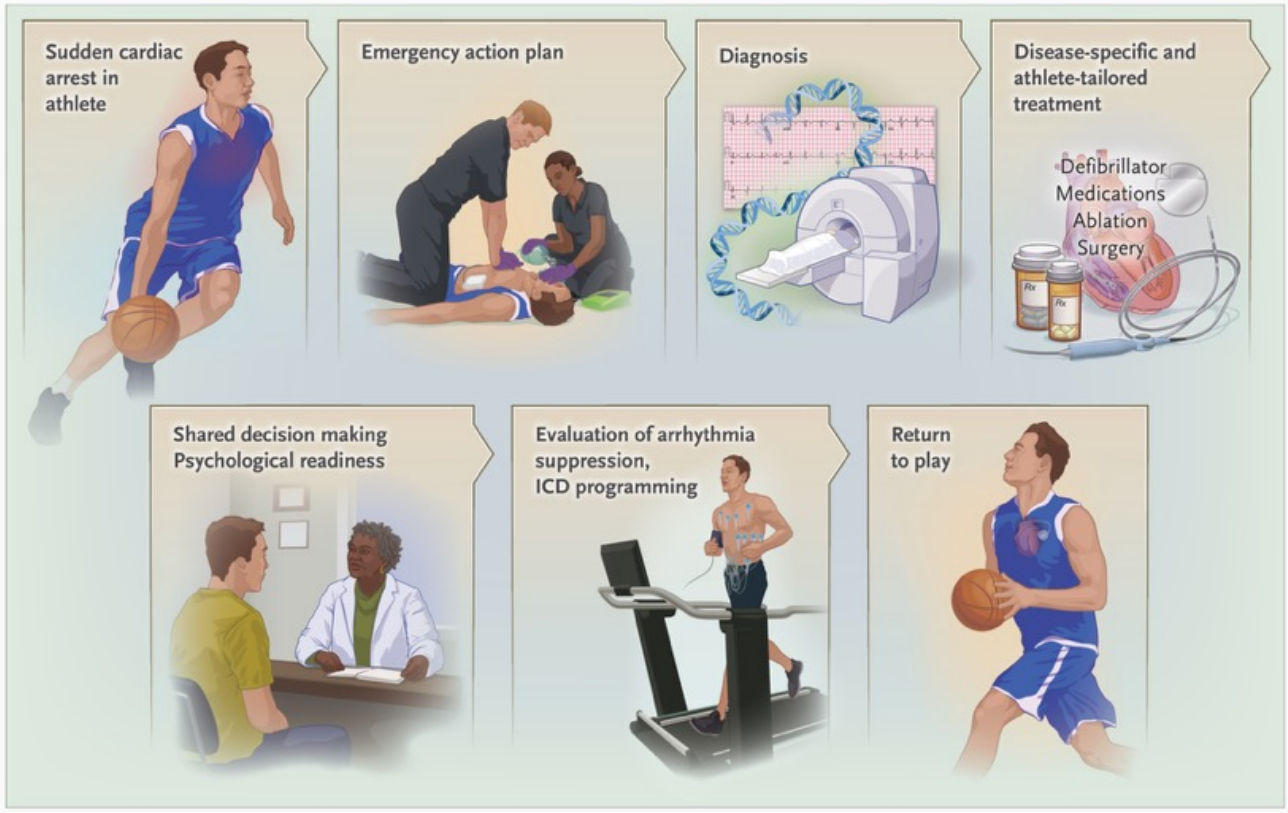

Return to Play for Athletes Who Survive Sudden Cardiac Arrest.

Current statements from professional societies support shared decision making regarding return to play for many athletes who survive sudden cardiac arrest, with factors such as underlying heart disease, the athlete's sport, and the athlete's goals and preferences taken into account.[16,48] ICD denotes implantable cardioverter–defibrillator.

Conclusions and Future Directions

Sudden death from cardiac causes in an athlete is a tragedy that may be preventable by means of screening before participation and emergency action planning. These approaches are complementary — screening will never be 100% sensitive, and emergency action plans will never cover all athletes in all locations. Further research is needed to determine the best screening methods and practices. Research on implementation will continue to enhance processes and protocols for emergency action plans. Advocacy at the state and federal levels to increase AED availability and to provide safer training environments is critical for improving the safety of athletes.

For the athlete who survives sudden cardiac arrest, ongoing research will enhance diagnostic capabilities and tailoring of treatments to prevent recurrence. Ongoing studies such as the Outcomes Registry for Cardiac Conditions in Athletes will continue to expand our understanding of outcomes in athletes with cardiovascular disease who return to play, at all levels of a sport. The overall goal is to prevent sudden cardiac arrest in athletes and, for survivors of cardiac arrest who wish to continue their participation in sports, to facilitate a return to play while minimizing risk.

Granulomatosis with Polyangiitis

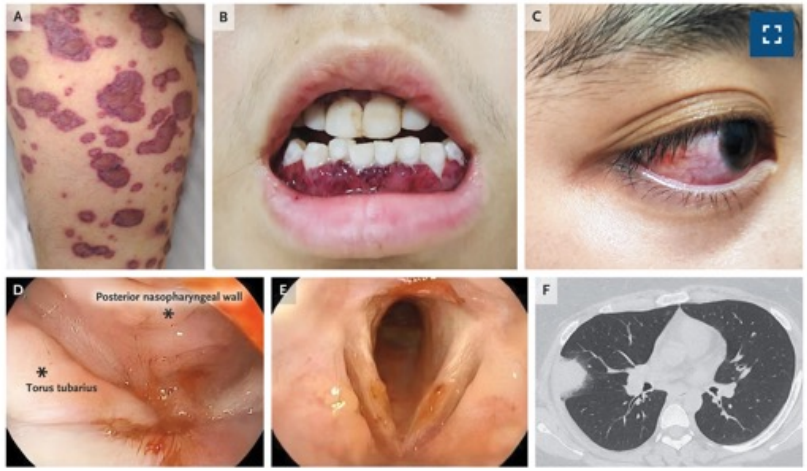

A previously healthy 20-year-old woman presented to the ophthalmology clinic with a 9-day history of pain and decreased vision in the right eye, as well as a 2-week history of a rash and gum swelling. On physical examination, purpura with overlying vesicles and bullae were seen on her chest, back, and anterior legs (Panel A, anterior surface of the left shin). Edema and dark-red discoloration of the gingiva with overlying petechiae were observed — findings consistent with "strawberry gingivitis" (Panel B). Scleral and conjunctival injection with a focal overlying nodule — findings consistent with nodular scleritis — were noted in the right eye (Panel C). Findings on funduscopic examination of the right eye aroused concern about optic neuritis. The patient was admitted to the hospital for further evaluation. Fever, dyspnea, and hemoptysis developed. Friable, hemorrhagic nasopharyngeal mucosa (Panel D) and edematous, ulcerated laryngeal mucosa (Panel E) were seen on endoscopy. Urinalysis showed proteinuria and hematuria. Computed tomography of the chest showed nodules in both lungs (Panel F). A test for proteinase 3 antineutrophil cytoplasmic antibodies was positive. A diagnosis of granulomatosis with polyangiitis was made. Treatment with pulse-dose intravenous methylprednisolone and cyclophosphamide (which was chosen instead of rituximab in this case), followed by a tapering dose of prednisone, was initiated. At the 3-month follow-up, the patient's condition had improved substantially.

PR3 ANCA

Primary Palmoplantar Pustulosis

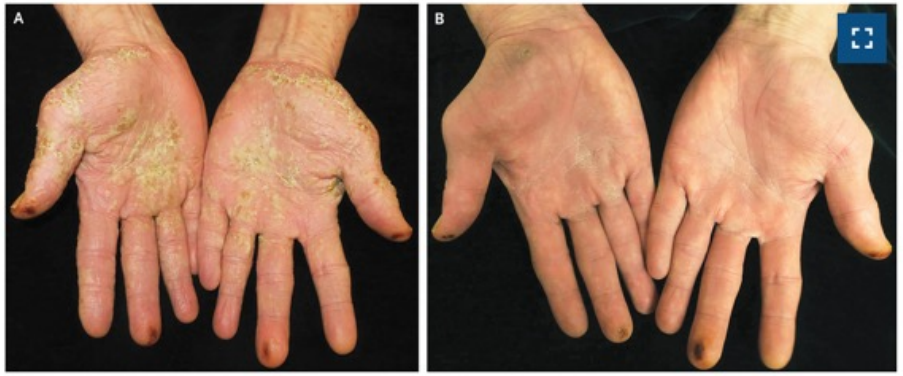

A 60-year-old man with a 30-pack-year smoking history presented to the dermatology clinic with a 2-year history of a painful rash on his palms and soles. Previous treatment with various antibacterial agents had been ineffective. Physical examination was notable for numerous pustules, with superficial erosions, purulent crusting, and surrounding erythema, on the palms (Panel A) and soles. Brown macules consistent with nicotine stains were also noted on several fingertips. Laboratory testing revealed neutrophilic leukocytosis and an elevated C-reactive protein level. A potassium hydroxide preparation of a skin scraping from the right sole was negative for fungal elements. A diagnosis of primary palmoplantar pustulosis was made. Primary palmoplantar pustulosis is a chronic inflammatory skin condition characterized by sterile pustules and is highly associated with cigarette smoking. Treatment with a brief course of topical triamcinolone, applied under occlusion, and oral cyclosporine was initiated. Cyclosporine was discontinued owing to drug-induced hypertension, and treatment with dapsone was started because of its antineutrophilic properties and because the dose can be adjusted as needed to maintain a response. At a follow-up visit 1 month after the initial presentation, the rash had abated (Panel B). At 9 years after presentation, the rash remained in remission, with the patient continuing to receive dapsone at a twice-weekly dose of 25 mg. Smoking cessation resources were recommended, but the patient declined.

9 years passed. I guess it was not cancer

Case 2-2026: A 63-Year-Old Man with Pulmonary Nodules, Liver Mass, and Vision Loss

A 63-year-old man was admitted to this hospital with fever, cough, and vision loss in the right eye.
The patient had been in his usual state of health until 3 weeks before the current presentation, when vomiting and diarrhea developed, which the patient attributed to his having eaten spoiled meat.
During the subsequent 2 weeks, vomiting and diarrhea abated, but a new cough productive of grayish-brown sputum developed, along with intermittent fever and chills.
Five days before the current presentation, the patient fell in the shower and hit the back of his head.
There was no loss of consciousness. Three days before the current presentation, the cough worsened, and his wife took him to the emergency department of another hospital.
On evaluation, the patient reported fever, chills, cough, and mild shortness of breath. He had had an unintentional weight loss of 3 kg in the previous few weeks. Vomiting and diarrhea had resolved, and no abdominal pain, anorexia, or rash was present.
The temporal temperature was 36.7°C, the blood pressure 109/71 mm Hg, the heart rate 104 beats per minute, the respiratory rate 19 breaths per minute, and the oxygen saturation 91% while the patient was breathing ambient air. Auscultation of the lungs revealed scattered crackles, and the abdomen was not tender on palpation. He had no rash or lymphadenopathy. The white-cell count was 19,300 per microliter (reference range, 4800 to 11,200).

Supplemental oxygen was administered through a nasal cannula, empirical treatment with ceftriaxone and azithromycin was started, and intravenous fluids were administered.

The patient was admitted to the other hospital.

On the second hospital day, the chills and cough persisted. Specimens of blood, urine, and induced sputum were obtained for culture. On the third hospital day, the patient awoke with loss of vision in the right eye. He had no eye pain or headache. On examination, marked periorbital edema was present, and the lids could not open spontaneously.

Variable	Reference Range, Other Hospital	On Admission, Other Hospital	Reference Range, Adults, This Hospital†	On Admission, This Hospital
White-cell count (per μl)	4800–11,200	19,300	4500–11,000	24,750
Differential count (per μl)				
Neutrophils	2200–9500	17,200	1800–7700	22,790
Lymphocytes	700–5000	500	1000–4800	640
Monocytes	0–1300	1600	200–1200	1310
Sodium (mmol/liter)	136–145	139	135–145	140
Potassium (mmol/liter)	3.5–5.1	2.5	3.4–5.0	3.7
Chloride (mmol/liter)	98–107	100	98–108	106
Carbon dioxide (mmol/liter)	20–31	28	23–32	25
Urea nitrogen (mg/dl)	9–23	38	8–25	16
Creatinine (mg/dl)	0.50–1.00	1.55	0.60–1.50	0.90
Glucose (mg/dl)	70–100	129	70–110	75
Calcium (mg/dl)	8.7–10.4	7.9	8.5–10.5	8.1
Aspartate aminotransferase (U/liter)	13–40	37	10–40	21
Alanine aminotransferase (U/liter)	7–40	38	10–55	40
Alkaline phosphatase (U/liter)	46–160	124	45–115	98
Total bilirubin (mg/dl)	0.2–1.0	3.5	0.0–1.0	1.6
Direct bilirubin (mg/dl)	—	—	0.0–0.4	0.8
Albumin (g/dl)	3.2–4.8	3.1	3.3–5.0	2.4
Total protein (g/dl)	5.7–8.2	6.6	6.0–8.3	6.3
Hematocrit (%)	40.0–52.0	36.8	41.0–53.0	30.5
Hemoglobin (g/dl)	14.0–17.2	12.8	13.5–17.5	9.7
Platelet count (per μl)	150,000–400,000	135,000	150,000–400,000	237,000

Where are inflammatory and coagulation markers?

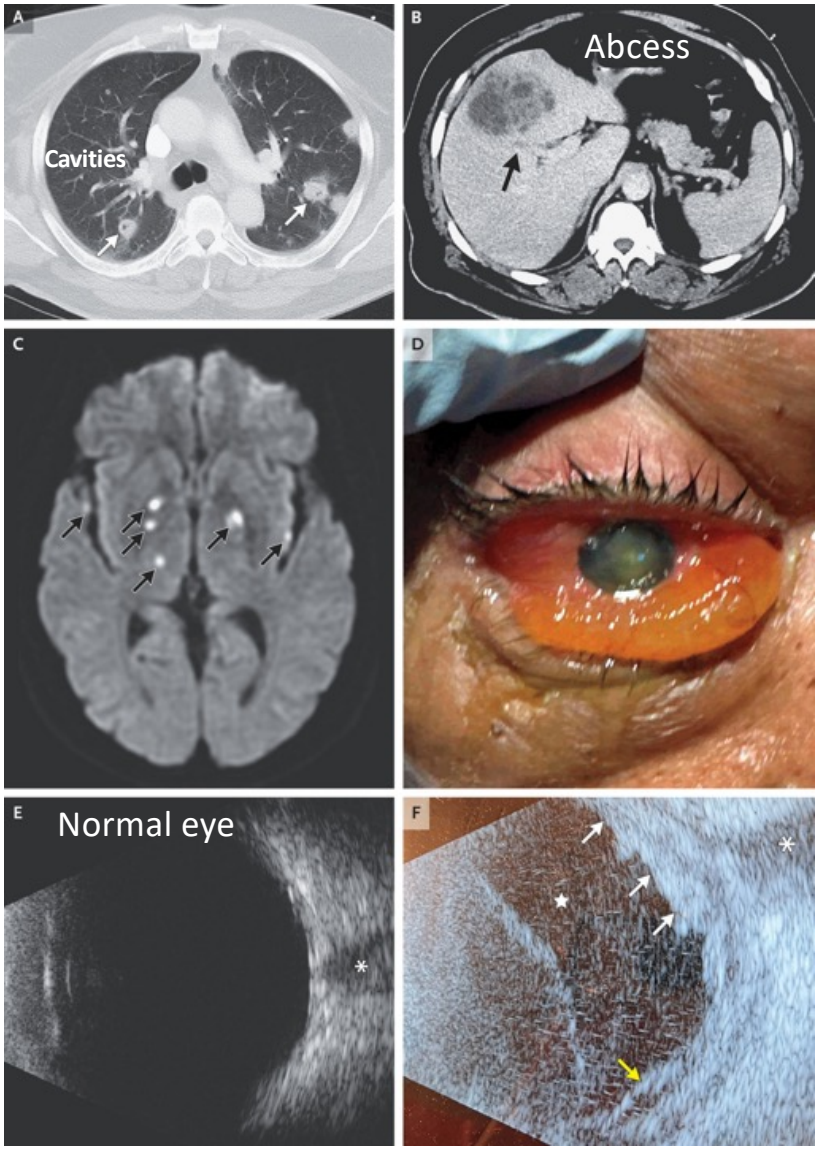

Imaging Studies and Clinical Photograph Obtained at the Other Hospital.

CT of the chest and abdomen was performed on admission to the other hospital after the administration of intravenous contrast material. An axial view of the chest (Panel A) shows multiple diffusely distributed pulmonary nodules with predominance in the middle and upper lung zones, many of which are cavitated (arrows). An axial view of the abdomen (Panel B) reveals a large mass with heterogeneous enhancement in the liver and a filling defect in the middle hepatic vein (arrow). Diffusion-weighted MRI of the head (Panel C) reveals multiple small lesions of restricted diffusion (arrows). On transfer to this hospital, an external photograph of the right eye with mechanical elevation of the eyelid (Panel D) reveals conjunctival injection and chemosis, corneal edema, anterior chamber fibrin, and a cataract. As compared with normal B-scan ultrasound of a healthy eye from a different patient (Panel E), the lower-quality image obtained on bedside B-scan ultrasonography in this patient (Panel F) shows dense vitreous hyperechoic material (star), a subretinal abscess (white arrows), and retinal detachment (yellow arrow). The optic nerve is denoted by an asterisk in Panels E and F.

Transthoracic echocardiography showed hyperdynamic left ventricular function and no valvular vegetations. Ceftriaxone and azithromycin were discontinued, and empirical treatment with vancomycin, cefepime, and metronidazole was started. The patient was transferred to this hospital. On presentation to this hospital, additional information was obtained. He had no known medical history or adverse reactions to medications. Medications included acetaminophen and ibuprofen as needed for fever. He had not subsequently traveled internationally and lived in a coastal area of New England. He drank alcohol rarely and did not take illicit drugs or smoke cigarettes; he smoked marijuana occasionally. The right eyelids were mildly erythematous, tender on palpation, and swollen such that the patient could not open the eyelids without assistance. The right eye had limited extraocular movement, had mild proptosis, and could only perceive light. The left eye had full extraocular movement and a visual acuity of 20/60. The intraocular pressure was 26 mm Hg in the right eye and 17 mm Hg in the left eye (reference range, 10 to 21). The right pupillary reaction to light was obscured by corneal haze and fibrin in the anterior chamber; the left pupil reacted normally. An afferent pupillary defect was observed in the right eye. Slit-lamp examination of the right eye revealed bullous chemosis involving the entire circumference of the conjunctiva, diffuse corneal edema with an inferior epithelial defect, and fibrin in the anterior chamber. The right iris was only faintly visible, with a faint view to an intact crystalline lens, and there was no view to the fundus. The anterior segment of the left eye was normal, and the vitreous was clear. Dilated fundoscopic examination of the left eye revealed a cotton-wool spot in the inferior retina. B-scan ultrasonography of the right eye showed dense vitreous opacities, subretinal hyperechoic material, and marked choroidal thickening

Differential Diagnosis

This 63-year-old man initially presented to another hospital after a nearly 3-week illness that was characterized by self-limited vomiting and diarrhea followed by fever, chills, and productive cough. He had leukocytosis, a large liver mass, and multiple cavitary pulmonary nodules. On the third hospital day, acute right periorbital edema and vision loss developed. MRI of the head revealed brain lesions in multiple vascular territories. Given the rapid onset of illness and these findings, an infectious cause seems most likely, and I will discuss infections that account for the liver, lung, brain, and eye findings.

Liver Abscess

The heterogeneously enhancing, mixed cystic and solid mass in the liver is consistent with an abscess. The adjacent filling defect in the middle hepatic vein most likely represents septic thrombophlebitis.

Cavitary Lung Nodules

This patient had multiple, widely distributed pulmonary nodules, many of which were cavitated. Metastatic cancer is an unlikely diagnosis given the acute onset of his symptoms. In patients with granulomatosis with polyangiitis, lung nodules are usually larger than those seen in this patient, and he had no history of nosebleeds or hemoptysis. Cavitary lung lesions commonly occur in persons with tuberculosis, aspergillus infection, or lung abscess with pneumonia.

Septic pulmonary emboli produce nodules and masses that are usually widespread, are often located in the peripheral lung, and frequently have cavitation — all features that were present in this patient's lung lesions. The most likely source of septic emboli in this patient is septic thrombophlebitis of the hepatic vein.

Brain Lesions

MRI of the patient's head showed multiple small lesions that were distributed across different vascular territories. These lesions, which most likely represent small infarcts, probably occurred recently because they were bright on both diffusion-weighted imaging and FLAIR sequences.

Eye Findings

The patient's left eye appeared normal, but fundoscopic examination showed a cotton-wool spot, a finding that is most common in patients with diabetes and hypertension but can occur in patients with other conditions, such as bacteremia. The blood cultures in this patient were negative, but they were obtained after the administration of antibiotic agents. This patient had multiple examination findings that were consistent with fulminant bacterial endophthalmitis. Corneal edema often occurs in patients with this condition because intraocular inflammation leads to increased intraocular pressure and interferes with the corneal endothelial "pump" that maintains appropriate corneal hydration. Slit-lamp examination nearly always shows white cells in the aqueous and, in many cases, a hypopyon, which is a layer of white cells in the anterior chamber.

A Unifying Infection

I believe this patient had invasive *K. pneumoniae* syndrome, which includes a primary liver abscess with metastatic infection. This syndrome is caused by a hypervirulent type of *K. pneumoniae*. As compared with liver abscesses caused by other bacteria, those caused by *K. pneumoniae* are more often single, solid lesions or contain necrotic debris, and they are often associated with thrombophlebitis and metastatic infection.

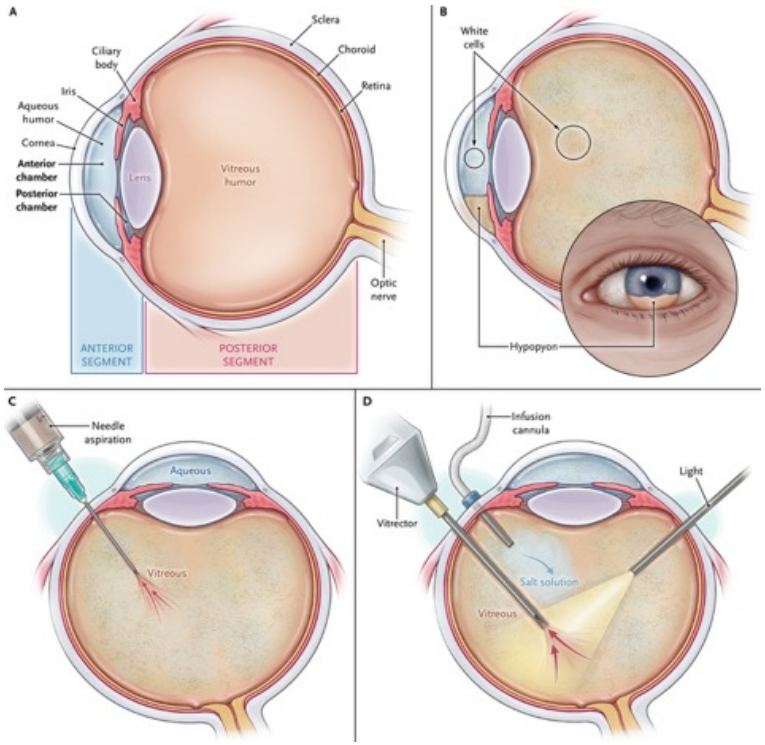

Eye Anatomy and Endophthalmitis.

The eye is anatomically divided into anterior and posterior segments by the lens (Panel A). The anterior segment is further divided into the anterior and posterior chambers. Aqueous humor, a liquid that is continuously produced by the ciliary body and reabsorbed into the systemic circulation, fills the anterior segment and is completely turned over every 100 minutes. The posterior segment is filled with vitreous humor, which is not regenerated but may be surgically removed by vitrectomy. In most cases of endophthalmitis (Panels B, C, and D), white cells are present throughout the aqueous and vitreous (Panel B). Although it was absent in this patient, a hypopyon, a layer of white cells in the anterior chamber, is often present in patients with acute bacterial endophthalmitis. Inflammation may be so intense that it obscures the view of the retina. A fine-needle aspiration of the vitreous (Panel C) or aqueous may be performed to obtain a fluid sample for culture in cases of suspected endophthalmitis. However, because the vitreous is gel-like, sometimes no sample can be obtained (known as a “dry tap”). Antibiotics are injected into the vitreous after aspiration of the vitreous for culture. A vitrectomy (Panel D) involves the use of a vitrector to cut and aspirate the vitreous, while balanced salt solution is infused to maintain eye turgor. An undiluted sample of vitreous may be obtained for culture at the start of the procedure, and the dilute vitreous washings, which are continuously collected during the surgery, may also be cultured. The yield of positive intraocular cultures in endophthalmitis is highest with vitrectomy, followed by vitreous aspirate, and then aqueous aspirate. Antibiotics are injected into the vitreous through a syringe at the end of a vitrectomy. A vitrectomy serves to débride the infected vitreous in endophthalmitis (similar to draining an abscess), and vitrectomy plus intravitreal antibiotic injection is preferred to intravitreal antibiotic injection alone in patients with severe endophthalmitis. However, vitrectomy cannot be safely performed in some inflamed eyes.

Discussant‘s Diagnosis

Disseminated infection due to hypervirulent *Klebsiella pneumoniae*.

Initial Management and Hospital Course

On the day of transfer to this hospital, intraocular needle aspirations were performed. The vitreous aspiration yielded no material owing to a highly viscous and inflamed vitreous, and the aqueous aspiration yielded 200 µl of fluid for microbiologic studies. In addition to intravenous antimicrobial therapy, treatment with intravitreal ceftazidime, vancomycin, and voriconazole was administered. The corneal clouding and widespread multilayer abscess with a compromised scleral wall precluded safe vitrectomy.The patient reported no light perception in the right eye after the procedure, most likely because of the near-complete loss of vision by the time of transfer to this hospital and the subsequent increase in intraocular pressure. Despite attempts to lower the intraocular pressure, vision in his right eye was not restored. Treatment with topical glucocorticoids and eye drops to reduce the intraocular pressure was started for comfort. During the first week in this hospital, proptosis and chemosis worsened. The right eye had severe preseptal soft-tissue inflammatory changes and marked orbital proptosis with abnormal elongation of the ocular globe. Circumferential scleral enhancement was noted in the right eye, along with extensive postseptal soft-tissue inflammatory changes affecting the right extraocular muscles and lacrimal gland and a small focus with peripheral enhancement, medial to the right globe, that most likely represented a periscleral abscess. The patient had severe stretching of the right optic nerve and extensive perineural enhancement along the right optic nerve. Given that the patient had no possibility of visual recovery, was at risk for spontaneous globe perforation, and had a rapidly worsening orbital infection despite appropriate treatment with antibiotics, enucleation of the right eye was performed.

Pathological Discussion

On the second hospital day, Gram's staining of an expectorated sputum sample showed a moderate number of neutrophils but no organisms. Culture grew rare gram-negative rods, which were identified as *K. pneumoniae* with the use of mass spectrometry. At the request of the infectious diseases team, a string test (an informal, nonstandardized test in which an inoculation loop is touched to a bacterial colony and then lifted to see whether a viscous string forms) was performed. A positive result occurs when a string height of greater than 5 mm is formed and represents hypermucoviscosity, a classic feature of hypervirulent *K. pneumoniae*. This patient's isolate was readily positive. Susceptibility testing revealed that the isolate was broadly susceptible to common antibacterial agents, including those that had been administered empirically before the first diagnostic procedure.

Discussion of Hypervirulent *Klebsiella pneumoniae*

Hypervirulent *K. pneumoniae* was first recognized in the 1980s in Taiwan as the cause of a distinct clinical syndrome. Since that time, isolates of hypervirulent *K. pneumoniae* have become endemic in Southeast Asia, and there have been reports of sporadic cases in Europe and the Americas. The disease course typically associated with hypervirulent *K. pneumoniae* begins with the development of a pyogenic liver abscess, often in persons who are otherwise healthy, before spreading through the bloodstream to distant sites, where it can cause endophthalmitis, meningitis, ventriculitis, pneumonia, or even skin and soft-tissue infections — conditions that are generally considered to be uncommon manifestations of infection with classical *K. pneumoniae*.

Viscous string test

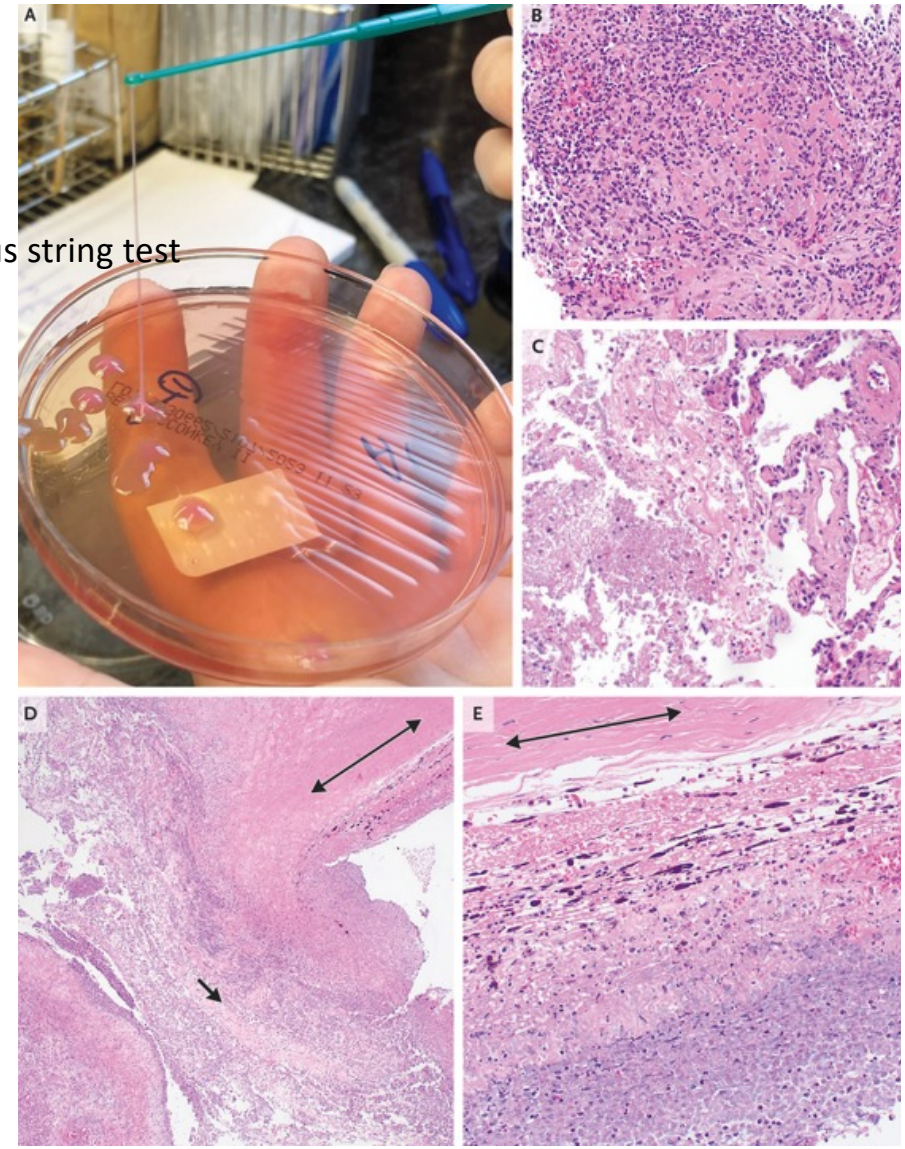

Microbiologic Studies and Specimens of the Enucleated Eye.

A string test performed on the rare growth of *Klebsiella pneumoniae* from the sputum culture shows a positive result, with the formation of a viscous string with a height of greater than 5 mm (Panel A). Hematoxylin and eosin staining of a liver-biopsy specimen (Panel B) shows a patch of necrosis and neutrophilic inflammation, findings consistent with an abscess. Hematoxylin and eosin staining of a lung-biopsy specimen (Panel C) shows acutely inflamed alveoli and airways (right side of image) and necrosis (left side). Hematoxylin and eosin staining of an enucleated eye specimen (Panel D) shows scleral perforation and abscess formation. The sclera (double-sided arrow) is discontinuous with an abscess (single-sided arrow) that extends into the globe. At higher magnification (Panel E), an area with intact sclera (double-sided arrow) shows that the deeper layers of the eye are disorganized, acutely inflamed, and necrotic, findings consistent with endophthalmitis.

The patient had a fluctuating hospital course that was complicated by acute kidney injury and an episode of worsening mental status. Repeat brain imaging revealed increased perilesional edema despite treatment with antibiotics. He received a 10-day course of dexamethasone, and his mental status improved. Five weeks after transfer to this hospital, he was discharged to an acute rehabilitation facility where he continued to receive intravenous ceftriaxone. After 2 weeks, he was discharged home and transitioned to treatment with oral levofloxacin.

Follow-up imaging studies were obtained during the 6 months after discharge. MRI of the head showed a marked decrease in the number and size of the enhancing lesions throughout the brain. CT of the abdomen showed a marked reduction in the size of the liver lesion, which no longer showed enhancement. CT of the chest revealed near resolution of the pulmonary nodules.

The patient reestablished care with a primary care physician, and a colonoscopy was recommended. He completed a total of 9 months of treatment with antibiotics, which was discontinued after follow-up CT confirmed resolution of the liver abscess.

Final Diagnosis

Disseminated infection with hypervirulent *Klebsiella pneumoniae*.

An **Abluminus Drug-Eluting Stent (DES)**, like the Abluminus DES+, is a next-generation coronary stent designed to deliver the anti-restenosis drug **Sirolimus** specifically to the artery's outer (abluminal) surface using a biodegradable polymer, aiming for better outcomes, especially in diabetic patients, by providing uniform drug delivery and transitioning to a bare-metal structure faster. It uses unique balloon technology for precise drug placement, addressing limitations of older stents by reducing late complications and improving outcomes in challenging patient groups.

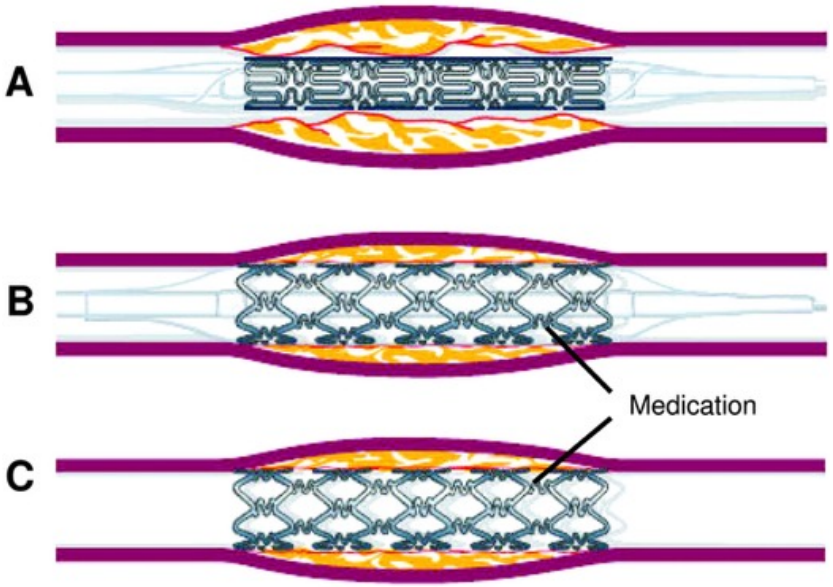

Abluminus DES+ sirolimus-eluting stent versus everolimus-eluting stent in patients with diabetes and coronary artery disease (ABILITY Diabetes Global): results from a multicentre, randomised controlled trial

Summary

Background In patients with coronary artery disease, diabetes increases the risk of restenosis and adverse cardiovascular events after percutaneous coronary intervention (PCI). The Abluminus DES+ is a thin-strut cobalt–chromium sirolimus-eluting stent (SES) with abluminal and balloon-surface coating intended to enhance drug delivery to the vessel wall. We aimed to compare the efficacy and safety of the Abluminus DES+ SES versus the XIENCE durable-polymer everolimus-eluting stent (EES) in patients with diabetes undergoing PCI.

Methods ABILITY Diabetes Global was a multicentre, prospective, open-label, randomised controlled trial conducted at 74 sites in 16 countries. Adults (aged ≥18 years) with type 1 or type 2 diabetes undergoing PCI for at least one de novo coronary lesion due to chronic coronary syndrome or non-ST-elevation acute coronary syndrome were eligible. Patients were randomly assigned (1:1) to the Abluminus DES+ SES or the XIENCE EES. Randomisation was stratified by site using a secure web-based system with concealed allocation and randomly varying block sizes (4, 6, and 8). Operators were unmasked to allocation; staff performing clinical follow-up and the independent clinical events committee were masked. For the Abluminus DES+ SES, a balloon inflation time of at least 45 s was recommended to facilitate drug transfer; dual antiplatelet therapy was prescribed to all patients according to clinical guidelines and local practice. The primary hypothesis of the study was the non-inferiority of the Abluminus DES+ SES compared with the XIENCE EES for the two coprimary endpoints at 12 months (in the per-protocol population): ischaemia-driven target-lesion revascularisation (2·8% non-inferiority margin) and target-lesion failure (3·0% margin), defined as a composite of cardiovascular death, target-vessel myocardial infarction, or ischaemia-driven target-lesion revascularisation. Time-to-event analyses were conducted with Kaplan–Meier estimates and Cox proportional hazards models. This trial is registered with ClinicalTrials.gov (NCT04236609) and is complete.

Findings Between June 12, 2020, and Sept 9, 2022, 3032 patients were randomly assigned to the Abluminus DES+ SES (n=1514) or XIENCE EES (n=1518). 2931 (96·7%) of 3032 patients completed follow-up to death or 24-month follow-up. Median age was 68·0 years (IQR 60–74). 879 (29·0%) of 3032 patients were female and 2153 (71·0%) were male. At 12 months, in the per-protocol analysis, the Abluminus DES+ SES did not meet the criteria for non-inferiority for ischaemia-driven target-lesion revascularisation compared with XIENCE EES (67 of 1421 patients [Kaplan–Meier estimate 4·8%, 95% CI 3·9–6·2] *vs* 30 of 1446 [2·1%, 95% CI 1·6–3·2]; absolute risk difference 2·7%, 95% CI 1·3–4·1; $p_{non\text{-}inferiority}$=0·44) and target lesion failure (137 [9·7%, 8·4–11·5] *vs* 89 [6·2%, 5·3–7·8]; 3·5%, 1·5–5·5; $p_{non\text{-}inferiority}$=0·68). For both endpoints, the lower bound of the 95% CI for the absolute risk difference excluded zero. Target-vessel myocardial infarction occurred more frequently in the Abluminus DES+ SES group (73 of 1421 patients [Kaplan–Meier estimate 5·2%, 95% CI 4·1–6·5] *vs* 44 of 1446 patients [3·1%, 2·4–4·3]) but there were no significant differences in cardiovascular death (41 of 1421 patients [2·9%, 2·1–3·9] *vs* 30 of 1446 patients [2·1%, 1·5–3·0]) and all-cause death (52 of 1421 patients [3·7%, 2·8–4·8] *vs* 48 of 1446 patients [3·3%, 2·5–4·4]). Results were consistent at 24 months in the intention-to-treat analysis, however no significant differences were observed between the two groups in landmark analyses between 12 and 24 months.

Interpretation In patients with diabetes undergoing PCI, the Abluminus DES+ SES was not non-inferior to the XIENCE EES, resulting in higher rates of ischaemia-driven target-lesion revascularisation and target lesion failure at 12-month follow-up. Event rates between 12 and 24 months were similar between groups. These findings highlight the persistent challenge of optimising outcomes in patients with diabetes and underscore the need for continued innovation in stent design and adjunctive pharmacotherapy to reduce residual ischaemic risk in this population.

Funding Concept Medical.

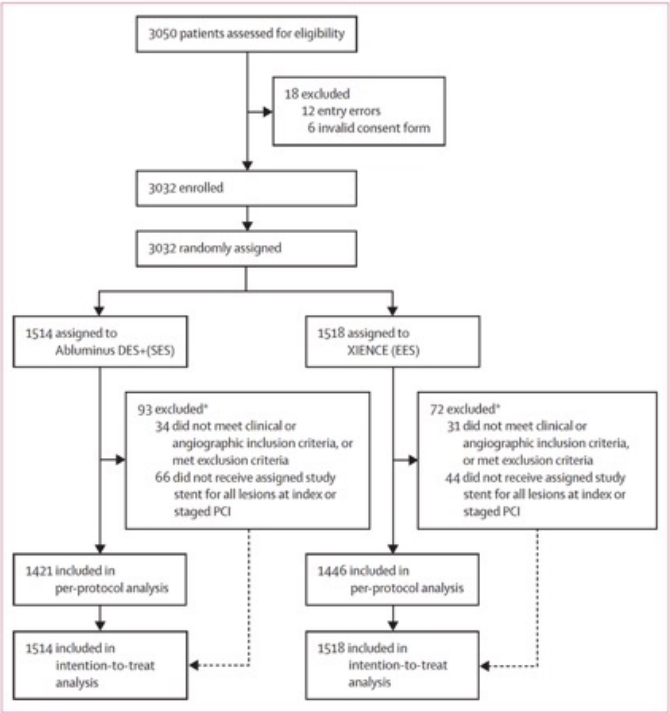

Figure 1: **Trial profile**
EES=everolimus-eluting stent. PCI=percutaneous coronary intervention. SES=sirolimus-eluting stent. *Reasons for exclusion were not mutually exclusive.

	Abluminus DES+ SES (n=1514)	XIENCE EES (n=1518)
Age, years	68 (60–75)	68 (61–74)
Sex		
Female	462/1514 (30·5%)	417/1518 (27·5%)
Male	1052/1514 (69·5%)	1101/1518 (72·5%)
BMI, kg/m²	28 (25–32)	29 (26–32)
Region of enrolment		
Europe	1166/1514 (77·0%)	1174/1518 (77·3%)
South America	206/1514 (13·6%)	206/1518 (13·6%)
Asia	142/1514 (9·4%)	138/1518 (9·1%)
Clinical presentation		
Silent ischaemia	277/1508 (18·4%)	293/1513 (19·4%)
Stable angina	680/1508 (45·1%)	695/1513 (45·9%)
Unstable angina	203/1508 (13·5%)	192/1513 (12·7%)
NSTEMI	348/1508 (23·1%)	333/1513 (22·0%)
Medical history		
Current smoker	242/1494 (16·2%)	233/1502 (15·5%)
Hypertension	1246/1509 (82·6%)	1294/1514 (85·5%)
Hypercholesterolemia	999/1509 (66·2%)	1003/1513 (66·3%)
Family history of CAD	393/1500 (26·2%)	418/1506 (27·8%)
Congestive heart failure	152/1507 (10·1%)	132/1514 (8·7%)
LVEF, %	55% (50–60%)	55% (50–60%)
Chronic kidney disease	173/1510 (11·5%)	148/1514 (9·8%)
Liver disease	23/1510 (1·5%)	34/1514 (2·2%)
Peripheral artery disease	137/1510 (9·1%)	132/1514 (8·7%)
Previous stroke	79/1510 (5·2%)	92/1514 (6·1%)
Previous myocardial infarction	315/1510 (20·9%)	317/1512 (21·0%)
Previous PCI	349/1510 (23·1%)	319/1513 (21·1%)
Previous CABG	71/1510 (4·7%)	55/1513 (3·6%)
Atrial fibrillation	177/1510 (11·7%)	164/1513 (10·8%)
Chronic lung disease	114/1509 (7·6%)	115/1512 (7·6%)
High bleeding risk	508/1510 (33·5%)	500/1514 (32·9%)

(Table 1 continues in next column)

	Abluminus DES+ SES (n=1514)	XIENCE EES (n=1518)
(Continued from previous column)		
Diabetes status		
Diabetes type		
Type 1	49/1509 (3·2%)	57/1512 (3·8%)
Type 2	1396/1509 (92·5%)	1397/1512 (92·4%)
Medically treated diabetes treatment	1446/1509 (95·8%)	1463/1515 (96·6%)
Insulin	530/1509 (35·1%)	535/1515 (35·3%)
Sensitisers	1090/1509 (72·2%)	1086/1515 (71·7%)
Secretagogues	371/1509 (24·6%)	367/1515 (24·2%)
GLP-1 or GIP agonists	77/1509 (5·1%)	93/1515 (6·2%)
DPP-4 inhibitors	220/1509 (14·6%)	205/1515 (13·5%)
SGLT2 inhibitors	190/1509 (12·6%)	190/1515 (12·5%)
Baseline laboratory values		
HbA_{1c}	7·6% (6·9–8·8)	7·5% (6·7–8·6)
Serum Creatinine, mg/dL	0·9 (0·8–1·2)	0·9 (0·8–1·2)
eGFR, mL/min per 1·73 m²	74·0 (60·0–90·0)	75·8 (60·0–90·0)
LDL, mg/dL	85·5 (37·8)	88·2 (37·8)
Antithrombotic therapy at discharge		
Aspirin	1407/1508 (92·9%)	1421/1514 (93·6%)
$P2Y_{12}$ inhibitor	1480/1508 (97·8%)	1486/1514 (97·9%)
Clopidogrel	1171/1480 (77·3%)	1197/1486 (78·9%)
Ticagrelor	237/1480 (15·7%)	205/1486 (13·5%)
Prasugrel	72/1480 (4·8%)	84/1486 (5·5%)
Oral anticoagulant	182/1508 (12·0%)	184/1486 (12·1%)

Data are n (%), median (IQR), or mean (SD). CABG=coronary artery bypass grafting. CAD=coronary artery disease. DES=drug eluting stent. DPP-4=dipeptidyl peptidase-4. EES=everolimus-eluting stent. eGFR=estimated glomerular filtration rate. GIP=glucose-dependent insulinotropic polypeptide. GLP-1=glucagon-like peptide-1. HbA_{1c}=glycated haemoglobin. LVEF=left ventricle ejection fraction. NSTEMI=non-ST-elevation myocardial infarction. PCI=percutaneous coronary intervention. SES=sirolimus-eluting stent. SGLT2=sodium–glucose cotransporter-2.

***Table 1*: Summary of demographic and baseline clinical characteristics**

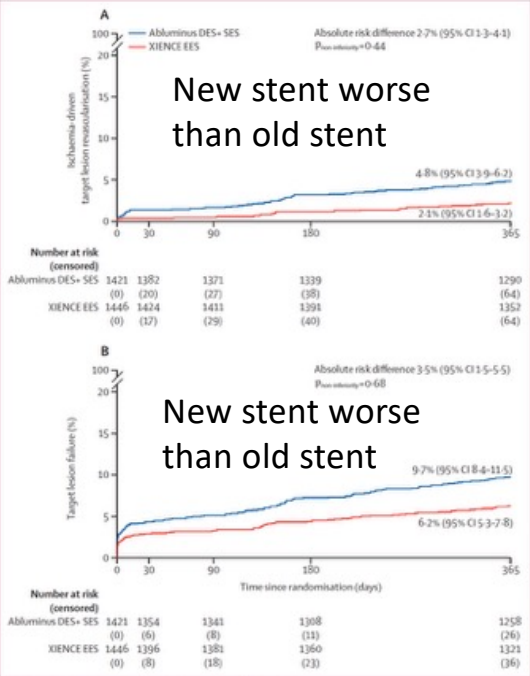

Figure 2: Kaplan–Meier curves for the coprimary efficacy endpoints
Ischemia-driven target lesion revascularisation (A) and target lesion failure (B) at 12 months in the per-protocol population. DES=drug-eluting stent. EES=everolimus-eluting stent. SES=sirolimus-eluting stent.

	Abluminus DES+ SES (n=1421)	XIENCE EES (n=1446)	Hazard ratio (95% CI)	Absolute risk difference, (95% CI)	Non-inferiority margin	$p_{non\text{-}inferiority}$
Target lesion failure	137 (9·7%, 8·4–11·5)	89 (6·2%, 5·3–7·8)	1·59 (1·22–2·07)	3·5% (1·5–5·5)	3·0%	0·68*
Ischaemia-driven target lesion revascularisation	67 (4·8%, 3·9–6·2)	30 (2·1%, 1·6–3·2)	2·31 (1·50–3·55)	2·7% (1·3–4·1)	2·8%	0·44*
Cardiovascular death	41 (2·9%, 2·1–3·9)	30 (2·1%, 1·5–3·0)	1·39 (0·87–2·23)	..	..	..
Target-vessel myocardial infarction	73 (5·2%, 4·1–6·5)	44 (3·1%, 2·4–4·3)	1·70 (1·17–2·47)	..	..	..
Periprocedural	31 (2·2%, 1·5–3·1)	30 (2·1%, 1·5–3·0)	1·05 (0·64–1·74)	..	..	..
Spontaneous	42 (3·0%, 2·3–4·2)	14 (1·0%, 0·7–1·8)	3·09 (1·68–5·65)	..	..	..
Cardiovascular death with target-vessel myocardial infarction	106 (7·5%, 6·2–9·0)	70 (4·9%, 4·0–6·3)	1·55 (1·15–2·10)	..	..	..
All-cause death	52 (3·7%, 2·8–4·8)	48 (3·3%, 2·5–4·4)	1·10 (0·74–1·63)	..	..	..
Definite or probable stent thrombosis	27 (1·9%, 1·3–2·8)	16 (1·1%, 0·7–1·8)	1·73 (0·93–3·21)	..	..	..
Stroke	17 (1·2%, 0·8–2·0)	20 (1·4%, 0·9–2·2)	0·86 (0·45–1·65)	..	..	..
Target-vessel revascularisation (non-target lesion failure)	16 (1·2%, 0·8–2·1)	11 (0·8%, 0·5–1·6)	1·48 (0·69–3·19)	..	..	..
BARC type 2–5 bleeding	50 (3·6%, 2·7–4·7)	51 (3·6%, 2·7–4·7)	1·00 (0·68–1·48)	..	..	..

BARC=Bleeding Academic Research Consortium. DES=drug-eluting stent. EES=everolimus-eluting stent. SES=sirolimus-eluting stent. Non-inferiority was assessed using Farrington–Manning with a one-sided α of 0·025. *Absolute risk differences are shown with two-sided 95% CIs.

***Table 2:* Primary analysis and secondary outcomes at 12 months in the per-protocol population**

	Abluminus DES+ SES (n=1514)	XIENCE EES (n=1518)	Hazard ratio (95% CI)
Target lesion failure	184 (12·4%, 10·8–14·2)	142 (9·6%, 8·2–11·2)	1·32 (1·06–1·65)
Ischaemia-driven target lesion revascularisation	95 (6·6%, 5·4–7·9)	57 (3·9%, 3·0–5·1)	1·71 (1·23–2·37)
Cardiovascular death	63 (4·3%, 3·3–5·4)	53 (3·6%, 2·8–4·7)	1·19 (0·83–1·72)
Target-vessel myocardial infarction	87 (5·9%, 4·8–7·2)	57 (3·8%, 3·0–4·9)	1·54 (1·11–2·16)
Periprocedural	34 (2·2%, 1·6–3·1)	32 (2·1%, 1·5–3·0)	1·07 (0·66–1·73)
Spontaneous	53 (3·8%, 2·9–4·9)	25 (1·7%, 1·2–2·5)	2·24 (1·39–3·59)
Cardiovascular death with target-vessel myocardial infarction	139 (9·3%, 8·0–10·9)	105 (7·1%, 5·9–8·5)	1·34 (1·04–1·73)
All-cause death	87 (5·9%, 4·8–7·2)	93 (6·3%, 5·2–7·7)	0·94 (0·70–1·26)
Definite or probable stent thrombosis	33 (2·2%, 1·6–3·1)	23 (1·6%, 1·0–2·4)	1·45 (0·85–2·47)
Stroke	26 (1·8%, 1·2–2·7)	28 (2·0%, 1·4–2·9)	0·93 (0·55–1·59)
Target-vessel revascularisation (non-TLR)	28 (2·0%, 1·3–2·8)	26 (1·8%, 1·2–2·7)	1·08 (0·63–1·84)
Bleeding BARC 2–5	62 (4·2%, 3·3–5·4)	64 (4·4%, 3·4–5·6)	0·98 (0·69–1·38)

BARC=Bleeding Academic Research Consortium. DES=drug-eluting stent. EES=everolimus-eluting stent. SES=sirolimus-eluting stent.

Table 3: **Primary and secondary outcomes at 24 months in the intention-to-treat population**

Research in context

Evidence before this study

We searched PubMed, Embase, and major cardiology meeting proceedings from database inception to Aug 31, 2025, without language restrictions, using the terms "diabetes", "drug-eluting stents", "PCI", and "randomized clinical trial". Previous randomised trials and meta-analyses consistently showed that patients with diabetes have higher rates of restenosis and repeat revascularisation than patients without diabetes, despite improvements in new-generation drug-eluting stents (DES). Small mechanistic studies and observational studies of the Abluminus DES+ suggested feasibility and safety, but clinical evidence from large-scale randomised trials was absent.

Added value of this study

The ABILITY Diabetes Global trial is the largest randomised study to date focused exclusively on patients with diabetes undergoing percutaneous coronary intervention and showed that the Abluminus DES+ sirolimus-eluting stent did not meet criteria for non-inferiority compared with the XIENCE everolimus-eluting stent for ischaemia-driven target lesion revascularisation and target lesion failure. The excess risk with the Abluminus DES+ was confined to the first year, driven by higher rates of target-vessel myocardial infarction and revascularisation, whereas outcomes were similar thereafter. This trial provides definitive, large-scale comparative data for two contemporary stent platforms in this high-risk population.

Implications of all the available evidence

Patients with diabetes remain at high risk of adverse events after percutaneous coronary intervention. The absence of an incremental benefit with the Abluminus DES+ highlights the ongoing unmet need for innovation in stent technology and adjunctive therapies to reduce residual ischaemic risk in patients with diabetes and coronary artery disease requiring percutaneous coronary intervention. Future research should explore device designs and pharmacological strategies that specifically address the biological challenges of diabetes. When feasible, surgical revascularisation should remain the preferred option for patients with diabetes and multivessel disease.

Socioeconomic inequalities in cancer survival and access to health care among children and adolescents in China, 2018–24: a prospective nationwide cohort study

Summary

Background To improve health equity, as a Sustainable Development Goal, timely evaluation of inequalities in cancer survival is essential. We aimed to assess the latest nationwide 5-year survival for childhood and adolescent cancers in China and disparities in survival, especially those associated with health-care access.

Methods Using data from the National Center for Pediatric Cancer Surveillance (covering 1388 surveillance sites and 82·3% of new cases in China), we applied the Kaplan–Meier method to estimate 5-year observed survival for 95 189 cases in patients aged 0–19 years who were diagnosed with cancer between 2018 and 2020. We assessed survival by age group, sex, cancer type (based on the International Classification of Childhood Cancer, third edition), regional Socio-demographic Index (SDI) category, and whether patients were treated within (intraprovincial) or outside (interprovincial) their province of residence. We categorised the 31 provinces into four regions according to the distribution of their SDI scores, a composite metric reflecting overall regional socioeconomic development. We examined survival disparities across regional SDI categories and within each region. We used the densities of seven health-care provision indicators (per 1000 children and adolescents) as proxies for health-care accessibility. We applied random survival forest models to estimate potential reductions in mortality risk among intraprovincial patients under simulated scenarios, where provincial-level indicator densities were set to the highest levels observed either nationally or within their respective regional SDI categories, relative to their actual values.

Findings The 5-year survival of patients with cancer was 77·8% (95% CI 77·4–78·1) among children aged 0–14 years and 75·3% (74·7–75·9) among adolescents aged 15–19 years, with an overall 5-year survival of 77·2% (76·9–77·5) in the entire cohort. Survival was higher in girls (79·0% [78·6–79·4]) than in boys (75·8% [75·4–76·2]). Among the 12 main cancer groups, retinoblastoma had the highest survival (91·2% [90·0–92·3]), whereas malignant bone tumours had the lowest (60·4% [59·0–61·9]). For all cancers combined, survival ranged from 72·6% (71·8–73·4) in low SDI regions to 84·9% (83·8–86·1) in high SDI regions, indicating significantly higher survival in regions with higher socioeconomic status ($p<0·0001$ for trend). This absolute survival difference between the high and low SDI regions was more pronounced in adolescents (13·4% [13·3–13·5]) than in children (11·7% [11·7–11·8]). Notably, within-region survival disparities existed in each regional SDI category and were most marked in low SDI regions, with provincial 5-year survival ranging from 61·4% to 81·1% (hazard ratio [HR] 2·68 [95% CI 1·99–3·62] for mortality risk). Compared with intraprovincial patients (n=72 867; 5-year survival 76·4% [76·0–76·7]), interprovincial patients (n=22 322) had a significantly higher survival (79·9% [79·3–80·4]; HR 0·81 [0·78–0·84]). Higher socioeconomic areas had greater densities of health-care provision indicators for diagnosis and treatment. Based on scenario-based simulations, the key indicators associated with estimated reductions in mortality risk varied by region, but included the density of the pathology workforce and institutions providing surgery, radiotherapy, and post-treatment supportive care for paediatric cancer.

Interpretation China has achieved major progress in childhood cancer survival, but inequalities remain across and within regions at different levels of socioeconomic development. The level of inequality appears greater among adolescents. While interprovincial health-care seeking was generally associated with higher survival, disparities in outcomes persisted, aligned with the socioeconomic development of patients' residence and treatment locations. Tiered resource allocation for paediatric cancer care at provincial and regional levels should be prioritised in China's health system to advance health equity.

An honest assessment; no such data comes from Russia

	Eligible cases diagnosed in 2018–20	Invalid cases excluded from survival analysis	Valid cases for survival analysis	Deaths for survival analysis	Data quality indicators					
					Uncertain primary site	Unspecified morphology	Unspecified ICCC-3 code	Lost to follow-up	Died within 30 days	Follow-up time, months
Total	99708	4519 (4·5%)	95189	20725 (21·8%)	4664 (4·9%)	4002 (4·2%)	7002 (7·4%)	4450 (4·7%)	5645 (5·9%)	58·8 (43·1–60·0)
Age group, years										
0–14	76756	2870 (3·7%)	73886	15588 (21·1%)	4257 (5·8%)	2774 (3·8%)	5069 (6·9%)	4024 (5·4%)	4895 (6·6%)	58·7 (42·3–60·0)
15–19	22952	1649 (7·2%)	21303	5137 (24·1%)	407 (1·9%)	1248 (5·9%)	1933 (9·1%)	426 (2·0%)	750 (3·5%)	59·1 (45·9–60·0)
Sex										
Boys	55901	2468 (4·4%)	53433	12331 (23·1%)	2395 (4·5%)	2181 (4·1%)	3901 (7·3%)	2522 (4·7%)	3193 (6·0%)	58·2 (35·0–60·0)
Girls	43803	2047 (4·7%)	41756	8394 (20·1%)	2269 (5·4%)	1841 (4·4%)	3101 (7·4%)	1928 (4·6%)	2452 (5·9%)	59·6 (48·5–60·0)
Unknown	4	4 (100·0%)	0	NA	NA	NA	NA	NA	NA	NA
Regional SDI										
High	3931	104 (2·6%)	3827	556 (14·5%)	247 (6·5%)	86 (2·2%)	172 (4·5%)	106 (2·8%)	99 (2·6%)	60·0 (50·9–60·0)
Upper-middle	47798	1792 (3·7%)	46006	9032 (19·6%)	2271 (4·9%)	1283 (2·8%)	2518 (5·5%)	1935 (4·2%)	2509 (5·5%)	60·0 (48·9–60·0)
Lower-middle	34438	2004 (5·8%)	32434	7857 (24·2%)	1471 (4·5%)	2038 (6·3%)	3171 (9·8%)	1310 (4·0%)	1934 (6·0%)	58·1 (31·1–60·0)
Low	13541	619 (4·6%)	12922	3280 (25·4%)	675 (5·2%)	615 (4·8%)	1141 (8·8%)	1099 (8·5%)	1103 (8·5%)	56·1 (16·1–60·0)
Cancer type										
Leukaemias	32327	57 (0·2%)	32270	7427 (23·0%)	3 (<0·1%)	0	1943 (6·0%)	1493 (4·6%)	2279 (7·1%)	58·8 (32·4–60·0)
Lymphomas	9906	3 (<0·1%)	9903	1381 (13·9%)	129 (1·3%)	0	554 (5·6%)	452 (4·6%)	530 (5·4%)	60·0 (51·0–60·0)
CNS tumours	16192	15 (0·1%)	16177	4158 (25·7%)	83 (0·5%)	1720 (10·6%)	1721 (10·6%)	777 (4·8%)	1011 (6·2%)	56·9 (23·9–60·0)
Neuroblastomas	4917	1 (<0·1%)	4916	1220 (24·8%)	2438 (49·6%)	0	0	342 (7·0%)	347 (7·1%)	56·8 (27·0–60·0)
Retinoblastoma	2458	1 (<0·1%)	2457	211 (8·6%)	1 (<0·1%)	0	25 (1·0%)	80 (3·3%)	56 (2·3%)	60·0 (53·5–60·0)
Renal tumours	2587	1 (<0·1%)	2586	409 (15·8%)	36 (1·4%)	83 (3·2%)	83 (3·2%)	157 (6·1%)	111 (4·3%)	60·0 (49·8–60·0)
Hepatic tumours	2152	0	2152	623 (28·9%)	2 (0·1%)	118 (5·5%)	118 (5·5%)	140 (6·5%)	199 (9·2%)	55·4 (10·9–60·0)
Malignant bone tumours	4385	1 (<0·1%)	4384	1686 (38·5%)	79 (1·8%)	330 (7·5%)	413 (9·4%)	83 (1·9%)	97 (2·2%)	53·6 (22·4–60·0)
Soft-tissue sarcomas	4597	0	4597	1551 (33·7%)	692 (15·1%)	0	354 (7·7%)	212 (4·6%)	248 (5·4%)	54·4 (17·4–60·0)
Germ cell tumours	6439	2 (<0·1%)	6437	801 (12·4%)	637 (9·9%)	176 (2·7%)	196 (3·0%)	376 (5·8%)	324 (5·0%)	60·0 (51·0–60·0)
Malignant epithelial tumours and melanomas	7450	2 (<0·1%)	7448	793 (10·6%)	164 (2·2%)	0	0	187 (2·5%)	209 (2·8%)	60·0 (52·5–60·0)
Other cancers	1870	8 (0·4%)	1862	465 (25·0%)	400 (21·5%)	1595 (85·7%)	1595 (85·7%)	151 (8·1%)	234 (12·6%)	55·8 (11·5–60·0)
Not classified	4428	4428 (100·0%)	0	NA	NA	NA	NA	NA	NA	NA

Data are presented as n, n (%), or median (IQR). Invalid cases include unknown sex, sex-site errors, missing morphology or primary site codes, discordance between the ICD-10 diagnosis and the ICD-O-3 behaviour code, cases not classifiable under ICCC-3, implausible date sequences (date of birth, diagnosis, and last known vital status), and unknown vital status. ICCC-3= International Classification of Childhood Cancer, third revision. ICD-O-3=International Classification of Diseases for Oncology, third edition. NA=not applicable (no valid cases for survival analysis). SDI=Socio-demographic Index.

Table 1: **Data quality indicators of childhood and adolescent cancer cases diagnosed during 2018–20 in China**

	Overall		Boys		Girls	
	n	Survival (95% CI)	n	Survival (95% CI)	n	Survival (95% CI)
Age 0–19 years (children and adolescents)						
All cancers combined	95 189	77·2% (76·9–77·5)	53 433	75·8% (75·4–76·2)	41 756	79·0% (78·6–79·4)
Leukaemias	32 270	75·9% (75·5–76·4)	18 928	75·9% (75·3–76·6)	13 342	76·0% (75·2–76·7)
Lymphoid leukaemias	19 946	80·3% (79·8–80·9)	11 900	79·6% (78·9–80·4)	8046	81·4% (80·6–82·3)
Acute myeloid leukaemias	7803	67·5% (66·4–68·5)	4366	68·4% (67·0–69·8)	3437	66·3% (64·7–68·0)
Chronic myeloproliferative diseases	1318	91·2% (89·6–92·8)	809	90·6% (88·5–92·7)	509	92·1% (89·7–94·5)
Myelodysplastic syndrome and other myeloproliferative diseases	1260	69·4% (66·8–72·1)	747	69·6% (66·2–73·1)	513	69·2% (65·2–73·5)
Unspecified and other specified leukaemias	1943	55·9% (53·5–58·3)	1106	56·9% (53·8–60·2)	837	54·5% (51·0–58·2)
Lymphomas	9903	85·5% (84·8–86·2)	6647	85·0% (84·1–85·9)	3256	86·4% (85·2–87·7)
Hodgkin lymphomas	1363	93·8% (92·5–95·1)	976	93·6% (92·1–95·2)	387	94·4% (92·1–96·8)
Non-Hodgkin lymphomas (except Burkitt lymphoma)	3966	77·1% (75·8–78·4)	2676	76·4% (74·8–78·0)	1290	78·5% (76·3–80·8)
Burkitt lymphoma	1073	84·1% (81·9–86·4)	869	84·4% (81·9–86·8)	204	83·1% (78·1–88·4)
Miscellaneous lymphoreticular neoplasms	2947	96·4% (95·7–97·1)	1776	96·6% (95·8–97·5)	1171	95·9% (94·7–97·1)
Unspecified lymphomas	554	71·3% (67·6–75·4)	350	71·2% (66·5–76·3)	204	71·6% (65·4–78·4)
CNS tumours	16 177	72·9% (72·2–73·6)	9063	71·9% (70·9–72·8)	7114	74·3% (73·3–75·4)
Ependymomas and choroid plexus tumour	1725	71·9% (69·8–74·2)	1028	70·6% (67·7–73·6)	697	73·9% (70·6–77·3)
Astrocytomas	3996	77·4% (76·1–78·7)	2204	76·8% (75·0–78·6)	1792	78·2% (76·3–80·2)
Intracranial and intraspinal embryonal tumours	2814	57·8% (56·0–59·8)	1702	55·5% (53·1–58·0)	1112	61·4% (58·5–64·4)
Other gliomas	1996	54·1% (51·9–56·4)	1059	54·5% (51·5–57·7)	937	53·7% (50·6–57·1)
Other specified intracranial and intraspinal neoplasms	3925	91·5% (90·6–92·4)	2140	91·6% (90·4–92·8)	1785	91·3% (90·0–92·7)
Unspecified intracranial and intraspinal neoplasms	1721	66·9% (64·6–69·3)	930	65·1% (62·0–68·4)	791	69·0% (65·7–72·4)
Neuroblastomas	4916	73·4% (72·1–74·7)	2656	70·6% (68·8–72·4)	2260	76·6% (74·8–78·4)
Neuroblastoma and ganglioneuroblastoma	4824	73·0% (71·7–74·3)	2605	70·2% (68·4–72·1)	2219	76·3% (74·5–78·1)
Other peripheral nervous cell tumours	92	90·9% (85·0–97·1)	51	89·5% (81·2–98·6)	41	NA
Retinoblastoma	2457	91·2% (90·0–92·3)	1315	91·0% (89·4–92·6)	1142	91·4% (89·7–93·0)
Renal tumours	2586	83·3% (81·8–84·8)	1363	84·1% (82·1–86·1)	1223	82·3% (80·2–84·6)
Nephroblastoma and other non-epithelial renal tumours	2187	84·7% (83·2–86·3)	1148	85·3% (83·2–87·4)	1039	84·1% (81·8–86·4)
Renal carcinomas	316	76·9% (72·2–82·0)	163	80·8% (74·6–87·4)	153	72·7% (65·6–80·6)
Unspecified malignant renal tumours	83	70·1% (60·5–81·1)	52	68·8% (56·9–83·2)	31	NA
Hepatic tumours	2152	69·4% (67·4–71·4)	1275	67·6% (65·0–70·2)	877	72·0% (69·0–75·2)
Hepatoblastoma and mesenchymal tumours of liver	1704	77·1% (75·1–79·2)	983	76·3% (73·6–79·1)	721	78·3% (75·3–81·5)
Hepatic carcinomas	330	38·6% (33·6–44·3)	228	37·8% (31·8–44·8)	102	40·4% (31·8–51·3)
Unspecified malignant hepatic tumours	118	42·6% (34·1–53·2)	64	37·3% (26·6–52·3)	54	49·0% (36·6–65·6)
Malignant bone tumours	4384	60·4% (59·0–61·9)	2600	59·2% (57·3–61·1)	1784	62·2% (60·0–64·6)
Osteosarcomas	3060	58·0% (56·2–59·8)	1798	56·0% (53·7–58·4)	1262	60·7% (58·1–63·6)
Chondrosarcomas	178	82·2% (76·6–88·3)	119	85·2% (79·0–92·0)	59	76·4% (65·7–88·8)
Ewing tumour and related sarcomas of bone	523	55·3% (51·1–59·9)	327	56·1% (50·8–61·9)	196	54·0% (47·4–61·7)
Other specified malignant bone tumours	210	83·6% (78·6–88·9)	117	82·2% (75·3–89·6)	93	85·5% (78·5–93·1)
Unspecified malignant bone tumours	413	64·1% (59·5–69·0)	239	63·4% (57·4–70·0)	174	65·1% (58·3–72·7)
Soft tissue sarcomas	4597	64·6% (63·2–66·0)	2549	63·7% (61·8–65·6)	2048	65·7% (63·6–67·8)
Rhabdomyosarcomas	1999	55·4% (53·2–57·7)	1186	55·3% (52·5–58·3)	813	55·4% (52·0–59·0)
Fibrosarcomas, peripheral nerve sheath tumours, and other fibrous neoplasms	614	78·7% (75·4–82·1)	293	76·7% (71·8–81·9)	321	80·5% (76·1–85·0)
Kaposi sarcoma	7	NA	4	NA	3	NA
Other specified soft tissue sarcomas	1623	71·2% (69·0–73·5)	863	70·9% (67·8–74·0)	760	71·7% (68·4–75·0)
Unspecified soft tissue sarcomas	354	61·0% (56·0–66·5)	203	62·6% (56·1–69·8)	151	59·0% (51·5–67·6)
Germ cell tumours	6437	86·9% (86·0–87·7)	3125	83·8% (82·4–85·1)	3312	89·8% (88·7–90·8)
Intracranial and intraspinal germ cell tumours	2487	80·5% (78·9–82·1)	1735	81·6% (79·7–83·4)	752	78·0% (75·0–81·1)
Malignant extracranial and extragonadal germ cell tumours	1072	83·2% (80·9–85·6)	469	73·5% (69·5–77·8)	603	90·7% (88·3–93·2)

(Table 2 continues on next page)

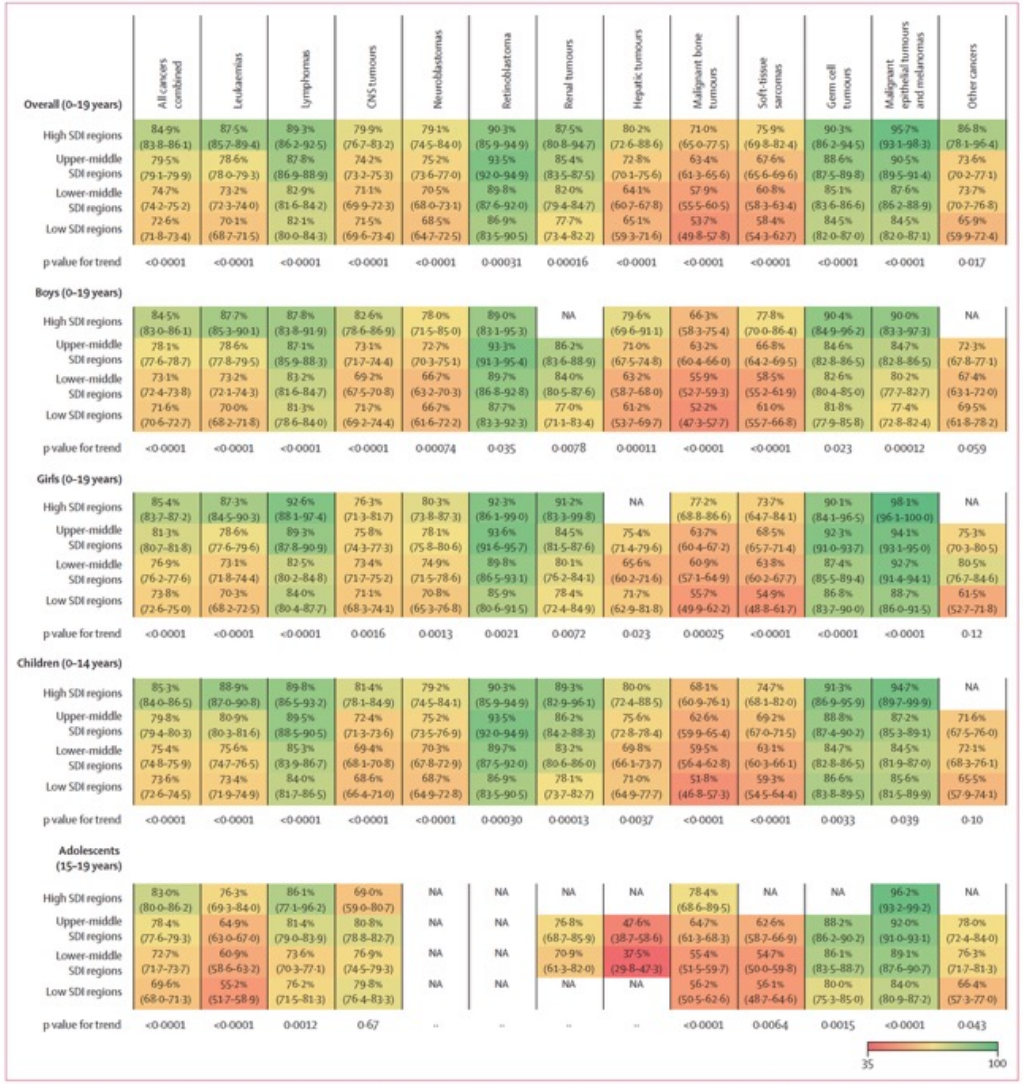

Figure 1: **Heatmap of 5-year observed survival for cancer cases, across 12 main cancer groups, diagnosed during 2018–20 in China, by regional SDI category, sex, and age group**
Data are % (95% CI). Linear trend tests were done by treating SDI as a continuous variable. SDI=Socio-demographic Index. NA=not applicable (number of cases <50).

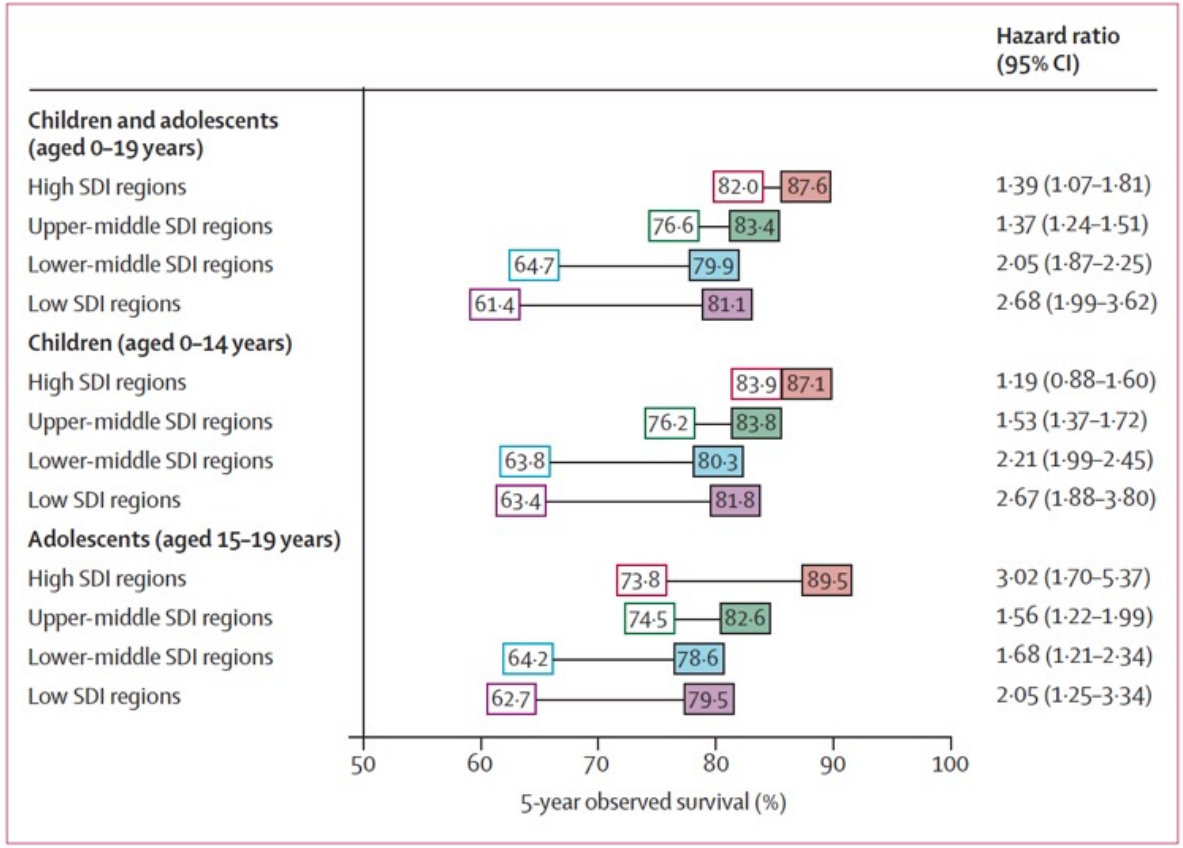

Figure 2: **Within-region survival disparities between provinces for childhood and adolescent cancers diagnosed during 2018–20 in China, by SDI and age group**

Unfilled boxes represent the lowest 5-year survival among all provinces within the SDI category, while filled boxes represent the highest. Hazard ratios represent mortality risk in provinces with the lowest versus highest 5-year survival within the same regional SDI category, adjusted for whether patients were treated within or outside the province of residence (intraprovincial patients *vs* interprovincial patients), age group, sex, cancer type, and year of diagnosis. SDI=Socio-demographic Index.

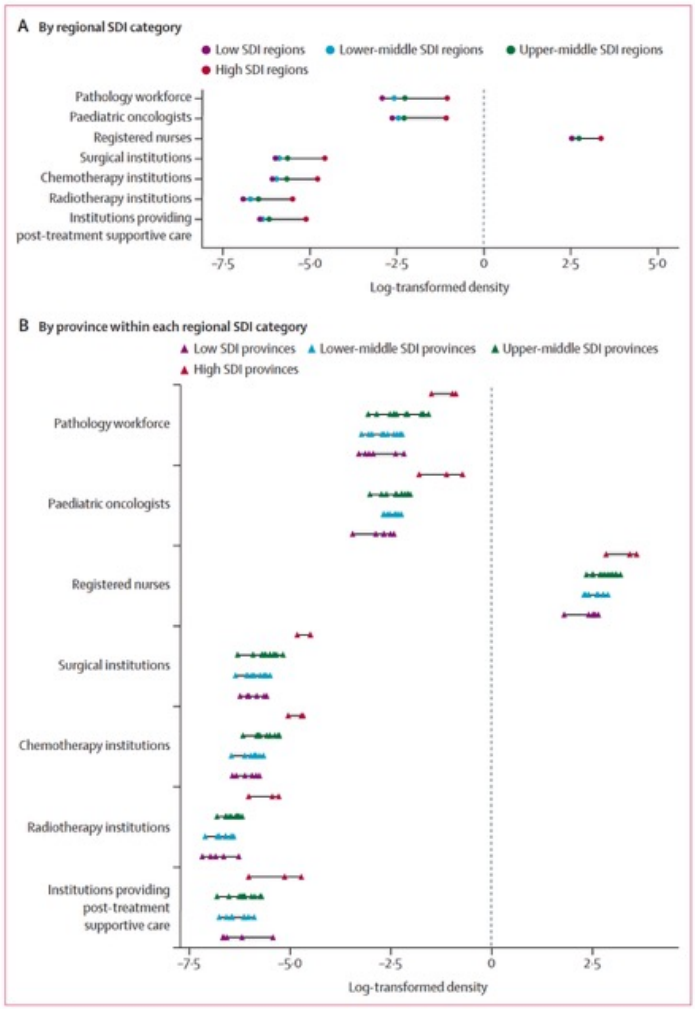

***Figure 3*: Distribution of densities for seven health-care provision indicators for paediatric cancer in China**
Listed institutions represent hospitals providing paediatric cancer-specific services (surgery, chemotherapy, radiotherapy, or post-treatment supportive care), not standalone paediatric cancer hospitals. Density refers to the number of each indicator per 1000 children and adolescents. Densities were log-transformed for visualisation. SDI=Socio-demographic Index.

	Patients, n/N (%)*	5-year survival, % (95% CI)	Hazard ratio (95% CI)†	p value for trend‡
Nationwide				..
Intraprovincial patients	72 867/95 189 (76·5%)	76·4% (76·0–76·7)	1 (ref)	
Interprovincial patients	22 322/95 189 (23·5%)	79·9% (79·3–80·4)	0·81 (0·78–0·84)	
Intraprovincial patients				<0·0001
High SDI regions	3032/72 867 (4·2%)	86·5% (85·3–87·8)	1 (ref)	
Upper-middle SDI regions	35 569/72 867 (48·8%)	78·6% (78·2–79·1)	1·68 (1·52–1·86)	
Lower-middle SDI regions	26 140/72 867 (35·9%)	74·0% (73·5–74·6)	2·07 (1·87–2·29)	
Low SDI regions	8126/72 867 (11·2%)	69·8% (68·7–70·8)	2·45 (2·20–2·73)	
Interprovincial patients				<0·0001
To high SDI regions	13 126/22 322 (58·8%)	82·5% (81·8–83·1)	1 (ref)	
To upper-middle SDI regions	5266/22 322 (23·6%)	78·7% (77·5–79·8)	1·29 (1·20–1·40)	
To lower-middle SDI regions	3466/22 322 (15·5%)	73·0% (71·5–74·6)	1·69 (1·57–1·84)	
To low SDI regions	464/22 322 (2·1%)	70·5% (66·3–75·0)	1·86 (1·55–2·24)	
By regional SDI category				
Residing in high SDI regions				0·36
Intraprovincial patients	3032/3827 (79·2%)	86·5% (85·3–87·8)	1 (ref)	
Interprovincial patients	795/3827 (20·8%)	78·9% (76·0–81·8)	1·46 (1·21–1·75)	
To high SDI regions	174/795 (21·9%)	80·2% (74·3–86·5)	1·29 (0·90–1·84)	
To upper-middle SDI regions	330/795 (41·5%)	78·0% (73·6–82·8)	1·60 (1·23–2·07)	
To lower-middle SDI regions	232/795 (29·2%)	81·0% (76·0–86·4)	1·28 (0·93–1·76)	
To low SDI regions	59/795 (7·4%)	71·9% (61·2–84·6)	2·00 (1·21–3·33)	
Residing in upper-middle SDI regions				<0·0001
Intraprovincial patients	35 569/46 006 (77·3%)	78·6% (78·2–79·1)	1 (ref)	
Interprovincial patients	10 437/46 006 (22·7%)	82·5% (81·8–83·3)	0·76 (0·72–0·80)	
To high SDI regions	8463/10 437 (81·1%)	83·4% (82·6–84·2)	0·71 (0·67–0·76)	
To upper-middle SDI regions	1243/10 437 (11·9%)	80·6% (78·4–82·9)	0·89 (0·78–1·02)	
To lower-middle SDI regions	622/10 437 (6·0%)	76·0% (72·5–79·6)	1·07 (0·91–1·27)	
To low SDI regions	109/10 437 (1·0%)	69·4% (60·4–79·6)	1·47 (1·01–2·13)	
Residing in lower-middle SDI regions				<0·0001
Intraprovincial patients	26 140/32 434 (80·6%)	74·0% (73·5–74·6)	1 (ref)	
Interprovincial patients	6294/32 434 (19·4%)	77·6% (76·6–78·7)	0·84 (0·79–0·89)	
To high SDI regions	2596/6294 (41·2%)	80·6% (79·1–82·2)	0·71 (0·64–0·78)	
To upper-middle SDI regions	2336/6294 (37·1%)	76·7% (75·0–78·5)	0·86 (0·79–0·95)	
To lower-middle SDI regions	1259/6294 (20·0%)	73·3% (70·9–75·9)	1·04 (0·93–1·16)	
To low SDI regions	103/6294 (1·6%)	75·1% (67·0–84·3)	0·98 (0·66–1·47)	
Residing in low SDI regions				<0·0001
Intraprovincial patients	8126/12 922 (62·9%)	69·8% (68·7–70·8)	1 (ref)	
Interprovincial patients	4796/12 922 (37·1%)	77·2% (76·0–78·4)	0·73 (0·68–0·79)	
To high SDI regions	1893/4796 (39·5%)	80·9% (79·1–82·8)	0·59 (0·52–0·67)	
To upper-middle SDI regions	1357/4796 (28·3%)	80·5% (78·3–82·7)	0·60 (0·53–0·69)	
To lower-middle SDI regions	1353/4796 (28·2%)	70·0% (67·5–72·5)	1·02 (0·92–1·14)	
To low SDI regions	193/4796 (4·0%)	68·3% (61·7–75·5)	1·05 (0·80–1·37)	

***Figure 4*: 5-year observed survival and hazard ratios for cancers diagnosed during 2018–20 among intraprovincial and interprovincial patients in China, at national and regional levels**
Intraprovincial patients were those who received their initial diagnosis and treatment within their province of residence. Interprovincial were those who travelled outside their province of residence for their initial diagnosis and treatment. SDI=Socio-demographic Index. *The sum of proportions might not equal 100% because of rounding. †Hazard ratios represent the difference in mortality risk for interprovincial versus intraprovincial patients, and the difference in mortality risk across regional SDI categories, adjusted for sex, age group, cancer type, year of diagnosis. ‡To assess linear trends in hazard ratios across SDI categories, we assigned ordinal integer scores to each SDI level (from low to high) and included this variable as a continuous covariate in the Cox proportional hazards model.

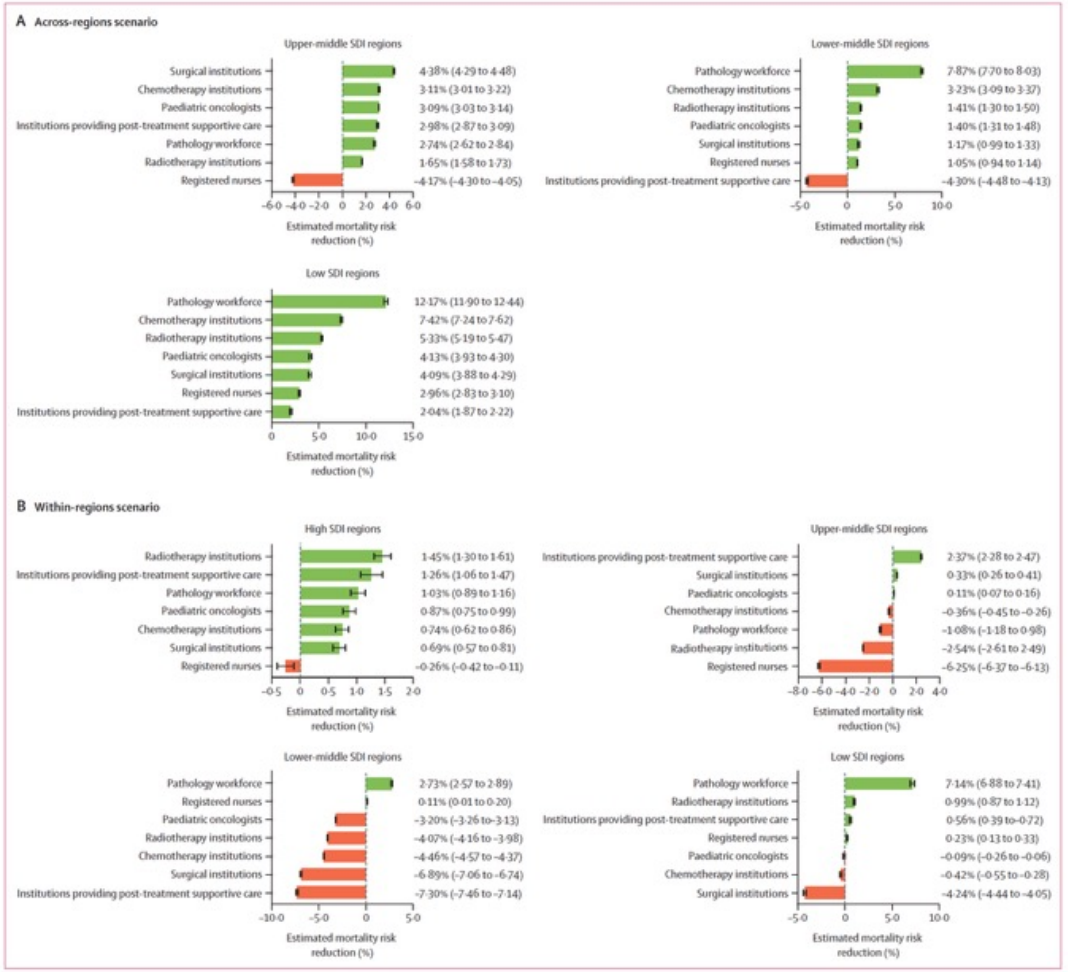

Figure 5: **Scenario-based simulation of mortality risk reductions by setting health-care provision densities to the highest observed provincial levels among intraprovincial patients**
Densities of seven health-care provision indicators were calculated at the provincial level as proxies for health-care accessibility, measured per 1000 children and adolescents. The seven health-care indicators included four types of institution (surgical, chemotherapy, radiotherapy, and post-treatment supportive care) and three types of workforce (pathology, paediatric oncologists, and registered nurses); institutions refer to those providing paediatric cancer-related services. Using scenario-based simulations with random survival forest models, mortality risk among intraprovincial patients was estimated by setting local health-care provision densities to the highest observed values. (A) In the across-regions scenario, the highest provincial-level density observed among all provinces was applied. (B) In the within-region scenario, the highest value observed within each regional SDI category was used. Estimated mortality risk reductions (%) for each indicator were calculated as the difference between simulated mortality risk at the highest observed provincial-level density and the actual provincial-level density. Green bars denote positive reductions in estimated mortality risk, while red bars indicate an increase in estimated risk. SDI=Socio-demographic Index.

Research in context

Evidence before this study

We systematically searched PubMed, Google Scholar, and China National Knowledge Infrastructure up to July 31, 2025 for studies on childhood cancer survival, socioeconomic status, and health-care access, using terms including "cancer survival", "survival outcomes", "children and adolescents", "paediatric", "socioeconomic status", "inequality", "disparity", "access", "accessibility", "healthcare", and "health service", without language or publication date restrictions. Cancer survival is a key metric for evaluating the effectiveness of health systems and informing global cancer control policy. Large-scale studies, such as the CONCORD and EUROCARE studies, have quantified international differences in cancer survival among children and adolescents. However, in low-income and middle-income countries, assessments of recent progress and disparities in childhood cancer survival at national and subnational levels remain scarce. While socioeconomic status and health-care access are known to influence childhood cancer survival, existing evidence has been based on modelling, qualitative research, or small-scale studies, rather than nationwide, real-world data analyses. Furthermore, the effect of medical travel on childhood cancer survival remains inconsistently documented, particularly among Chinese children and adolescents. To the best of our knowledge, no studies have yet systematically assessed the latest 5-year survival between 2018 and 2024, or examined survival disparities associated with health-care access among children and adolescents at both national and subnational levels in China.

Added value of this study

For the first time, using nationwide cohort data from the National Center for Pediatric Cancer Surveillance, we report 5-year survival for children (aged 0–14 years) and adolescents (aged 15–19 years) diagnosed with cancer from 2018 to 2020 at both the national and subnational levels in China. Our findings show that the latest 5-year observed survival for all cancers combined was 77·2% (95% CI 76·9–77·5), revealing substantial regional inequalities, ranging from 72·6% in low Socio-demographic Index (SDI) regions to 84·9% in high SDI regions. The absolute survival difference between high and low SDI regions was greater for adolescents than for children with cancer, particularly for leukaemias, lymphomas, malignant bone tumours, and malignant epithelial tumours and melanomas. Within-region survival disparities among children were more pronounced in low SDI regions, with an absolute survival difference of 18·4% between provinces with the highest and lowest survival; among adolescents, substantial disparities between provinces were observed in both low and high SDI regions, with absolute survival differences of 16·8% and 15·7%, respectively. Across socioeconomic strata, we observed a maximal survival disparity of 18·2% (18·0–18·5) between patients who travelled across provinces to seek medical care and those who remained within their province. These findings provide important information for service planning.

Implications of all the available evidence

Our study provides the first nationally representative, real-world data assessing China's health system performance in childhood cancer care. These findings highlight China's contribution to global efforts to meet the WHO Global Initiative for Childhood Cancer 2030 target, with at least 60% 5-year survival nationally among patients aged 0–19 years. Despite this achievement, substantial regional disparities in survival remain, driven by structural and multifaceted factors including uneven health-care resource distribution, financial hardship, and deficiency in insurance and social support systems. Although travelling to seek health care was associated with better survival, disparities persisted, aligned with the socioeconomic development of both the patients' home regions and the locations where they received care. Our findings highlight the need for targeted interventions to address these disparities. Based on existing literature, potential strategies could include establishing regional paediatric cancer centres, standardising referral pathways, and applying artificial intelligence to improve diagnostics in resource-limited settings. These efforts are especially important for cancers with considerable unmet needs, including leukaemias, hepatic tumours, malignant bone tumours, and soft tissue sarcomas, particularly among adolescents. Health systems should also ensure continuity of care during the transition from childhood to adolescence and from adolescence to adulthood. Sustained investment and coordinated policy efforts across regions are essential to achieve equitable and high-quality childhood cancer care, a conclusion which could also be relevant for other regions facing similar challenges.

Mpox (früher Affenpocken) ist eine durch Viren verursachte Infektionskrankheit, die im Januar 2026 weiterhin weltweit und in Deutschland zirkuliert. Die Situation ist durch verschiedene Virusvarianten (Kladen) geprägt, wobei die neue Variante **Klade Ib** seit Anfang 2026 auch durch lokale Übertragungen in Deutschland (speziell in Berlin) nachgewiesen wurde.

The main vaccine for monkeypox (now called mpox) is JYNNEOS (MVA-BN), a safe, two-dose shot approved for preventing both mpox and smallpox, used as pre-exposure or post-exposure prophylaxis for high-risk groups like men who have sex with men, people with multiple partners, or those exposed to the virus.

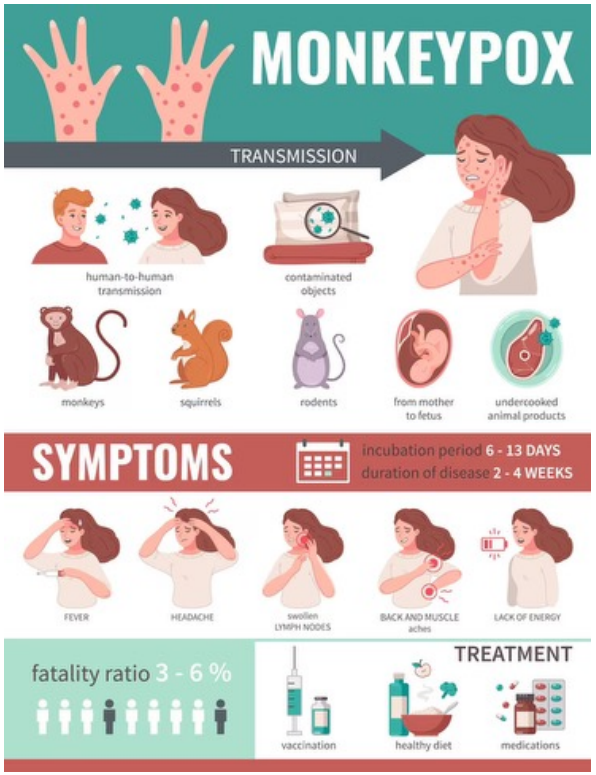

Maternal and neonatal outcomes after infection with monkeypox virus clade I during pregnancy in DR Congo: a pooled, prospective cohort study

Summary

Background Monkeypox virus (MPXV) has been linked to vertical transmission, but systematic data are scarce. We aimed to describe the sociodemographic, clinical, and virological characteristics and assess the frequency and determinants of adverse outcomes in pregnant women with MPXV clade I infection.

Methods In this prospective cohort study, we pooled data from three cohort studies (MBOTE-SK, PREGMPOX, and Uvira mpox) and one randomised controlled trial (PALM007) conducted in the South Kivu, Maniema, and Sankuru provinces of DR Congo between Dec 29, 2022, and June 20, 2025. Pregnant women and adolescent girls with a PCR-confirmed diagnosis of mpox were followed up throughout hospitalisation for mpox, delivery, and until discharge during the postpartum period. We extracted data on sociodemographic characteristics, MPXV exposure, clinical and obstetric presentation, and laboratory results. In a univariable analysis, we examined factors associated with the following adverse outcomes: spontaneous or missed abortion (<20 weeks of gestation), stillbirth (≥20 weeks of gestation), preterm birth (<37 weeks of gestation), live birth of a neonate with macroscopic mpox-like lesions, early (first 7 days) neonatal death, congenital anomaly, or maternal death (during pregnancy or discharge postpartum).

Findings We collected data from 89 pregnant women in the first (25 [28%]), second (31 [35%]), and third (33 [37%]) trimesters across all four studies: MBOTE-SK (36 [40%]), PREGMPOX (24 [27%]), PALM007 (25 [28%]), and Uvira mpox (four [4%]). All participants recovered from mpox; no maternal deaths were reported. During hospitalisation for mpox, fetal loss was reported in 17 (19%) women. Final pregnancy outcomes were known for 69 (78%) participants; adverse outcomes were reported in 35 (51%) women (95% CI 38–63), including fetal loss in 31 (45%; 95% CI 33–57; 16 [52%] spontaneous abortions, four [13%] missed abortions, and 11 [35%] stillbirths). Of the 38 live births, four neonates had congenital mpox-like lesions; one infant died a few hours after birth. No preterm births or congenital abnormalities were recorded. MPXV infection during the first trimester was associated with a higher risk of adverse pregnancy outcomes than during the second (risk ratio [RR] 0·6 [95% CI 0·4–0·9]) and third (0·2 [0·1–0·4]) trimesters (p=0·0008). Adverse outcomes were also associated with high viral load in skin lesions (PCR cycle threshold ≤30; RR 3·5 [95% CI 1·0–12·3]; p=0·045), direct sexual contact with the index case (1·6 [1·1–2·4]; p=0·026), positive HIV status (2·0 [1·4–2·9]; p=0·0002), and the presence of genital lesions (1·9 [1·1–3·2]; p=0·025).

Interpretation MPXV clade I infection in pregnancy is associated with a high risk of fetal loss and congenital infection, particularly during the first trimester. Targeted preventive and clinical strategies are urgently needed to protect pregnant women and their infants in settings that are endemic and epidemic for mpox.

Funding The European and Developing Countries Clinical Trials Partnership, the Belgian Directorate-General Development Cooperation and Humanitarian Aid, the Swiss National Science Foundation, the Research Foundation–Flanders, the Gates Foundation, the Intramural Research Program of the National Institutes of Health, and the National Cancer Institute.

	Participants (n=89)
Study settings	
Original study	
MBOTE-SK	36 (40%)
PREGMPOX	24 (27%)
PALM007	25 (28%)
Uvira mpox	4 (4%)
Province	
South Kivu	64 (72%)
Maniema	17 (19%)
Sankuru	8 (9%)
Suspected MPXV clade*	
Clade Ib/sh2023	64 (72%)
Endemic zoonotic clade Ia	25 (28%)
Participant demographics	
Age, years	24 (20–30)
Age group, years	
≤18	14 (16%)
19–34	61 (69%)
≥35	14 (16%)
Primary occupation	
Home maker	35 (39%)
Farmer	24 (27%)
Businesswoman	18 (20%)
Sex worker	4 (4%)
Unemployed	4 (4%)
Student	1 (1%)
Other	3 (3%)
MPXV exposure characteristics	
Exposure in past 3 weeks	
Hunting	1/88 (1%)
Consumption of rodents	4/87 (5%)
Manipulation of wildlife meat	10/86 (12%)
Consumption of wildlife meat	4/85 (5%)
Contact with another mpox case	57/73 (78%)
Type of contact with index case†	
Direct, skin-to-skin, non-sexual contact	35/55 (64%)
Sexual contact	20/55 (36%)
Fomite	0

(Table 1 continues in next column)

(Continued from previous column)

	Participants (n=89)
Medical history	
Childhood smallpox vaccination	0
Mpox vaccination with MVA-BN	3/85 (4%)
Coinfection‡	
HIV	3/35 (9%)
Syphilis	0
Malaria	12/86 (14%)
Treated with tecovirimat§	8 (9%)

Data are n (%), median (IQR), or n/N (%). Denominators represent the number of participants with available data. MPXV=monkeypox virus. *Attributed based on health zone. According to genomic sequencing analyses, no co-circulation of clade Ib/sh2023 and zoonotic clade Ia has been reported in the study areas as of May, 2025. †Classified as the main exposure only. ‡Diagnosed as part of routine clinical care, either during hospitalisation or prenatal care. §Participants in the PALM007 trial, including pregnant women, were randomly assigned (1:1) to receive either placebo or tecovirimat (three 200 mg capsules twice daily for 14 days for those weighing 40–120 kg).

Table 1: **Study settings and participant demographics, MPVX exposure characteristics, and medical history**

	Participants (n=89)
Time between symptom onset and enrolment, days	7·0 (4·0–10·0)
Symptoms	
Fever	33/88 (38%)
Fatigue	55/88 (63%)
Itching	77/89 (87%)
Myalgia or arthralgia	48/88 (55%)
Pain in lesions	71/89 (80%)
Headache	43/89 (48%)
Sore throat or dysphagia	41/89 (46%)
Cough	19/89 (21%)
Anorexia	39/85 (46%)
Abdominal pain	24/85 (28%)
Vomiting or nausea	24/89 (27%)
Diarrhoea	10/89 (11%)
Dysuria	28/85 (33%)
Genital pain	30/89 (34%)
Rectal pain	8/89 (9%)
Eye pain	9/85 (11%)
Convulsion or altered consciousness	1/83 (1%)
Signs	
Presence of skin lesions	89/89 (100%)
Number of lesions	62·0 (18·5–179·2)
WHO severity score by lesion count	
Mild (<25)	27/87 (31%)
Moderate (25–99)	26/87 (30%)
Severe (100–250)	20/87 (23%)
Grave (>250)	14/87 (16%)
Type of skin lesion	
Macule	13/85 (15%)
Papule	31/87 (36%)
Vesicle	69/87 (79%)
Small pustule	52/84 (62%)
Umbilicated pustule	31/83 (37%)
Ulcerated lesion	16/83 (19%)
Crust	16/83 (19%)
Scar	14/84 (17%)
Genital skin lesions	46/84 (55%)
Genital oedema	23/81 (28%)
Rectal lesions	11/83 (13%)
Lymphadenopathy	53/83 (64%)
Virological test results	
MPXV PCR-positive skin lesion	89/89 (100%)
Ct value of skin lesion swab	20·5 (18·1–25·0)
MPXV PCR-positive oropharyngeal swab	30/34 (88%)
Ct value of oropharyngeal swab	28·3 (23·8–31·2)
MPXV PCR-positive blood sample*	12/26 (46%)
Clinical outcomes during hospitalisation	
Duration of hospital stay, days	13·0 (7·0–15·0)
Maternal death	0

Data are median (IQR) or n/N (%). Denominators represent the number of participants with available data. Ct=cycle threshold. MPXV=monkeypox virus. *Only one Ct value available: 33·1.

Table 2: **Clinical presentation and outcomes of pregnant women with mpox**

	Participants (n=89)
Gestational trimester at the time of mpox diagnosis (weeks of gestation)	
First (1–13)	25/89 (28%)
Second (14–27)	31/89 (35%)
Third (≥28)	33/89 (37%)
Obstetric history	
Female genital mutilation	0
Number of previous pregnancies	
0	18/84 (21%)
1	8/84 (10%)
2	12/84 (14%)
≥3	46/84 (55%)
Previous caesarean section	15/83 (18%)
Previous miscarriage	16/83 (19%)
Previous premature delivery	1/67 (2%)
Previous stillbirth	4/67 (6%)
Previous birth of neonate with congenital anomalies	0
Attended prenatal consultation	8/60 (13%)
Diagnosed complications during current pregnancy*	
Gestational diabetes	0
Hypertension	0
Polyhydramnios	3/57 (5%)
Preterm pre-labour rupture of membranes (<37 weeks of gestation)	4/57 (7%)
Pregnancy complications during hospital admission for mpox	18/89 (20%)
Spontaneous abortion	11/89 (12%)
Missed abortion	3/89 (3%)
Stillbirth	3/89 (3%)
Vaginal bleeding and abdominal pain without pregnancy loss	1/89 (1%)
Pregnancy outcomes	
Participants with available outcome data	69/89 (78%)
Delivery of healthy neonate	34/69 (49%)
Adverse outcome	35/69 (51%)
Spontaneous abortion (<20 weeks of gestation)	16/69 (23%)
Missed abortion (<20 weeks of gestation)	4/89 (5%)
Stillbirth (>20 weeks of gestation)	11/69 (16%)
Preterm live neonate (<37 weeks of gestation)	0
Live neonate with macroscopic lesions	3/69 (4%)
Live neonate with macroscopic lesions and neonatal death	1/69 (1%)
Maternal death	0
Neonate with congenital anomalies	0
MPXV PCR-positive placental swab	9/12 (75%)
Ct value of placental swab	23·6 (20·9–32·2)
Duration from hospital admission to adverse outcome, days	
Spontaneous abortion	11·0 (6·8–14·0)
Missed abortion	20·5 (18·8–22·5)
Stillbirth	14·0 (12·5–15·0)

Data are n/N (%) or median (IQR). Denominators represent the number of participants with available data. Ct=Cycle threshold. MPXV=monkeypox virus. *Pregnancy complications occurring before discharge from the mpox treatment centre.

Table 3: **Obstetric history and outcomes in pregnant women with mpox**

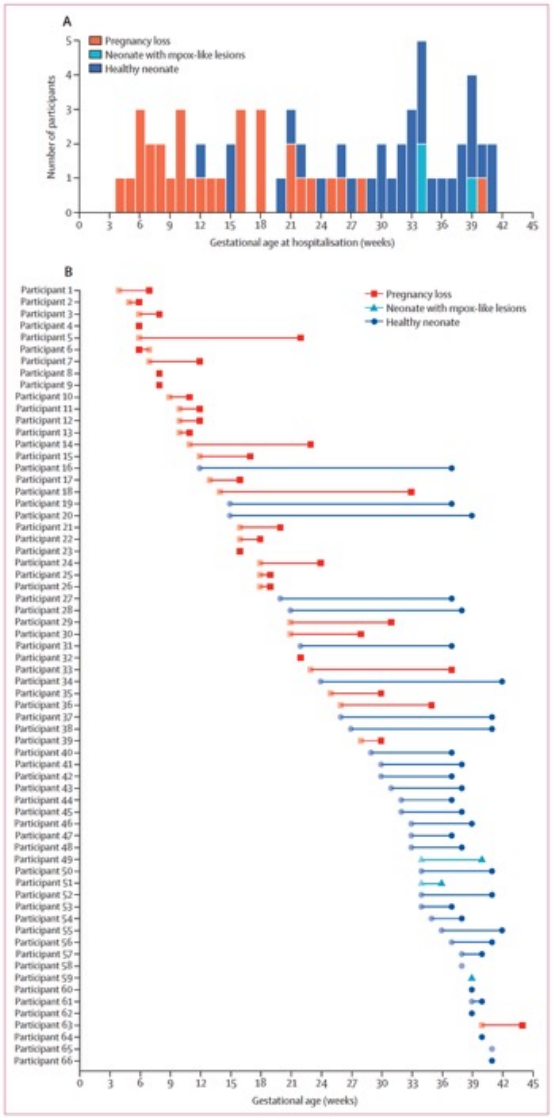

Figure: **Pregnancy outcomes among 66 women with mpox by gestational age**
(A) Frequency of pregnancy outcomes (pregnancy loss, delivery of a neonate with mpox-like lesions, or delivery of a healthy neonate) stratified by gestational age at hospitalisation. (B) Individual participant timelines between hospitalisation for mpox (pale symbol) and delivery according to pregnancy outcome (dark symbol). Gestational age at delivery was unknown for two women. Three women with an unknown exact gestational age at hospitalisation were excluded.

	Overall (n=69)	Healthy neonates (n=34)	Adverse outcomes (n=35)	Risk ratio* (95% CI)	p value†
Demographics					
Maternal age group, years					
≤18	10/69 (14%)	5/10 (50%)	5/10 (50%)	1 (ref)	0·48
19–34	46/69 (67%)	20/46 (44%)	26/46 (57%)	1·1 (0·6–2·2)	–
≥35	13/69 (19%)	9/13 (69%)	4/13 (31%)	0·6 (0·2–1·7)	–
Suspected MPVX clade					
Clade Ia	24/69 (35%)	11/24 (46%)	13/24 (54%)	1 (ref)	0·67
Clade Ib/sh2023	45/69 (65%)	23/45 (51%)	22/45 (49%)	0·9 (0·6–1·4)	–
Gestational characteristics at diagnosis					
Gestational age, weeks	23·5 (13·2–34·0)	33·0 (26·8–37·2)	15·0 (8·2–21·8)	–	–
Data missing	3/69 (4%)	2/34 (6%)	1/35 (3%)	–	–
Trimester					
First	18/69 (26%)	1/18 (6%)	17/18 (94%)	1 (ref)	0·0008
Second	22/69 (32%)	9/22 (41%)	13/22 (59%)	0·6 (0·4–0·9)	–
Third	29/69 (42%)	24/29 (83%)	5/29 (17%)	0·2 (0·1–0·4)	–
Type of MPXV exposure‡					
Direct, non-sexual, skin-to-skin contact with index case	30/43 (70%)	14/30 (47%)	16/30 (53%)	1 (ref)	0·026
Direct sexual contact with index case	13/43 (30%)	2/13 (15%)	11/13 (85%)	1·6 (1·1–2·4)	–
Clinical presentation					
Total lesion count	60·0 (13·0–164·5)	66·0 (9·0–183·0)	59·0 (25·0–150·0)	–	–
Data missing	7/69 (10%)	5/34 (15%)	2/35 (6%)	–	–
WHO severity score by lesion count					
Mild (<25)	22/67 (33%)	13/22 (59%)	9/22 (41%)	1 (ref)	0·69
Moderate (25–99)	19/67 (28%)	6/19 (32%)	13/19 (68%)	1·7 (0·9–3·0)	–
Severe (100–250)	16/67 (24%)	8/16 (50%)	8/16 (50%)	1·2 (0·6–2·5)	–
Grave (>250)	10/67 (15%)	5/10 (50%)	5/10 (50%)	1·2 (0·6–2·7)	–
Fever					
No	44/68 (65%)	21/44 (48%)	23/44 (52%)	1 (ref)	0·62
Yes	24/68 (35%)	13/24 (54%)	11/24 (46%)	0·9 (0·5–1·5)	–
Genital skin lesions					
No	28/64 (44%)	18/28 (64%)	10/28 (36%)	1 (ref)	0·025
Yes	36/64 (56%)	12/36 (33%)	24/36 (67%)	1·9 (1·1–3·2)	–
Living with HIV					
No	28/31 (90%)	14/28 (50%)	14/28 (50%)	1 (ref)	0·0002
Yes	3/31 (10%)	0	3/3 (100%)	2·0 (1·4–2·9)	–
Co-infection with malaria					
No	59/68 (87%)	30/59 (51%)	29/59 (49%)	1 (ref)	0·26
Yes	9/68 (13%)	3/9 (33%)	6/9 (67%)	1·4 (0·8–2·3)	–
Virological test results					
Ct value of skin lesion swab	20·6 (18·0–25·1)	23·5 (19·0–35·6)	20·1 (17·5–21·7)	–	–
Data missing	19/69 (28%)	14/34 (41%)	5/35 (14%)	–	–
Viral load of skin lesion swab					
Low (Ct value >30)	10/50 (20%)	8/10 (80%)	2/10 (20%)	1 (ref)	0·045
High (Ct value ≤30)	40/50 (80%)	12/40 (30%)	28/40 (70%)	3·5 (1·0–12·3)	–
Ct value of oropharyngeal swab	28·8 (23·7–31·5)	30·0 (27·7–33·4)	27·3 (23·1–31·0)	–	–
Data missing	44/69 (64%)	24/34 (71%)	20/35 (57%)	–	–
Viral load of oropharyngeal swab					
Low (Ct value >30)	11/25 (44%)	5/11 (45%)	6/11 (55%)	1 (ref)	0·63
High (Ct value ≤30)	14/25 (56%)	5/14 (36%)	9/14 (64%)	1·2 (0·6–2·3)	–

Data are n/N (%) or median (IQR), unless otherwise indicated. Denominators represent the number of participants with available data. Ct=cycle threshold. MPXV=monkeypox virus. *Calculated with Poisson regression with robust SEs. †Fisher's exact test for categorical variables and Wilcoxon rank-sum test for continuous variables. ‡Contact type classified as the main exposure only.

Table 4: **Factors associated with adverse pregnancy outcomes**

Research in context

Evidence before this study

Monkeypox virus (MPXV) infection in pregnancy has been linked to vertical transmission and adverse pregnancy outcomes. We searched PubMed, Google Scholar, medRxiv, and bioRxiv for articles published in English from database inception to Sept 12, 2025, using the following terms: ("monkeypox" OR "mpox" OR "monkeypox virus") AND ("pregnancy" OR "pregnancy outcome" OR "perinatal" OR "pregnancy complications" OR "pregnant people" OR "vertical transmission" OR "placenta"). We also searched websites and publications from WHO and the US Centers for Disease Control and Prevention. Our search identified 52 publications, of which 18 reported primary clinical data from 16 studies, three reported preclinical data, and four were systematic reviews; the other 27 publications were narrative reviews, guidelines, letters, or editorial commentaries without primary data. Seven publications from 16 studies were from DR Congo, where MPXV clade I is endemic. These publications described 64 pregnancies, with adverse outcomes reported in 21 (70%) of 30 pregnancies with known outcomes. The earliest report of mpox in pregnancy was published in 1988 in Zaire (present day DR Congo). A woman who presented with mpox in the third trimester gave birth to a premature infant with a generalised mpox rash who died 6 weeks later. Another study, conducted between 2007 and 2011 in an area of DR Congo endemic for MPXV clade Ia, reported MPXV infection in four pregnancies, of which two resulted in spontaneous abortion and one in a stillbirth with visible fetal lesions. Histopathological evidence confirmed vertical transmission. Three studies have reported pregnancy outcomes in the South Kivu province, where MPXV clade Ib/sh2023 was first identified in 2023. In a study of 21 pregnant women with mpox, known pregnancy outcomes for six women included three fetal deaths and one full-term infant with mpox skin lesions who died shortly after birth. A report on three cases, one from each trimester, provided histological and molecular evidence on the vertical transmission of MPXV. An additional report from the same region documented 14 pregnancies with eight adverse outcomes. An mpox surveillance-based study conducted between October, 2023, and September, 2024, documented pregnancy loss in two of 21 reported pregnancies.

Added value of this study

In this pooled, prospective cohort study, we collected data on 89 pregnant women from three provinces across DR Congo, including two where MPXV clade Ia is in circulation and one where clade Ib is in circulation. This study design provides evidence on the adverse outcomes of infection with mpox clade I in pregnancy, which is less biased and more precise than the conclusions of case reports and case series. The geographical coverage of the study, covering areas affected by both clade Ia and Ib/sh2023 MPXV, makes these findings more generalisable than studies from a single location in DR Congo. By studying women with mpox diagnosed at all stages of pregnancy and following them up until delivery, this study shows a higher risk of adverse outcomes with mpox infection during the first trimester than during the second or third trimester. The study identified factors that clinicians and researchers can use for future monitoring and investigation of pregnant women with mpox clade I infection.

Implications of all the available evidence

MPXV clade I infection is associated with a substantial risk of adverse pregnancy outcomes, particularly when infection occurs during the first trimester. MPXV acquired during pregnancy should be regarded as a congenital pathogen, with outcomes resembling those of other congenital viral infections. Pregnant women and women of childbearing age should be prioritised for preventive and therapeutic interventions, including vaccination. Long-term studies are needed to assess the developmental consequences of congenital mpox.

The *Lancet* Commission on improving population health post-COVID-19

Panel 1: **Priority recommendations**

- Replace harmful policies and interventions with actions to improve population health and the natural environment
- Enhance the effectiveness of governments, commercial actors, and civil society to improve population health
- Develop capability and capacity in systems level responses to the three threats, with demonstrable progress by 2030

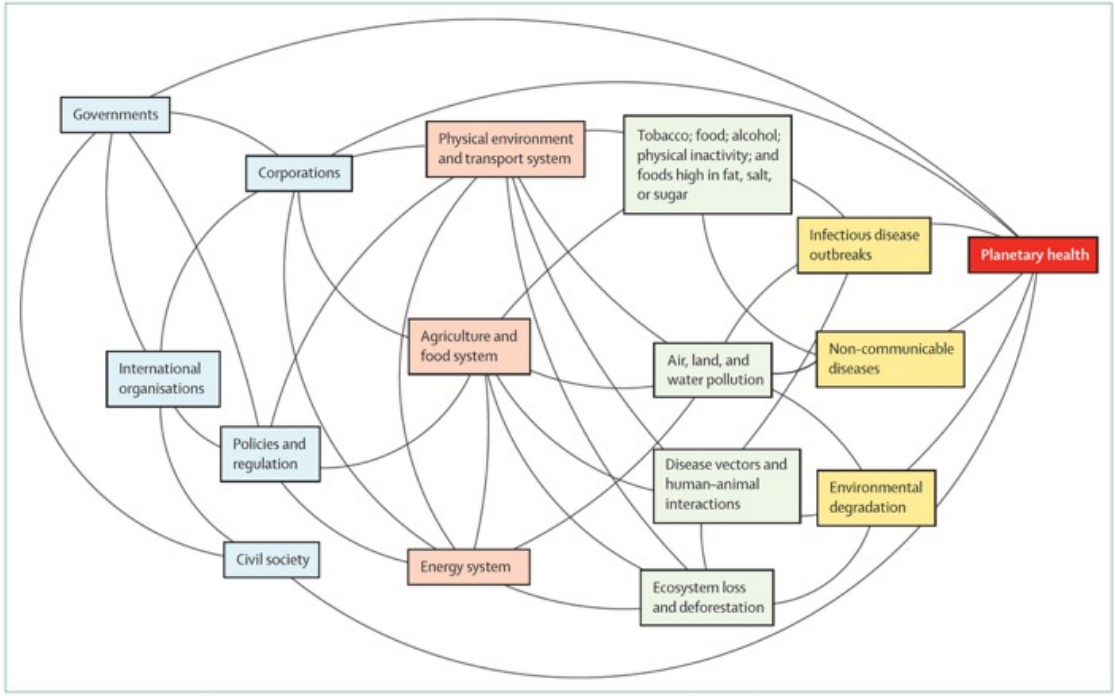

Figure: **Conceptual model of key actors, systems, and drivers of the three major threats to population health**
Blue=actors. Orange=systems. Green=drivers. Yellow=impacts. Red=outcome.

	Proposed interventions	Mitigating potential harms
Aim 1: Achieve healthy and sustainable physical environment and transport systems		
Objective 1: Ensure healthy and sustainable transport		
Design and build infrastructure in urban and rural areas to enable and prioritise safe, affordable, accessible, and convenient active travel and public transport.	Prioritise and invest in active travel infrastructure and public transport; make public and active transport more affordable and convenient than private cars.	Car ownership is strongly socially patterned. Removing advantages of private car use and providing safe, affordable, accessible, reliable, public, and active transport alternatives will help reduce inequalities; increased active travel and reduced car use will increase physical activity levels of the population, leading to reduced incidence and prevalence of non-communicable diseases, as well as concomitant benefits in outcomes from communicable diseases, such as COVID-19.
Objective 2: Reduce the need to travel		
Design, build, and manage urban and rural environments in which the need for vehicles is reduced.	Prioritise active travel and sustainable mobility over private car use; reallocate subsidies from harmful sectors to beneficial sectors.	Designing urban systems that prioritise walking, cycling, and free or low-cost public transport over private motorised travel reduces transport-related inequalities.
Objective 3: Healthy sustainable urban ecosystems		
Design habitations and associated areas to foster biodiversity and to support and restore ecosystems, including, where relevant, the provision of accessible public green and blue spaces (eg, rivers, lakes, and seas).	Planning and transport policy is designed to generate health, environmental, and sustainability benefits.	Incentivise biodiversity preservation in low-resource contexts; mandate requirements not to widen social, health, or other inequalities when protecting and restoring ecosystems; urban green space improves air quality, provides shade, reduces urban heat intensity, and contributes to increased physical activity and improved mental health.
Objective 4: Ensure healthy and sustainable construction		
Ensure all private and public buildings incorporate sanitation, ventilation, and temperature regulations that do not contribute to exceeding planetary boundaries or harm health.	Mandate planning and building regulations that prioritise sustainability, health, and resource efficiency; pricing to disincentivise high resource use and incentivise sustainable practice.	Mandating standards drives economies of scale; provide grants and subsidies for people with low income; place per-capita limits on resource use; design and construct healthier buildings that can reduce energy use (eg, through use of natural ventilation) and exposure to indoor air pollutants; and promote physical activity (eg, using stairs rather than lifts).
Aim 2: Achieve healthy and sustainable agriculture and food systems		
Objective 5: Ensure healthy and sustainable agriculture		
Conduct all activities within the agriculture and food system, including production, processing, packaging, distribution, and consumption, within planetary boundaries in proportion to yields, and ensure activities do not cause other harms such as increasing animal–human contact.	Regulation to reduce the impact of agriculture on the environment, based on robust and appropriate metrics; pricing to drive rapid and long-term reductions in carbon intensity; reallocate subsidies from harmful sectors to beneficial sectors.	Increases in prices of food should be addressed through food system measures and wider mitigation measures, such as welfare systems and redistributive taxation; maintain support for Indigenous people's land-use and food practices and traditional forms of agriculture, where these practices are beneficial in terms of health and environmental outcomes; sustainable agriculture reduces environmental harms, such as carbon emissions and biodiversity loss; reduced livestock production decreases the likelihood of zoonotic disease development.
Objective 6: Provide healthy and sustainable food for all		
Design production and distribution systems to ensure access to sufficient nutritious food (eg, fruit and vegetables) for everyone on the planet; reduce waste through supply and demand mechanisms; and reduce or eliminate environmentally harmful products.	Mandate food buying standards for healthy and sustainably grown food for the public and private sectors; mandate reporting for large food companies; reallocate subsidies from harmful sectors to beneficial ones.	Increases in prices of food should be addressed through food system measures and wider mitigation measures, such as redistributive taxation – healthier diets that result from these measures will lead to decreased prevalence of NCDs; maintain support for Indigenous people's land-use and food practices and traditional forms of agriculture, where these practices are beneficial in terms of health and environmental outcomes.
Objective 7: Reduce harmful produce		
Reduced production and consumption of alcohol; tobacco; foods high in fat, sugar, and salt; animal-sourced foods; and other produce that harms population health and the environment.	Regulate to reduce production, availability, and marketing of these products; fiscal and other pricing measures to reduce affordability.	Provide retraining and re-employment for people who lose employment in industries producing these harmful products.
Objective 8: Ensure sustainable land use		
Protect and restore land and marine ecosystems in rural areas through reforestation, rewilding, and reintroduction of native animals.	Conduct large-scale rewilding, protect pristine ecosystems, and incentivise restoration; subsidise agricultural activities that promote ecosystem protection and restoration, based on robust and appropriate metrics; purchase land to create areas for restoration.	Retraining and re-employment for people who lose employment in industries that destroy or damage ecosystems; support Indigenous people to act as custodians; global accounting systems and other mechanisms to prevent perverse incentives.

(Table 1 continues on next page)

(Continued from previous page)

	Proposed interventions	Mitigating potential harms
Aim 3: Achieve healthy and sustainable energy systems		
Objective 9: Achieve zero carbon energy		
Stop new fossil fuel exploration, extraction, or power stations from being built; end all fossil fuel use while ensuring energy security via a fair transition to net zero carbon energy sources.	Ban new fossil fuel power plants; rapidly reduce emission limits; accelerate construction of sustainable energy generation infrastructure; escalate carbon and other pricing measures; reallocate subsidies from harmful sectors to beneficial sectors.	Protect households from fuel poverty through welfare programmes and by reallocating subsidies; mandating relevant standards should drive economies of scale; retraining and redeployment programmes for the more than 18 million people globally working in fossil fuel and related industries.
Objective 10: Healthy sustainable energy production		
Reduce harms caused by energy production and from equipment for its storage and use; reduce production and consumption to reduce energy-related harms both during and after the energy transition, including any harms related to sustainable energy.	Control development of mining and extraction, with strict regulation of waste disposal; require recycling and reuse of raw materials; pricing measures to promote recycling and re-use of raw materials; disincentivise energy use.	Ensure global cooperation on transparency and reporting mechanisms, aligned with national agreements on restrictions to embedded emissions and other externalities.

Table 1: **Summary of Commission aims, objectives, interventions, and mitigations**

Panel 2: Summary of economic analyses of carbon pricing on land transport and food systems

Carbon pricing of US$385–560 tCO_2 by 2050 has the potential to:

- Reduce urban land transport emissions by up to 25%
- Reduce land use emissions by up to 85%, relative to business-as-usual emissions
- Prevent 200 million incident cases of non-communicable diseases by 2050, largely driven by increased physical activity and reduced red meat consumption
- Save more than $12 billion per year in health-care expenditure from type 2 diabetes alone
- Reverse biodiversity decline and reduce environmental risk factors for zoonotic diseases, water pollution, and antimicrobial resistance

Achieving these impacts on transport and agriculture is highly contingent on the suitability and availability of alternatives to current carbon-intensive transport and diets, and also on people's willingness to change their behaviours. The higher the price, the lower the emissions, but the greater the unwanted harmful impacts. As prices increase, so do the benefits, but not at the same rate of increase as a result of unwanted harmful impacts. Even high levels of carbon price will not reduce carbon emissions as much as is required to achieve net zero targets. Achieving the additional reductions in emissions necessary to achieve net zero will require much more ambitious policy responses than any governments have planned across land transport and agriculture and food. Carefully designed pricing policies and packages of measures will be needed to mitigate any unintended consequences for people with low income or vulnerable groups, adjusted for different global regions and levels of development.

	Potential solutions	Additional actions to address barriers
Action 1: Effective state institutions and political leadership at national, local, and international levels to achieve long-term objectives		
Competing ideologies and interests	Coalitions of leaders to develop a common vision and goals	Legally binding commitments to achieve a common vision
Corruption and state capture by businesses and elites	Effective governance frameworks, including legally binding commitments to increase accountabilty of governments	Reject industry-led voluntary pledges in favour of robust policy packages that include regulations that are enforced
Inadequate capability and relevant expertise within governments and the research community	Establish a platform to collate and share evidence and practices, while building capacity in systems approaches	Requirement of governments to increase representation of women in parliaments
Prioritising short-term over long-term objectives	Agreed metrics to measure progress against common vision and goals	Requirement of governments to consider the rights and interests of future generations to a healthy environment
Action 2: Businesses comply with regulations and policies		
Business interference in policy making through misinformation and other practices	Adopt and strengthen governance systems to protect policies from business interests that conflict with public interests in health and the natural environment	Establishing networks of activist investors holding businesses to account for long-term impacts on health and environment
Incentives for businesses to harm health and the natural environment (eg, subsidies on harmful products and activities) and insufficient disincentives for businesses harming health and the natural environment (eg, external costs not borne by businesses generating these harms)	Incentivise sustainable and healthy business activities and disincentivise unsustainable ones using fiscal and other regulatory measures, including legally binding standardised metrics for business reporting	Implement polluter-pays policies or equivalent to ensure businesses pay the full cost of any harm from the production or consumption of their products to health or the natural environment
Action 3: Engage and empower citizens and civil society		
Disengagement from democratic processes as reflected in declining voter turnout	Protect against misinformation and disinformation, including that which encourages inactivism	Embedding deliberative processes into policy making at all levels of government
Distrust of governments and politicians to serve the interests of citizens	Leaders acting in trustworthy ways (ie, being responsive to citizens; being reliable; and acting with integrity, openness, and fairness)	Governments to deliver on long-term interests of citizens with policy-making processes open to public scruitiny
Low public acceptability of interventions	Communicate the effectiveness of policies in ways understood by most people	Design policies fairly (ie, ensuring that those who are most vulnerable benefit most with least cost)
Exclusion and marginalisation of civil society actors and interests by leaders and regimes	Empower and fund civil society organisations to engage meaningfully in policy development	Governments to widen suffrage by lowering voting age to engage younger generations

Table 2: **Barriers to recommended actions for improving population health**

Panel 3: Which factors affect public support for carbon and other pricing measures?

We conducted a rapid review of evidence on public support for carbon and other pricing measures. This review was restricted to studies using experimental designs as described in a pre-registered protocol.[209] The 37 studies included in this review were all conducted in high-income counties, so their generalisability to low-income and middle-income countries remains unknown. Three principal aspects of policy design with potential to alter support were identified:

Price levels

27 sets of comparisons reported in 11 studies across ten publications assessed how changes in public support for carbon pricing depended on how revenues were used.[210–219] 19 of 27 comparisons had significantly lower support for higher prices, with eight of 27 comparisons reporting no difference. No studies reported that higher prices were associated with increased support.

Perceived fairness

Three of 11 studies also assessed perceived fairness of pricing levels. Each study found that lower perceived fairness was associated with lower support for higher prices.[214–216] One study assessed perceived effectiveness of higher prices,[214] and found it was unrelated to public support. The extent to which loss of support for higher pricing levels can be offset if revenues are used for environmental purposes (particularly public transport) or rebates remains to be determined.

Earmarking revenues

20 studies, reported across 11 publications, assessed changes in support with revenue use, reported in 91 sets of comparisons.[212,215,216,220–227] Within these sets, 36 of 59 comparisons reported increased support if the revenues went towards tax rebates, 14 of 18 comparisons reported increased support if the revenues were earmarked for environmental purposes, and seven of 26 comparisons reported increased support if the revenues used for non-environmental purposes. There was no increase in support in the 16 comparisons where revenues were allocated to general state funds.

Six studies reported across four publications[212,223–225] examined revenue use for environmental purposes. Across 17 sets of comparisons, energy efficient transport was the most frequently studied, with ten of 11 comparisons showing higher support. The other environmental purposes examined were renewable energy investments (one comparison), and unspecified environmental purposes (five comparisons). Four of these six studies[222,224,226,227] found that support was partly explained by perceived effectiveness of the revenue use at improving environmental problems.

Panel 4: Strategic litigation to protect public health and the natural environment

Strategic litigation aims for "an intended impact beyond a particular case to influence broader change at the level of law, policy, practice, or social discourse".[242] Strategic litigation can therefore expose and help to change the practices of industries that contribute to poor health or environmental degradation, and to challenge the failure of governments to regulate commercial practices that infringe human rights, especially the right to life, enjoyment of the highest attainable standard of health, and nutritious adequate food.

Specific population groups and civil society organisations are increasingly challenging governments for their failure to tackle climate change,[243] air pollution, and unhealthy diets. Some of these cases have started to yield interesting results. For example, on April 9, 2024, the European Court of Human Rights ruled that Switzerland had failed to comply with its positive obligations under the European Convention on Human Rights.[244] In this case, over 2000 older women complained of various failures by the Swiss authorities to mitigate climate change (particularly the effect of global warming), which adversely affected their lives, living conditions, and health. After emphasising that climate change was one of the most pressing issues of our times, the European Court of Human Rights held that states had a primary duty to adopt and apply regulations and measures capable of mitigating the existing and potentially irreversible future effects of climate change.[245]

Beyond engaging in legal disputes in courts, citizens (including children) have also relied on other human rights accountability mechanisms to complain against their governments for failure to respect, protect, and fulfil their human rights. The most prominent example is the petition to the Committee on the Rights of the Child in 2019 lodged by 16 children from around the world against five governments: Argentina, Brazil, France, Germany, and Türkiye.[246]

In some cases, the impact of strategic litigation has been tangible, leading to direct changes to policy or corporate practices. For example, ClientEarth repeatedly challenged the UK's government in court on the basis that its air quality plans were unlawful as they failed to address dangerous levels of air pollution. As a result, the UK was forced to amend these plans.[247] Alana, a consumer protection organisation in Brazil, filed an amicus curia brief in support of the Sao Paulo State Attorney in the challenge in 2016 against Pandurata Alimentos for a deceptive unhealthy food marketing campaign to children.[248]

In other cases, less tangible impacts have raised awareness of (and established) health problems as human rights concerns, therefore highlighting the need to ensure state accountability for human rights violations, supported citizen participation (directly or indirectly through civil society organisations), and increased political will for interventions, promoting better health for all. The potential of human rights-based approaches to population health and ecological justice remains underexplored, although there is growing momentum, particularly in relation to climate change and air pollution.[249]

Panel 5: Human rights-based approach to commercial determinants of health and environmental degradation

The constant legal and political challenges to public health measures from industry or states call for a reconsideration of how the law, particularly human rights law, is used to promote better health for all. A human rights-based approach calls for compliance with human rights standards and principles, particularly the principle of accountability. States must ensure that mechanisms are in place for people to hold them accountable for their actions or failures to act. There must be processes in place allowing people to claim their rights, and remedies allowing them to be compensated should these rights be violated. These processes can be judicial or extrajudicial (eg, an ombudsperson or other agency), and supported by civil society organisations. The benefits of a human rights-based approach in regulating the commercial determinants of health and environmental damage include:[250]

Accountability

A human rights-based approach guarantees a degree of accountability, making effective remedies more likely where rights are violated. This approach makes it easier for the commitments and obligations established in international human rights law to be translated into practicable, long-lasting, and realisable entitlements, guaranteed by independent monitoring bodies, including courts and national human rights institutions.

Empowerment

Once the concept of rights is introduced into policy making, the rationale for improving environments and preventing diseases comes from the fact that individuals not only have needs, but also rights—ie, legal entitlements that give rise to legal obligations on the part of states.

Legitimacy

As human rights are inalienable and universal, there is an inherent legitimacy. Arguments based on human rights can ensure that an issue is given special consideration and that competing interests lose legitimacy if they are incompatible with human rights.

Advocacy and participation

An approach based on human rights provides an opportunity to build strategic alliances, coalitions, and networks with other actors who share a similar vision and pursue common objectives. Such an approach might attract a broad range of actors who might not have previously viewed the work of this Commission as a human rights concern (eg, human rights civil society organisations and human rights protection agencies). This approach might help galvanise political will and increase pressure on states to comply with their human rights obligations and therefore address communicable and non-communicable diseases, as well as environmental degradation.

***Panel 6*: Case examples of replacing livelihoods in the tobacco industry**

In 2023, 48% of the world's tobacco was grown in China (36%) and India (12%).[378]

China

In China, the tobacco industry is a state monopoly with annual production of tobacco determined centrally. Reflecting government policies to reduce smoking through increased taxes and anti-smoking campaigns, the area of land devoted to tobacco farming has reduced from 1·55 million hectares in 2013 to 1·08 million hectares in 2023.[379] To our knowledge, no government-led programme has encouraged the farming of other crops. However, in the Yuxi municipality, collaborators from the Yuxi Bureau of Agriculture and the University of California at Los Angeles School of Public Health initiated a tobacco crop substitution project. At three sites, 458 farm families volunteered to participate in a new, for-profit cooperative model. Farmers at these sites increased their annual income by 21%–110% per acre compared with farmers who planted tobacco. Grapes were the most lucrative crop. Since 2011, the Yuxi Bureau of Agriculture has extended the project to other counties. Farmers themselves are taking the initiative to reduce tobacco cultivation in favour of other crops. From 2012 to 2015, the per capita net income of Yuxi municipality increased by more than ¥3000 (US$484).

India

In India, an important part of the tobacco industry is the production of cheap cigarettes in the form of beedis. Beedis are more lethal than manufactured cigarettes and consumed mainly by people with low income.[380] Up to 85% of people engaged in informal and highly exploitative beedi rolling are women.[381] Programmes to develop skills for alternative livelihoods have been underway for over 20 years,[382] but only 0·06% of India's beedi workers are involved.[383] Two southern states, Tamil Nadu and Karnataka, have been particularly successful at recruiting women to such programmes.[384] A pilot project by the International Labour Organisation in 2000, in partnership with local organisations and non-governmental organisations, recruited 4500 women who were beedi workers from the cities of Mangalore, Karnataka and Sagar, Madhya Pradesh to help build their skills, confidence, and status in society. The project identified other sources of income generation—such as jackfruit agriculture, tailoring, and baking, as well as linkages for marketing these products—and has increased income levels three-fold to four-fold.[382] Further action is still needed to help women move away from employment in an industry that disproportionately exploits and causes the death of people with low income.

Conclusion

Acting on these recommendations would help slow the harmful trajectories created by the three threats at the core of this Commission. The recommendations need to be combined with other major shifts, such as universal health coverage, achieving sex, gender, and racial parity, and the eradication of poverty, each of which is necessary but not sufficient alone to generate the required sustainable improvements in population health and natural environments worldwide. The three threats we confront in this Commission have developed over many years, and we are aware of the difficult challenges involved in effectively addressing them, especially in the face of stagnating economies, populist politics, and the increasing influence of commercial actors. Concerted action by governments, combined with the engagement of civil society, has the potential to halt and start to reverse these harmful trends to create a more sustainable, fairer, and healthier world.

"Beiges Fett" ist ein
induzierbarer Typ von Fettzellen im menschlichen Körper, der Energie verbrennen und zur Wärmeerzeugung beitragen kann, im Gegensatz zu weißem Fett, das hauptsächlich Energie speichert. Es handelt sich um ein biologisches Konzept, nicht um ein kommerzielles Produkt, das man kaufen kann.

Was ist beiges Fettgewebe?

Beiges Fettgewebe (auch als "brite fat", von "brown in white" adipose tissue, bekannt) ist eine Mischform aus weißem und braunem Fettgewebe.

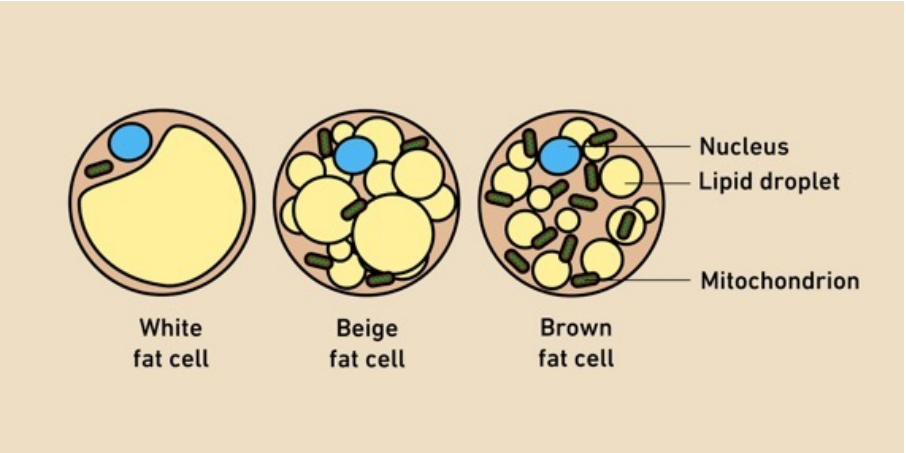

Funktion: Ähnlich wie braunes Fettgewebe verbrennen beige Fettzellen Kalorien, um Wärme zu erzeugen (Thermogenese), was dem Körper hilft, die Temperatur zu regulieren. Menschen mit einem höheren Anteil an aktivem beigem oder braunem Fettgewebe sind tendenziell schlanker und haben ein geringeres Risiko für Stoffwechselerkrankungen wie Diabetes und Herzerkrankungen.

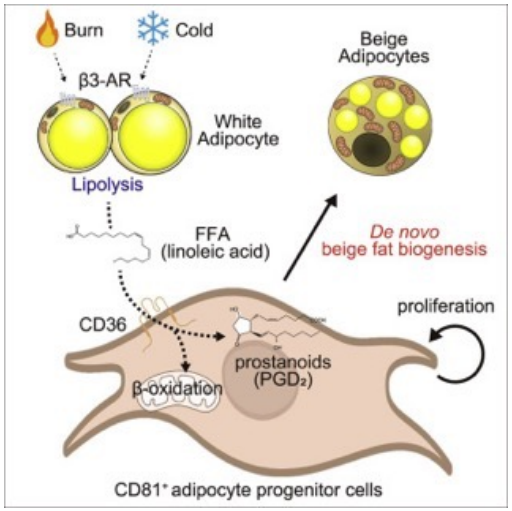

a

	UCP1 Expression	Mitochondrial Density	Lipid droplet	Primary Functions
White	-	Low	Uni-locular	Energy storage Endocrine
Beige	+	Medium	Multi-locular	Thermogenesis Endocrine
Brown	+++	High	Multi-locular	Thermogenesis Endocrine

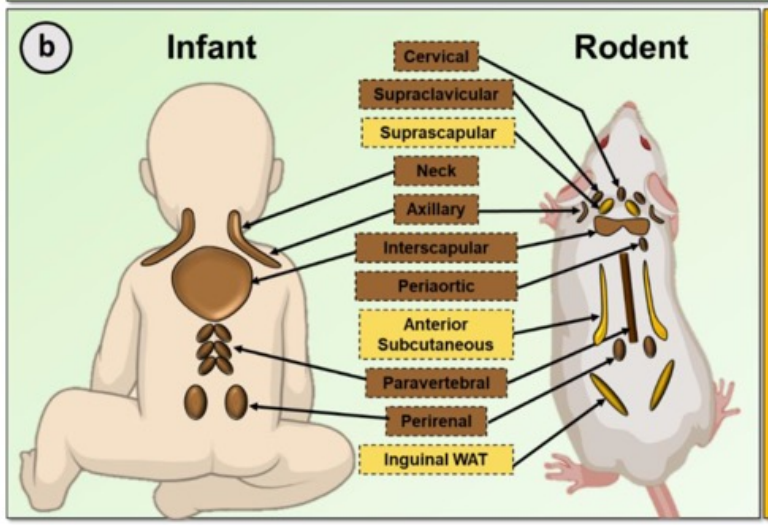

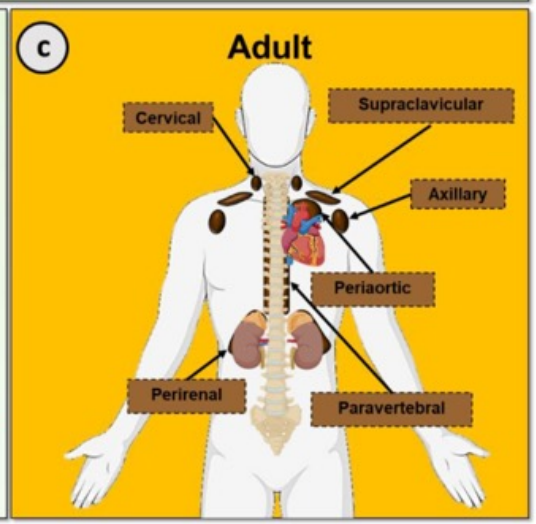

Brown fat releases various substances, including heat (thermogenesis), **lactate**, nucleosides (like **inosine**, adenosine), **lipids**, and proteins/peptides like **Neuregulin 4 (Nrg4)**, adiponectin, and irisin, which signal to other tissues to influence metabolism, glucose control, and energy expenditure, acting locally (paracrine) or systemically (endocrine) to burn calories and maintain body temperature.

Key Substances & Their Roles:

- **Heat (Thermogenesis):** The primary function, achieved by burning calories (glucose, fatty acids) to warm the body, especially in cold conditions.
- **Lactate:** Released during high metabolic activity, potentially acting as a local fuel or signaling molecule.
- **Nucleosides/Nucleotides:** Inosine, adenosine, xanthine, and other related compounds are released and can signal to affect brown fat function and differentiation.
- **Neuregulin 4 (Nrg4):** A protein that helps maintain healthy glucose and lipid metabolism, protecting against fatty liver disease.
- **Adiponectin:** Increases with cold exposure, improving insulin sensitivity and overall metabolic health, linked to longevity.
- **Irisin:** A hormone that improves insulin sensitivity, promotes muscle health, and can convert white fat to brown fat (browning).
- **Lipid Metabolites & Thyroid Hormones:** Act locally to modulate brown fat's development and heat production.

Beige fat releases various signaling molecules, known as "beigokines," that improve metabolic health and energy expenditure, including **FGF21**, **Interleukin-6 (IL-6)**, **Neuregulins (NRG4)**, **VEGF**, and **BAIBA**, affecting other organs, blood vessels (lowering blood pressure), and immune cells to boost thermogenesis and glucose regulation. It also secretes **NGF**, **BDNF**, and **S100b**, supporting nerve health and vasculature, while its activation involves complex interactions with immune cells like eosinophils.

Key Substances (Beigokines) & Their Roles

- **Fibroblast Growth Factor 21 (FGF21):** Improves whole-body insulin sensitivity, reduces food intake (especially sweets).
- **Interleukin-6 (IL-6):** A cytokine that helps regulate metabolism and energy use.
- **Neuregulin 4 (NRG4):** Supports nerve remodeling and vascular health.
- **Vascular Endothelial Growth Factor (VEGF):** Promotes new blood vessel formation (angiogenesis) for better nutrient/oxygen supply.
- **β-Aminoisobutyric Acid (BAIBA):** Increases energy expenditure and protects against weight gain.
- **Neurotrophic Factors (NGF, BDNF):** Promote nerve health and remodeling.
- **S100b:** A calcium-binding protein implicated in beige fat's function and innervation.

Das Gen
PRDM16 (*PR domain containing 16*) kodiert für einen Transkriptionsfaktor, der als zentraler Schalter für die Zellschicksalsbestimmung und den Stoffwechsel in verschiedenen Geweben fungiert. Besondere Bedeutung hat es für das Herz-Kreislauf-System, das Fettgewebe und die Hämatopoese.

Zentrale Funktionen
•**Herzfunktion und Entwicklung:** PRDM16 ist entscheidend für die normale Entwicklung des Herzmuskels, insbesondere des kompakten Myokards. Es reguliert den Fett- und Glukosestoffwechsel in Herzmuskelzellen.
•**Fettstoffwechsel:** Es gilt als Hauptregulator für die Entstehung von **braunem und beigem Fettgewebe**. Es aktiviert Gene für die Thermogenese (Wärmebildung), wie *UCP1*, und unterdrückt gleichzeitig Programme für weißes Fettgewebe.
•**Blutdruckregulation:** Aktuelle Forschungsergebnisse (Stand Januar 2026) zeigen, dass PRDM16 über das beige Fettgewebe und die Sekretion des Proteins *QSOX1* maßgeblich zur Aufrechterhaltung eines gesunden Blutdrucks beiträgt.
•**Hämatopoese:** Es spielt eine Rolle bei der Erhaltung hämatopoetischer Stammzellen

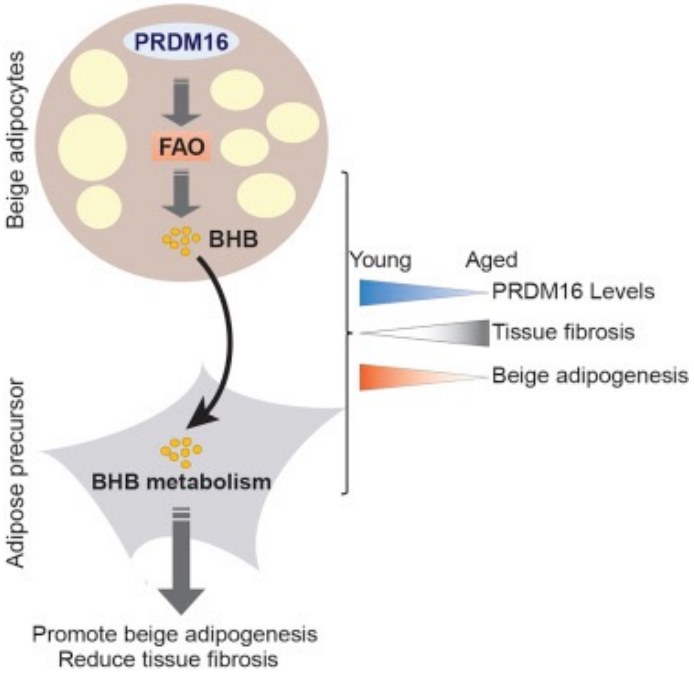

Fatty-acid oxydase and beta hydroxybutyrate

Blood vessels under pressure

A protein in perivascular fat cells protects mice against hypertension

Adipose tissue, the body's largest endocrine organ, is a major regulator of cardiovascular health. In humans, white adipose tissue stores fat and is associated with an increased risk of cardiovascular disease. By contrast, brown adipose tissue produces heat by burning fat and is linked to a decreased risk of cardiovascular disease. Perivascular adipose tissue (PVAT) surrounds blood vessels and has features of both white and brown adipose tissue. PVAT secretes adipokines (adipose tissue proteins that function as hormones), some of which cross the vessel wall and reach its inner layer. Koenen *et al.* report that deleting the PR domain containing 16 (*Prdm16*) gene in fat cells (adipocytes) attenuated PVAT's brown adipose tissue–like features and caused vascular remodeling and hypertension in mice. These findings support the view that therapeutic activation of brown adipose tissue could reduce the risk of cardiovascular disease.

PVAT was considered to be a passive protective cushion around blood vessels, but it is now recognized as an active vessel layer, called the tunica adiposa, with an important role in vascular homeostasis (see the figure). It is a heterogeneous tissue that hosts adipocytes, vascular cells, fibroblasts, immune cells, neurons, and connective tissue progenitor cells. PVAT has adipocytes containing one large lipid droplet, like white adipose tissue, and adipocytes containing many small lipid droplets that express proteins involved in heat production, like brown adipose tissue. There are two types of brown fat: the classic type, which is formed before birth, and the inducible postnatal type, which arises from white adipose tissue through a process called "beiging." The beige fat cells in PVAT in mice are functionally and molecularly similar to the inducible brown fat cells in adult humans.

QSOX1
(**Quiescin Sulfhydryl Oxidase 1**) ist ein Enzym, das eine entscheidende Rolle bei der Ausbildung von Disulfidbrücken in Proteinen spielt. Es als wiichtiger faktor für die Aufrechterhaltung von Barrierefunktionen im Körper.
Biologische Funktion
•**Disulfid-Katalysator:** QSOX1 katalysiert die Oxidation von Sulfhydryl-Gruppen zu Disulfidbrücken unter Reduktion von Sauerstoff zu Wasserstoffperoxid.

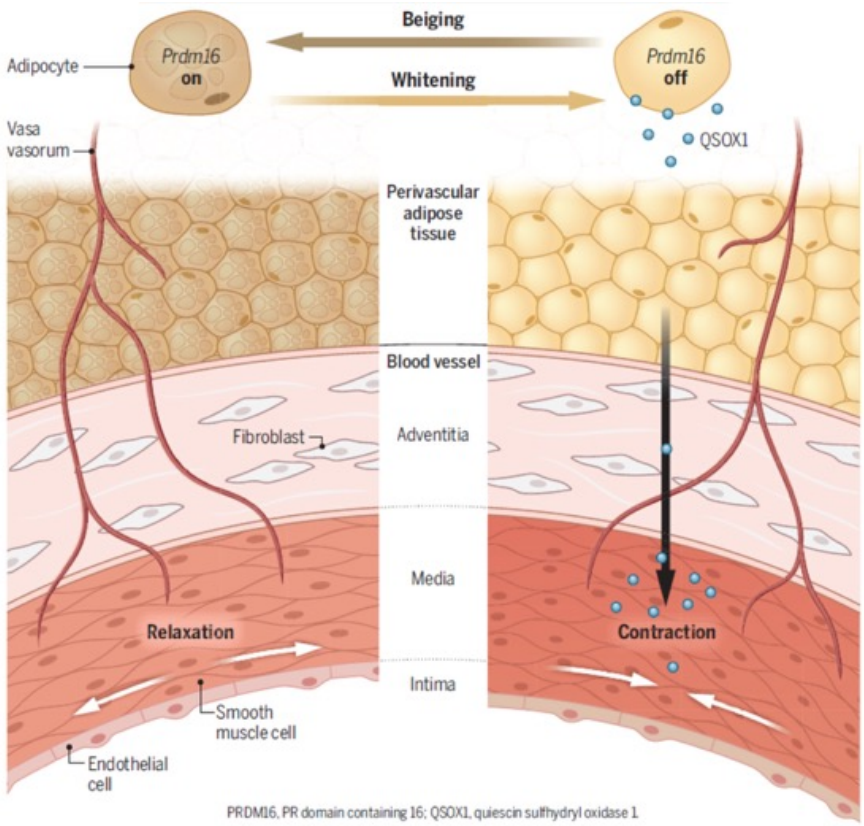

Pressured by fat
Absence of the transcription factor PRDM16 in mice causes remodeling of the perivascular adipose tissue that surrounds blood vessels. Adipocytes gain more white fat characteristics and release the enzyme QSOX1, which causes vascular constriction and increased blood pressure.

Changes in the composition and function of PVAT can promote atherosclerosis, a major cause of cardiovascular disease, through an “outside-in” mechanism in which PVAT-derived adipokines travel to the blood vessel wall, causing inflammation and vessel wall constriction. In rats, overexpression of the protein *PRDM16*—a major gene expression regulator of the beiging process—in PVAT caused white adipocytes to beige and decreased atherosclerotic plaque formation in blood vessels. By contrast, deletion of *Prdm16* inhibited PVAT beiging and led to more vascular lesions in mice. Koenen *et al.* demonstrated that in addition to atherosclerosis, changes in the composition and function of PVAT promote hypertension in mice. Absence of PRDM16 in PVAT adipocytes erased their beige identity, leading to accumulation of connective tissue (fibrosis), increased constriction in blood vessels, and elevated blood pressure. The absence of PRDM16 also changed the repertoire of adipokines released by PVAT. For example, there was increased expression of quiescin sulfhydryl oxidase 1 (QSOX1), an enzyme that drives vascular malfunction by increasing vascular fibrosis and constriction. Although these observations were independent of body weight changes, assessing the absence of PRDM16 in mice given a high-fat diet could help to clarify the role of PVAT and PRDM16 in obesity-related cardiovascular disease.

PRDM16 has been extensively studied as a regulator of adipocyte and heart muscle cell (cardiomyocyte) identity. More recently, PRDM16 was reported to have a role in endothelial cells, as its absence alters the ability of blood vessels to dilate, and in determining the identity of vascular smooth muscle cells. Koenen *et al.* investigated how Prdm16 deletion in PVAT adipocytes affected their adipokine-mediated communication with smooth muscle cells in the tunica media—the middle layer of blood vessels. How this deletion affects communication with endothelial cells in the tunica intima—the inner layer of blood vessels—remains undetermined. Whether *Prdm16* deletion in endothelial or vascular smooth muscle cells affects PVAT adipocytes through altered "inside-out" communication is another outstanding question. Notably, PVAT harbors part of the vasa vasorum, the network of microvessels that nourishes the walls of larger blood vessels and that provides a physical connection between the outer and inner vessel walls. Whether the vasa vasorum are involved in bidirectional communication within the vessel wall or in the function of PVAT is also unclear.

Koenen *et al.*'s meta-analysis of genome-wide association studies that used data from three biobanks reveals an overall positive association between *PRDM16* variants and hypertension in humans. However, PVAT has different features depending on its location: Thoracic PVAT typically has a beige fat phenotype, whereas intestinal PVAT is predominantly composed of white fat cells. The expression of PRDM16 might be different in distinct PVAT regions, so the absence of PRDM16 could have more- or less-pronounced effects in the vessel wall according to location. Notably, Koenen *et al.* observed that the expression level of *Prdm16* in thoracic PVAT is higher in male versus female mice and that the absence of PRDM16 led to prominent changes in vascular fibrosis and adipokine expression in male animals only. Previous studies in mice also revealed that PRDM16 has cell type–specific effects on blood pressure. Its absence in adipocytes resulted in hypertension, whereas in vascular smooth muscle cells, it had the opposite effect. Therefore, a tissue- and cell type–specific approach is warranted when considering the modulation of PRDM16 for therapeutic purposes.

Koenen *et al.*'s findings suggest that the activation of brown adipose tissue by boosting or stabilizing PRDM16 expression could have cardiovascular benefits. Although current human and nonhuman data are encouraging, well-controlled clinical trials are needed to determine whether triggering beiging of adipose tissue reduces the frequency of adverse cardiovascular events in patients. Future studies may elucidate the cross-talk between PVAT and the multilayered arterial wall in various cardiovascular disease conditions, such as atherosclerosis, potentially revealing new therapeutic opportunities.

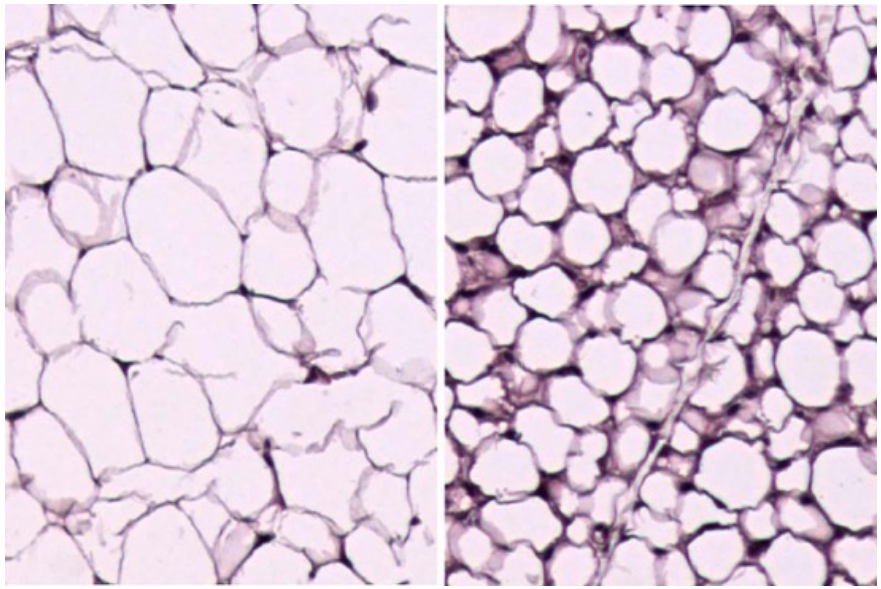

Scientists find way to convert bad body fat into good fat – WashU Medicine

These are the treatments dominating the business of living longer

The big money, big promises and uncertain evidence behind the booming longevity business.

LAS VEGAS — Just beyond the flashing slot machines and cigarette-saturated casino air, thousands of the health obsessed gathered in a convention hall here to demonstrate their hacks for living longer lives. They infused ozone into their blood streams, stood on vibrating mats, swallowed samples of supplements and took scans of their livers.

At its core, antiaging medicine revolves around the reality that the older we are — the weaker our hearts, the more brittle our bones — the more susceptible we become to afflictions like cancer, heart disease and dementia. The average American dies at about 76, with the last decade of life often spent in poor health, according to the World Health Organization. Longevity experts theorize that if humans can slow the natural aging process, then we can avoid debilitating ailments and live longer and healthier.

Cashing in

The boom in consumer demand has inspired as many as 800 longevity clinics to spring up around the country, according to some estimates. These clinics often charge as much as tens of thousands of dollars for a single visit.

Also in 2021, OpenAI CEO Sam Altman invested $180 million into Retro Biosciences, a start-up that says it is developing therapies to add "10 years to healthy human lifespan." The company is currently "fundraising for the next stage of expansion," said Joe Betts-LaCroix, CEO of Retro Biosciences.

Momentum around the industry hit a tipping point last year, as powerful allies of the industry ascended into the federal government. Health Secretary Robert F. Kennedy Jr., a longevity enthusiast himself, has described his own antiaging routines that include a "fistful" of vitamins, testosterone and a stem cell treatment he once received in Antigua. Kennedy has called for an overhaul of FDA funding and regulations, and said last year that if people want to take an experimental drug they "ought to be able to do that." A top adviser to Kennedy, Calley Means, was the closing speaker at the Las Vegas conference, LongevityFest, considered one of the largest annual gatherings of the industry.

This ozone therapy treatment, offered at the conference by a Michigan-based company, Simply O3, is an increasingly popular one among providers who claim the treatment helps boost immunity and reduce inflammation. It's also lucrative: The average clinic generates an additional $60,000 per year by adding IV ozone therapy, according to a company brochure. SimplyO3 did not respond to a request for comment.

Calley Means, a policy adviser to Health Secretary Robert F. Kennedy Jr., attends the longevity industry conference, where he said the United States is in an "existential moment" on health care. (Trisha Thadani/The Washington Post)